

NAVAL POSTGRADUATE SCHOOL

Monterey, California



19970311 005

THESIS

ERICA IOP 5A: MESOSCALE STRUCTURE AND FRONTAL EVOLUTION

by

Timothy G. Lane

September, 1996

Thesis Co-Advisors:

Carlyle H. Wash
Paul A. Hirschberg

Approved for public release; distribution is unlimited.

ERIC QUALITY INSPECTED

REPORT DOCUMENTATION PAGE			Form Approved OMB No. 0704-0188	
Public reporting burden for this collection of information is estimated to average 1 hour per response, including the time for reviewing instruction, searching existing data sources, gathering and maintaining the data needed, and completing and reviewing the collection of information. Send comments regarding this burden estimate or any other aspect of this collection of information, including suggestions for reducing this burden, to Washington Headquarters Services, Directorate for Information Operations and Reports, 1215 Jefferson Davis Highway, Suite 1204, Arlington, VA 22202-4302, and to the Office of Management and Budget, Paperwork Reduction Project (0704-0188) Washington DC 20503.				
1. AGENCY USE ONLY (Leave blank)	2. REPORT DATE September 1996	3. REPORT TYPE AND DATES COVERED Master's Thesis		
4. TITLE AND SUBTITLE : ERICA IOP 5A: Mesoscale Structure and Frontal Evolution		5. FUNDING NUMBERS		
6. AUTHOR Lane, Timothy Glenin				
7. PERFORMING ORGANIZATION NAME(S) AND ADDRESS(ES) Naval Postgraduate School Monterey CA 93943-5000		8. PERFORMING ORGANIZATION REPORT NUMBER		
9. SPONSORING/MONITORING AGENCY NAME(S) AND ADDRESS(ES)		10. SPONSORING/MONITORING AGENCY REPORT NUMBER		
11. SUPPLEMENTARY NOTES The views expressed in this thesis are those of the author and do not reflect the official policy or position of the Department of Defense or the U.S. Government.				
12a. DISTRIBUTION/AVAILABILITY STATEMENT Approved for public release; distribution is unlimited.		12b. DISTRIBUTION CODE		
13. ABSTRACT <p>A mesoscale investigation was conducted on the rapid coastal cyclogenesis that occurred during Intensive Observation Period (IOP 5A) of the Experiment on Rapidly Intensifying Cyclones over the Atlantic (ERICA). Forecasts from a double-nested version of the Navy Operational Regional Analysis and Prediction System (NORAPS) and Multiquadric Interpolation (MQI) objective analyses utilizing operationally available and some special ERICA data were examined to study the mesoscale structure and frontal evolution associated with this explosively deepening coastal cyclone. Additionally, the ability of NORAPS to accurately simulate the explosive cyclogenesis was investigated.</p> <p>The frontal evolution showed characteristics of a classical occlusion, similar to the Norwegian cyclone model, and marine frontal structure as described by Shapiro and Keyser (1990). The frontal evolution was highly influenced by the prior existence of strong Arctic and coastal fronts. These fronts intensified during the course of the storm development and did not develop as a result of the cyclogenesis.</p> <p>The NORAPS model forecasts were compared against satellite imagery, surface observations, MQI analyses, and observed soundings taken during the ERICA study. The double-nested version of NORAPS was found to be an excellent tool for forecasting the mesoscale frontal structure and intensity of this explosively deepening coastal cyclone.</p>				
14. SUBJECT TERMS Experiment on Rapidly Intensifying Cyclones over the Atlantic (ERICA); rapid cyclogenesis; mesoscale frontal evolution		15. NUMBER OF PAGES 93		
		16. PRICE CODE		
17. SECURITY CLASSIFICATION OF REPORT Unclassified	18. SECURITY CLASSIFICATION OF THIS PAGE Unclassified	19. SECURITY CLASSIFICATION OF ABSTRACT Unclassified	20. LIMITATION OF ABSTRACT UL	

Approved for public release; distribution is unlimited.

**ERICA IOP 5A: MESOSCALE STRUCTURE AND FRONTAL
EVOLUTION**

Timothy Glenn Lane
Lieutenant Commander, United States Navy
B.S., Southampton College, 1985

Submitted in partial fulfillment
of the requirements for the degree of

**MASTER OF SCIENCE IN METEOROLOGY AND PHYSICAL
OCEANOGRAPHY**

from the

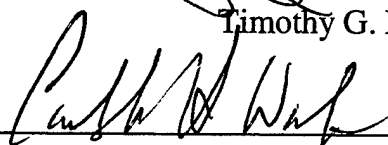
**NAVAL POSTGRADUATE SCHOOL
September 1996**

Author:



Timothy G. Lane

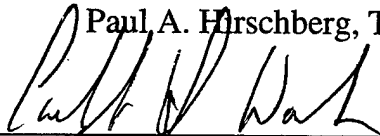
Approved by:



Carlyle H. Wash, Thesis Co-Advisor



Paul A. Hirschberg, Thesis Co-Advisor



Carlyle H. Wash, Chair
Department of Meteorology

ABSTRACT

A mesoscale investigation was conducted on the rapid coastal cyclogenesis that occurred during Intensive Observation Period (IOP 5A) of the Experiment on Rapidly Intensifying Cyclones over the Atlantic (ERICA). Forecasts from a double-nested version of the Navy Operational Regional Analysis and Prediction System (NORAPS) and Multiquadric Interpolation (MQI) objective analyses utilizing operationally available and some special ERICA data were examined to study the mesoscale structure and frontal evolution associated with this explosively deepening coastal cyclone. Additionally, the ability of NORAPS to accurately simulate the explosive cyclogenesis was investigated.

The frontal evolution showed characteristics of a classical occlusion, similar to the Norwegian cyclone model, and marine frontal structure as described by Shapiro and Keyser (1990). The frontal evolution was highly influenced by the prior existence of strong Arctic and coastal fronts. These fronts intensified during the course of the storm development and did not develop as a result of the cyclogenesis.

The NORAPS model forecasts were compared against satellite imagery, surface observations, MQI analyses, and observed soundings taken during the ERICA study. The double-nested version of NORAPS was found to be an excellent tool for forecasting the mesoscale frontal structure and intensity of this explosively deepening coastal cyclone.

TABLE OF CONTENTS

I. INTRODUCTION	1
II. MESOSCALE MODEL AND ANALYSES	5
A. MESOSCALE FORECAST MODEL	5
B. SURFACE ANALYSES	6
III. REVIEW AND METHODOLOGY	9
A. REVIEW OF PREVIOUS WORK	9
B. NESTED NORAPS MODEL PERFORMANCE	14
1. Position and Intensity	15
2. Time Series Comparisons	17
C. SUMMARY OF MODEL PERFORMANCE	18
IV. MESOSCALE EVOLUTION	23
A. INCIPIENT DEVELOPMENT STAGE (20/1200Z-21/0000Z)	24
B. EARLY MESOSCALE DEVELOPMENT	38
C. EXPLOSIVE DEVELOPMENT STAGE (21/0000Z - 21/1800Z)	48
D. MATURE CYCLONE STAGE (21/1800Z - 22/0000Z)	68
V. SUMMARY AND RECOMMENDATIONS	71

A.	SUMMARY	71
B.	RECOMMENDATIONS	75
LIST OF REFERENCES		77
INITIAL DISTRIBUTION LIST		81

ACKNOWLEDGMENTS

The author acknowledges the support, encouragement, and prayers of his wife Rebecca. I could not have made it through school without her understanding, and perseverance along side of me.

The author sincerely appreciates the time and support of his thesis advisors: Professor Carlyle Wash, for sharing his depth and breadth of knowledge in meteorology which I hope someday to achieve in my own life; and Professor Paul Hirschberg, for his patience and technical assistance throughout this project. Additionally, thanks are due to Ms. Olivera Haney and Professor Wendall Nuss for sharing their time, efforts and technical expertise in preparing the analyses.

And to my friends: John, Don, Scott, Jay and Tony - I wouldn't have graduated without you all!

I. INTRODUCTION

Rapid cyclogenesis at sea and in coastal areas can pose a severe threat to seagoing vessels and adversely impact military operations. These storms are associated with high winds and seas that also restrict visibility and pose substantial danger to both personnel and property. Consequently, accurate short-range as well as long-range forecasts are of great importance to the mariner. With the development of better position and intensity forecasts, it is likely that these storms will cause less damage because better evasive and preparatory actions will be possible. Of particular interest and concern are storms that intensify rapidly. Sanders and Gyakum (1980) define a rapidly deepening extratropical cyclone or a "meteorological bomb" as a storm exhibiting a central pressure fall exceeding 1 mb h^{-1} for 24 hr or more. While the large-scale processes that contribute to typical cyclogenesis are well understood, it appears that other processes beyond large-scale baroclinic dynamics contribute to the development of rapidly intensifying storms. Although there are variations between individual storms, certain physical processes such as latent and sensible heat fluxes (Nuss and Anthes 1987); strong upper-level forcing (Uccellini et al. 1985; Wash et al. 1988; Sanders 1986); and a pre-existing baroclinic zone (Bosart 1981) have been found to act independently or synergistically to produce a rapid developer.

Sanders (1986) discussed the composite structure and mean behavior of bombs forming in the west-central North Atlantic Ocean during the period January 1981- December 1984. He identified 54 cases of explosive deepening from the 12 h operational analyses prepared by the National Meteorological Center (NMC). Sanders noted that the average 500 mb vorticity advection was highly correlated with the period of maximum deepening, which

provides further evidence of the fundamentally baroclinic nature of the bomb. Sanders further speculated that the large response to the baroclinic forcing is due to the small lower-tropospheric static stability brought about by surface latent and sensible heat fluxes and the relatively small dissipation over the smooth sea surface. Manobianco (1989) extended the work of Sanders by describing the three-dimensional kinematic and thermodynamic synoptic and subsynoptic-scale structure for 24 of the 54 cases identified by Sanders (1986). The results of his work support the idea that explosive cyclogenesis is a baroclinic phenomenon in which the rapid development in the presence of strong upper tropospheric forcing appears to be enhanced by a more destabilized lower troposphere.

Because of inadequate knowledge and parameterizations of the processes involved, operational models often fail to adequately predict the development, intensification and storm track of these systems (Bosart 1981). This failure of numerical models to accurately simulate explosive cyclogenesis led to the Office of Naval Research (ONR) to sponsor Experiment on Rapidly Intensifying Cyclones over the Atlantic (ERICA).

ERICA was conducted in the oceanic region east of New England and the middle Atlantic states and south of Nova Scotia and Newfoundland during the period 1 December 1988 - 28 February 1989. The general area of ERICA measurements is shown in Fig. 1. The stippled area represents the region of greatest summed pressure falls for 104 pre-ERICA type storms and the area that was targeted for the highest concentration of ERICA measurements (Hadlock and Kreitzberg 1988). Throughout this period, the density of surface observations over the ocean was increased by measurements from specially deployed drifting buoys and ships of opportunity. During intensive observation periods (IOPs), additional low-level and

upper-air measurements were collected from instrumented aircraft, dropsondes released from the aircraft, and supplementary soundings taken in the eastern United States and Canada. Hadlock and Kreitzberg (1988) stated that the objectives of the experiment were to:

- (i) understand the fundamental physical processes occurring in the atmosphere during rapid intensification at sea;
- (ii) determine those physical processes that need to be incorporated into dynamical prediction models through efficient parameterizations if necessary and;
- (iii) identify measurable precursors that might be incorporated in the initial analysis for accurate and detailed operational model predictions.

The objectives of this paper are two fold: first, to document the evolution and mesoscale features of a rapidly developing coastal cyclone and its associated frontal structures observed during ERICA IOP 5A with all available data and second, to determine the ability of the nested Navy Operational Regional Atmospheric Prediction System (NORAPS) mesoscale model to diagnose the fronts and cyclone evolution. Chapter II describes the mesoscale model and analysis method used for the study. Chapter III reviews the previous work completed on IOP 5A and describes model performance. Chapter IV contains the synoptic and mesoscale description of the event as well as model verification through actual observations. A summary and conclusions is found in Chapter V.

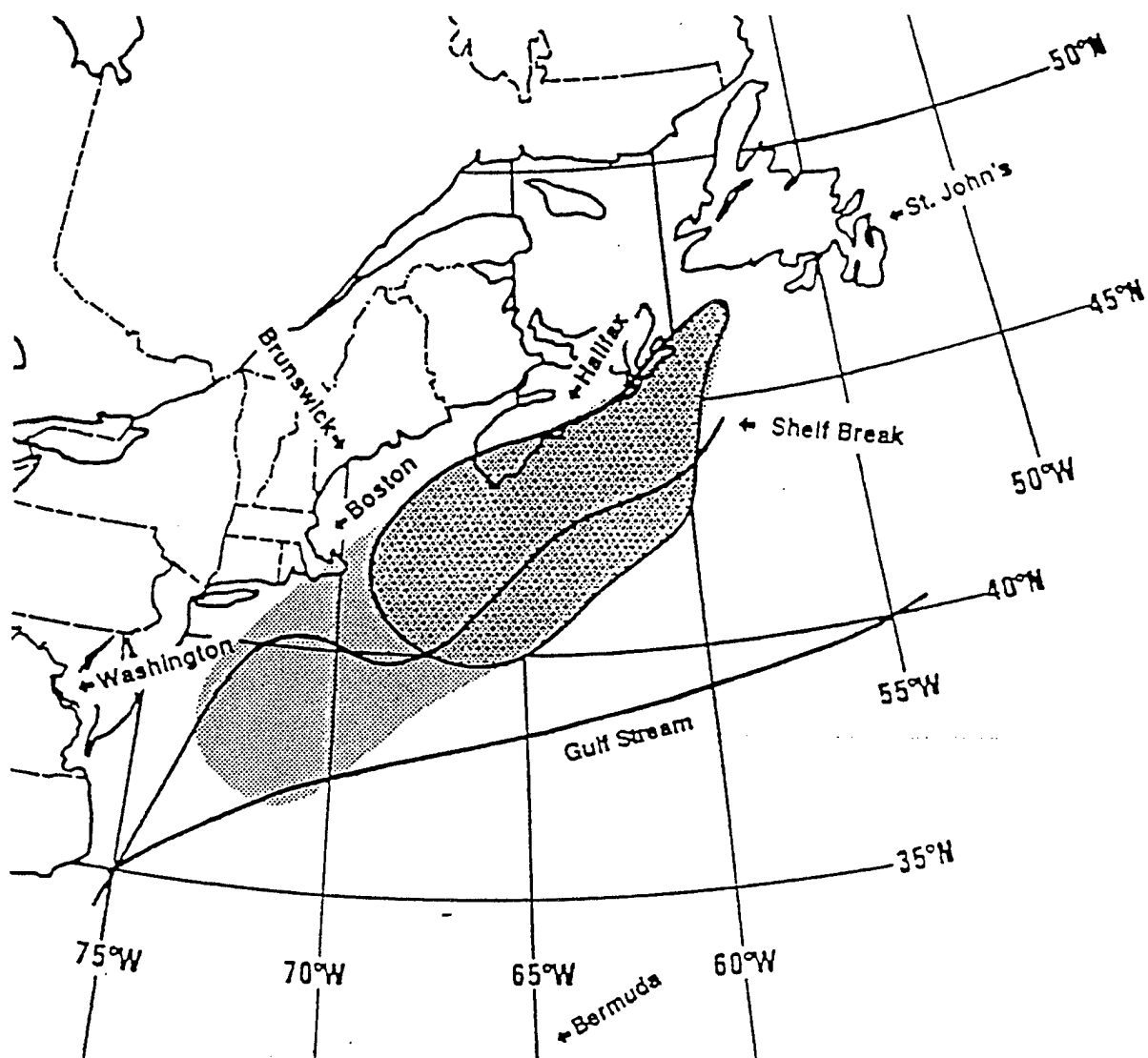


Figure 1. Primary (dark stippling) and secondary (light stippling) areas where rapidly developing storms are most likely to occur in the ERICA domain (from Hadlock et al. 1989).

II. MESOSCALE MODEL AND ANALYSES

A. MESOSCALE FORECAST MODEL

NORAPS version 6.1 is a globally relocatable, triple-nested mesoscale model run operationally by the Naval Fleet Numerical Meteorology and Oceanography Center for several areas of the world: the continental U.S. (including the Western Atlantic Ocean); Indian Ocean; Europe (including the Mediterranean); and Asia (including the Western Pacific Ocean). The NORAPS model has been described by Hodur (1987) and more recently by Liou et al. (1994). Initial conditions (analyses) are prepared on 16 standard pressure levels through multivariate optimum interpolation (MVOI) (Barker 1992). Model forecasts are obtained by integrating the hydrostatic primitive equations and physical parameterizations on a staggered Arakawa C-grid. The model atmosphere is divided into 24 layers from the surface to 50 mb. Of the 24 levels, 7 are concentrated below 850 mb to provide adequate resolution of the planetary boundary layer (PBL). Physical parameterizations for NORAPS include: radiative transfer, Kuo (1974) type cumulus parameterization for deep convection, and Tiedtke et al. (1989) parameterization for large-scale condensation. The multi-level boundary layer is parameterized by using K-theory for the surface (Louis 1979) and a 1.5 turbulent kinetic energy closure scheme for vertical eddy flux parameterization (Langland and Liou 1994). Precipitation falling into unsaturated layers is partially evaporated, depending on the relative humidity of the subcloud layers. NORAPS grids can be selected using any of the conformal projections: Lambert, Mercator, or polar stereographic. At inner lateral boundary zones, terrain heights of the inner fine mesh are matched with the terrain

heights of the coarser mesh so that sigma coordinates are consistent in those regions. During time integration, the boundary conditions for the two inner meshes are updated with each timestep, while the coarser outer grid is updated every 6 or 12 h by the forecasts of the Navy Global Atmospheric Predictions System (NOGAPS) (Liou et al. 1994). The U. S. Navy's ten minute data base provides the terrain fields used by NORAPS

A double-mesh version of NORAPS has been used in this study. The forecast domain for the fine mesh contains 121×121 grid points with a grid size of 20 km centered at 45°N , 65°W . The domain for the coarse mesh contains 109×89 grid points with a grid size of 60 km centered at 45°N , 65°W (Fig. 2). The forecast model was initialized with 60 km NORAPS OI analyses. The initialization was supplemented by regional operational surface data, rawinsonde data, and special ERICA data. The model simulation started at 1200 UTC 20 January and was integrated 36 h to 0000 UTC 22 January 1989.

B. SURFACE ANALYSES

In order to verify the model forecasts, reanalyses of the sea level pressure and surface temperatures were produced using a multiquadric interpolation (MQI) scheme on the NORAPS 60 km and 20 km grids. As described by Nuss and Titley (1994), the MQI fits surfaces through all observations in such a way that values can be interpolated to any point on a grid. NORAPS analysis fields were used as a first-guess. The degree of surface fit to the observations is determined by specification of filtering and smoothing parameters. The user may vary the root mean square difference between observations and the first-guess field. Similarly, the smoothing of the observations may be varied in the analysis. Nuss and Titley have demonstrated that the MQI technique has skill in the interpolation of scattered data.

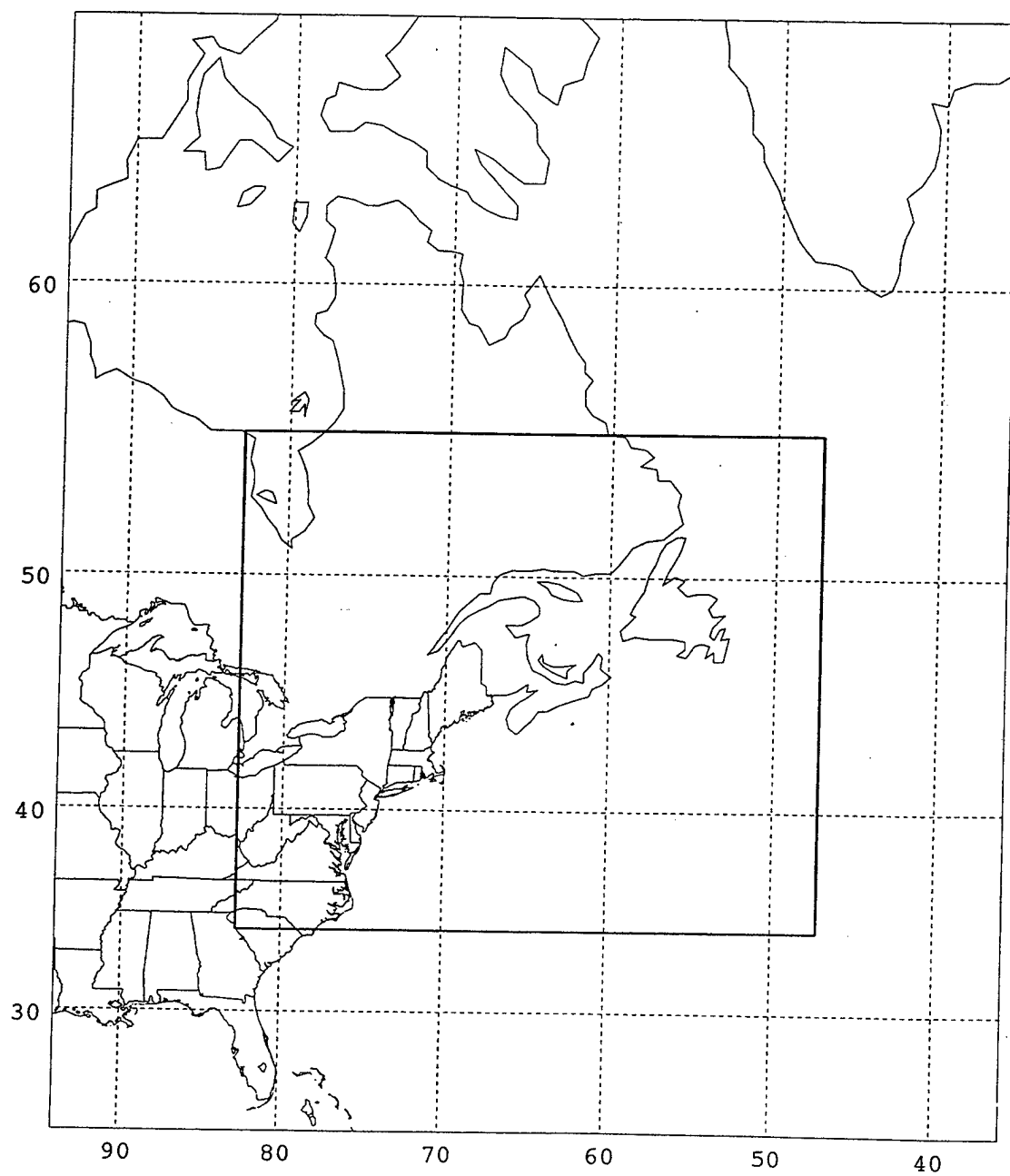


Figure 2. The NORAPS 60-km and 20-km domains used in this study.

III. REVIEW AND METHODOLOGY

The time period 18-22 January 1989 was one of the most active during the ERICA project. During this five day period, two rapidly intensifying cyclones developed within 36 h over the western North Atlantic Ocean. The first cyclone, IOP 5, developed off the mid-Atlantic coast and tracked along the north wall of the Gulf Stream, reaching a maximum deepening rate of $36 \text{ mb (18 h)}^{-1}$ (Hadlock et al. 1989). The second cyclone, IOP 5A, developed northeast of Lake Ontario and tracked along the Canadian Maritimes coast, reaching a maximum deepening rate of 21 mb (9 h)^{-1} (Fig. 3). This latter storm is of particular interest because it is a coastal developing storm, which exhibited characteristics of rapid deepening over land as described by Mass and Schultz (1993), and marine development as summarized by Shapiro and Keyser (1990). Of particular interest, pre-existing frontal zones intensified during the rapid cyclogenesis and evolved into cyclone frontal structures rather than forming as a result of the cyclogenesis.

A. REVIEW OF PREVIOUS WORK

Spinelli (1992) conducted a synoptic investigation of IOP 5A and determined several factors that contributed to the rapid development of the cyclone. Those factors were: (i) significant lower tropospheric thermal advection preceding the rapid intensification; (ii) favorable superposition of a mobile 500 mb trough over the frontal wave providing upper-level support; (iii) the presence of a jet streak on the eastern side of the 300 mb trough and; (iv) intense upward vertical motions within the frontal cloud band of the cyclone. In addition, an evaluation of the 60 km NORAPS model forecast versus the 60 km NORAPS OI

NMC 3-HRLY NORTH AMERICAN CHART DATA

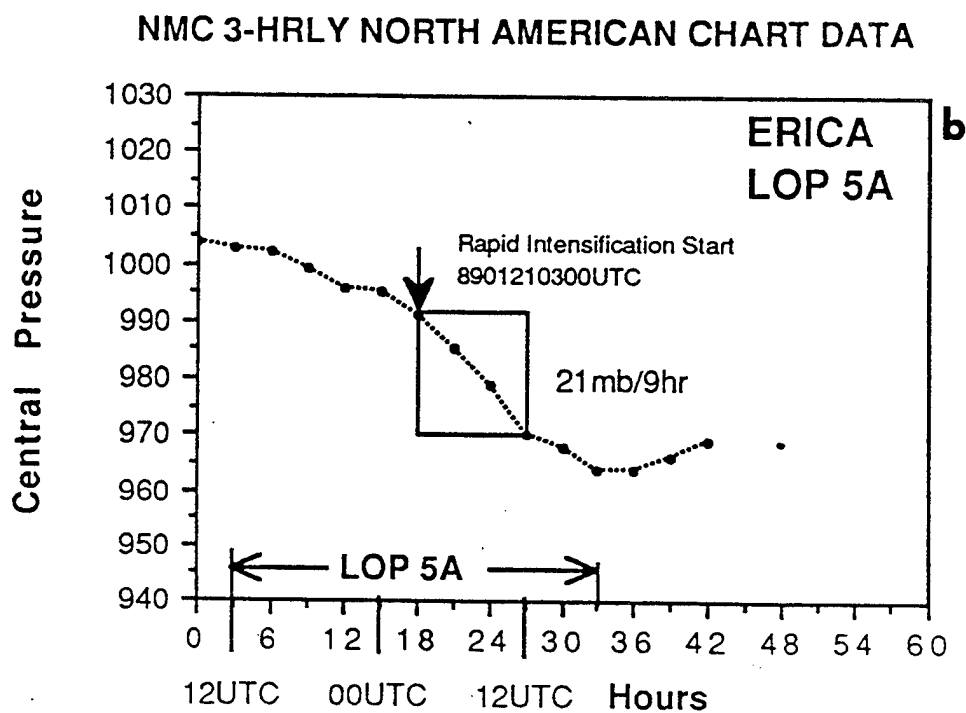
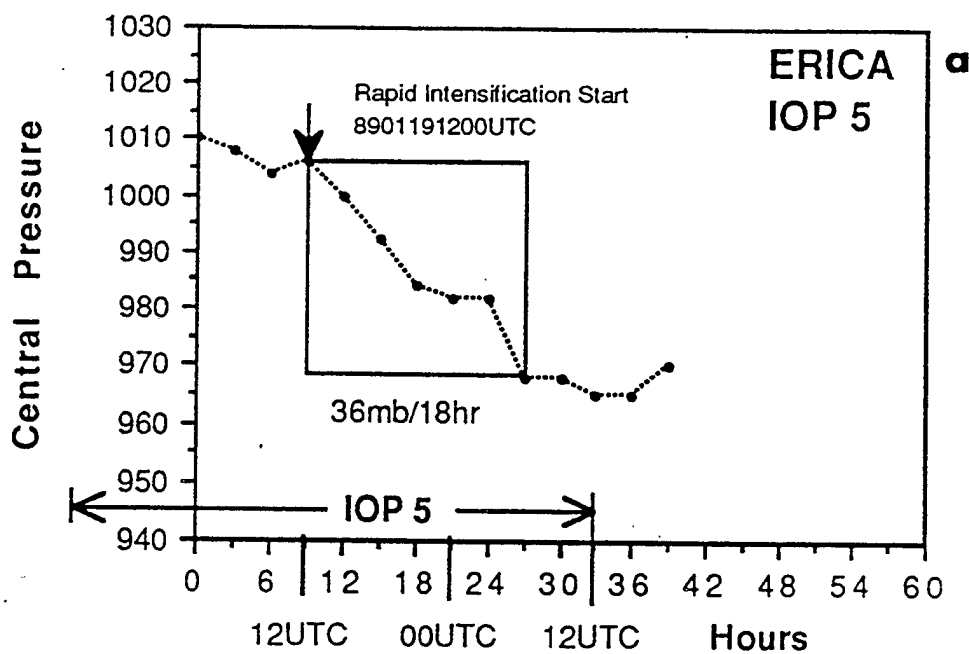


Figure 3: NMC SLP (mb) vs time for (a) ERICA IOP 5 (b) ERICA IOP 5A

analyses was conducted to determine the performance of the model in simulating a rapidly developing coastal storm.

In evaluating the NORAPS model, Spinelli (1992) noted that the NORAPS 60 km models forecasts of the synoptic-scale features, (e.g., jet streaks, vorticity centers, upper-level troughs) position and intensity were "relatively accurate." However, the 60 km NORAPS analyses and forecasts were too coarse to resolve the mesoscale features that may have played an important role in the rapid development of the IOP 5A cyclone. To resolve these features, Spinelli performed a hourly subjective analysis, which revealed the development of a secondary low pressure center well to the southeast of the primary low (Fig. 4). This secondary development was not indicated in the synoptic NORAPS analyses. Based on the topography of the region (Fig. 5), Spinelli speculated that this low was probably a result of lee cyclogenesis on the lee (eastern) side of the northern Appalachian Mountains. The coastal low continued to progress northeast and deepen rapidly and likely became the primary low center for the IOP 5A cyclone. Figure 6 shows the tracks of the two separate lows from 20/1500Z to 21/0300Z as derived from the subjective analyses. The 6-h positions of the IOP 5A cyclone as analyzed by the 60 km NORAPS are represented by the open square symbols. One significant result of these detailed analyses is that there is a clear indication that mesoscale processes not necessarily captured by the 60 km NORAPS analysis or forecasts were occurring during the time period examined.

Further assessment of the NORAPS model to predict mesoscale features was also conducted by Cameron (1993). Specifically, a comparison between the frontal evolutions associated with other rapidly deepening storms and the coastal IOP 5A storm was performed

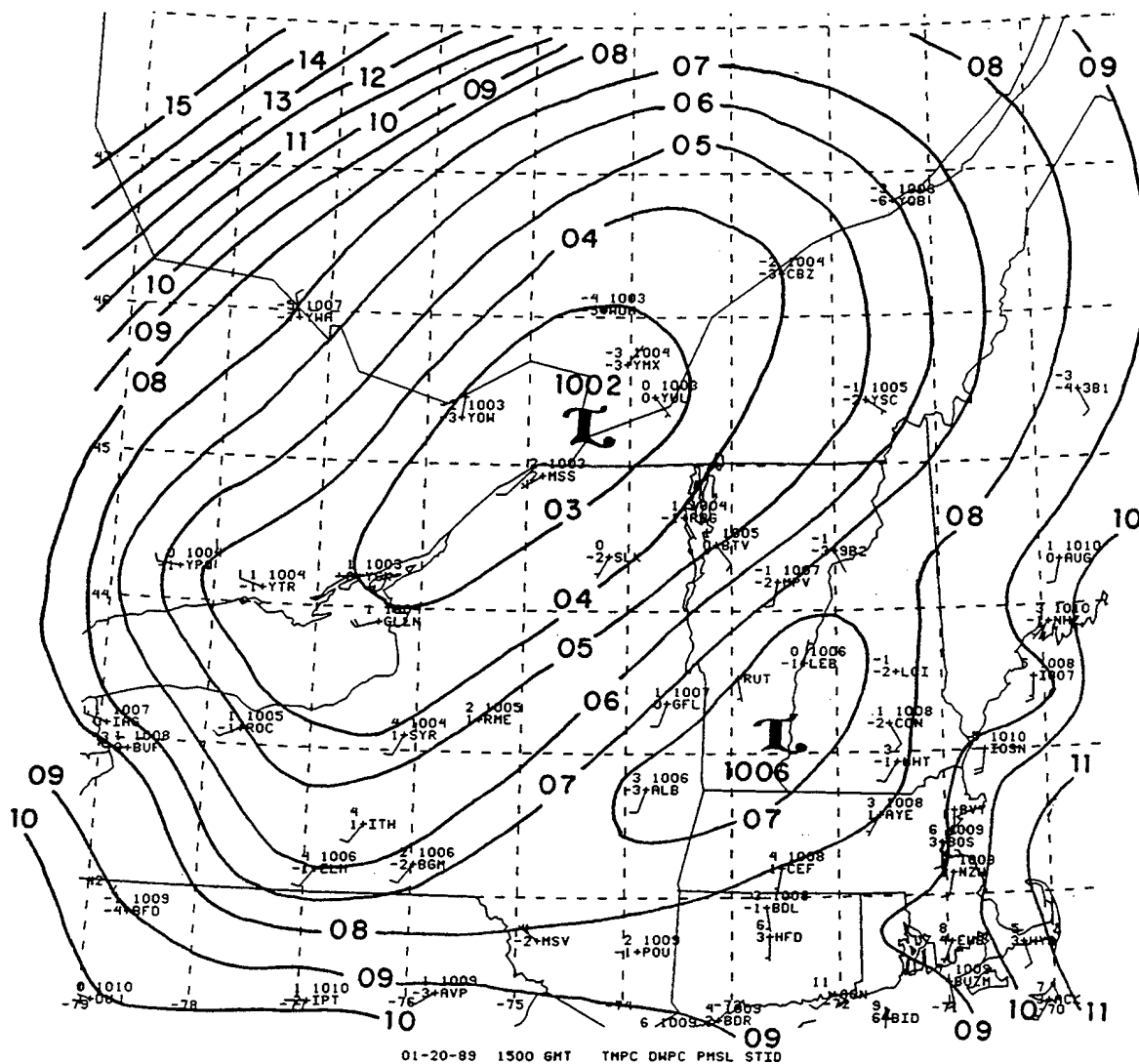


Figure 4. Subjective surface pressure analysis (solid, contour interval 4 mb) with subjective temperature analysis added (dashed, contour interval 2°C) at 20/15Z January 1989 (from Spinelli 1992).

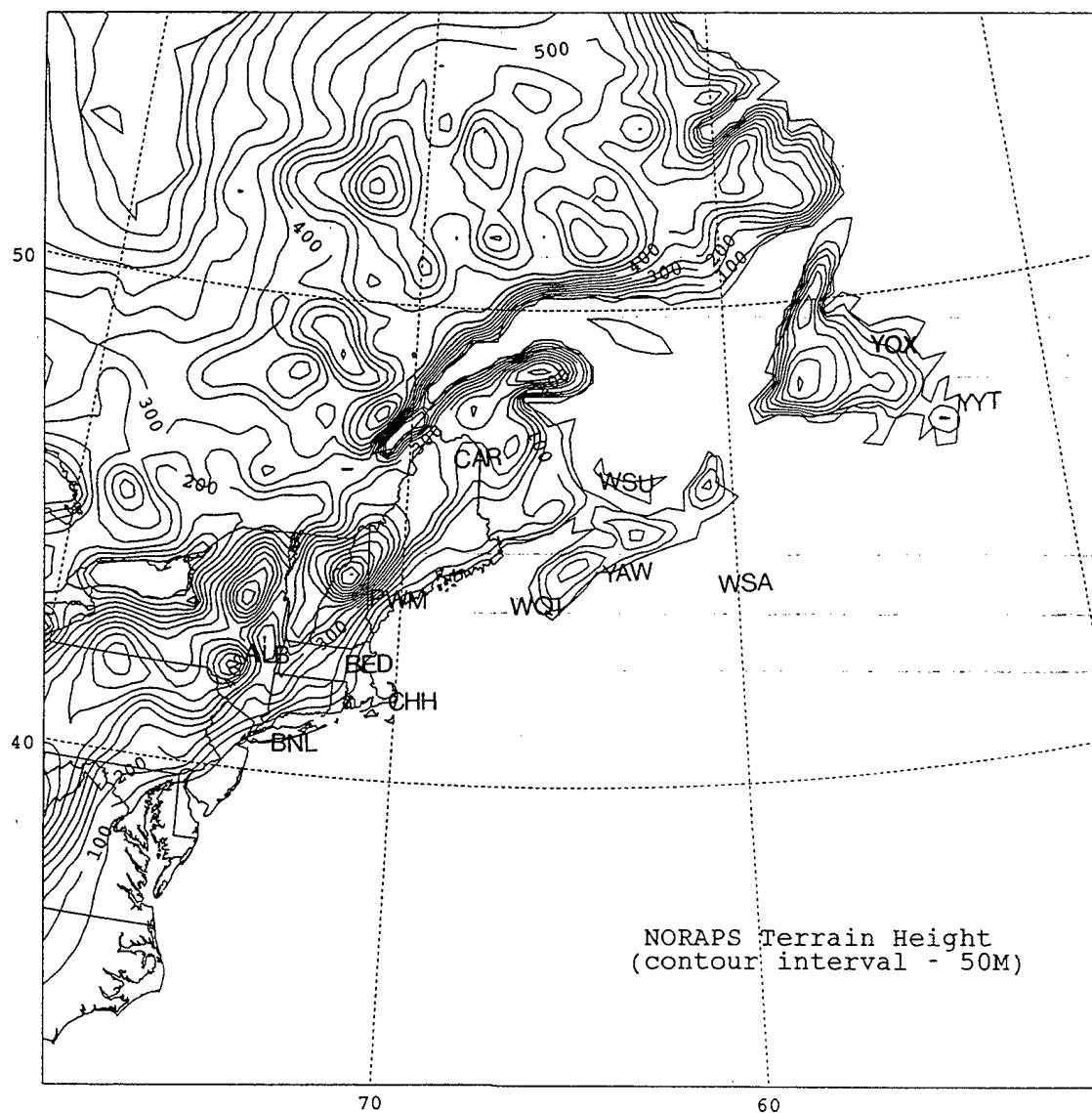


Figure 5. NORAPS terrain height (contour interval 50 m).

to determine if maritime frontal evolution can be generalized to a coastal environment. In his investigation, Cameron found that the frontal evolution of IOP 5A did not neatly fit into a single category of development. Rather, the storm exhibited properties similar to a classical occlusion and some evidence of the bent-back warm front structure described by Shapiro and Keyser (1990). For example, composite of the Arctic front evolution as depicted by the 60 km NORAPS model is shown in Fig. 7 at 12 h intervals from 20/1200Z to 22/0000Z. Figure 8 is a coastal front composite every six hours from 20/1200Z to 22/0000Z. These composites show that strong Arctic and coastal fronts present at the incipient stage of cyclone development intensified as a result of the rapid cyclogenesis and became an integral part of the synoptic-scale frontal structure.

B. NESTED NORAPS MODEL PERFORMANCE

A significant result of these two previous studies was that the need for a higher resolution mesoscale model to accurately predict secondary cyclogenesis and further investigate the mesoscale features. This study utilizes the results from a 36-h NORAPS simulation on the 20 km mesh previously described. A 20 km MQI analysis of the SLP and surface temperatures is also utilized to: determine the SLP and positions of IOP 5A; perform frontal analysis; and to validate NORAPS output. In evaluating forecast model performance, time series from Sable Island, MQI and National Meteorological Center (NMC) analyses, in situ observations, and the NORAPS 60 km analysis were used. In this manner, the model skill in predicting the evolution and mesoscale features of the IOP 5A cyclone will be compared closely to the observations.

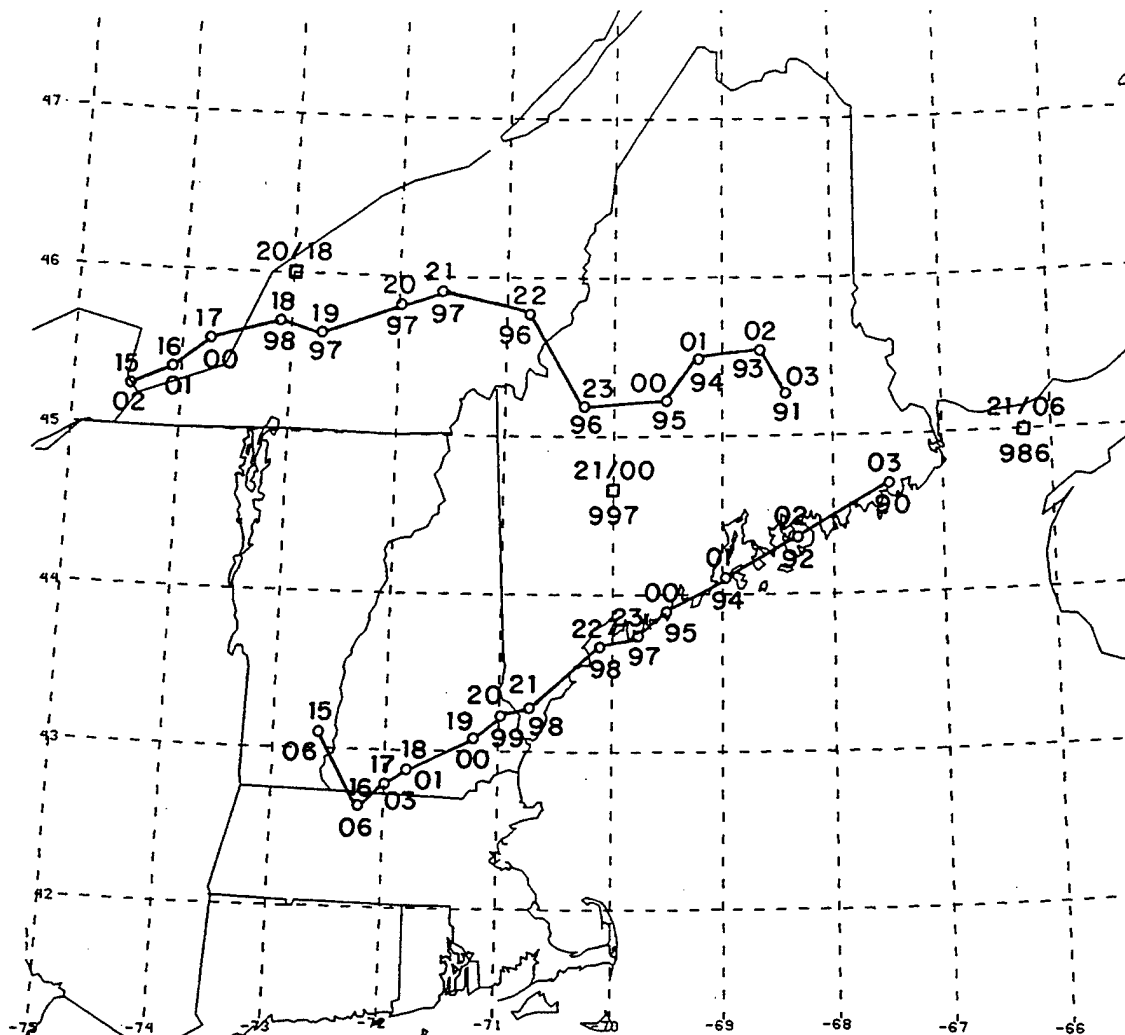


Figure 6. Tracks (solid lines connecting open circles) and central pressures (mb) of primary and secondary lows from 20/1500Z to 21/0300Z. The hour and last two digits of the central pressure are shown above and below the position markers. Open squares are positions of main low derived from NORAPS analyses.

1. Position and Intensity

NORAPS did an excellent job in forecasting the rapid development of the IOP 5A cyclone. A comparison of intensity and position forecasts is provided in Table 1. While the 6-h forecast central pressure of the low was 2 mb too high, the model was 2 mb too deep by tau 24, but remained 2 mb weak for the remaining period. The 36-h analysis and NORAPS

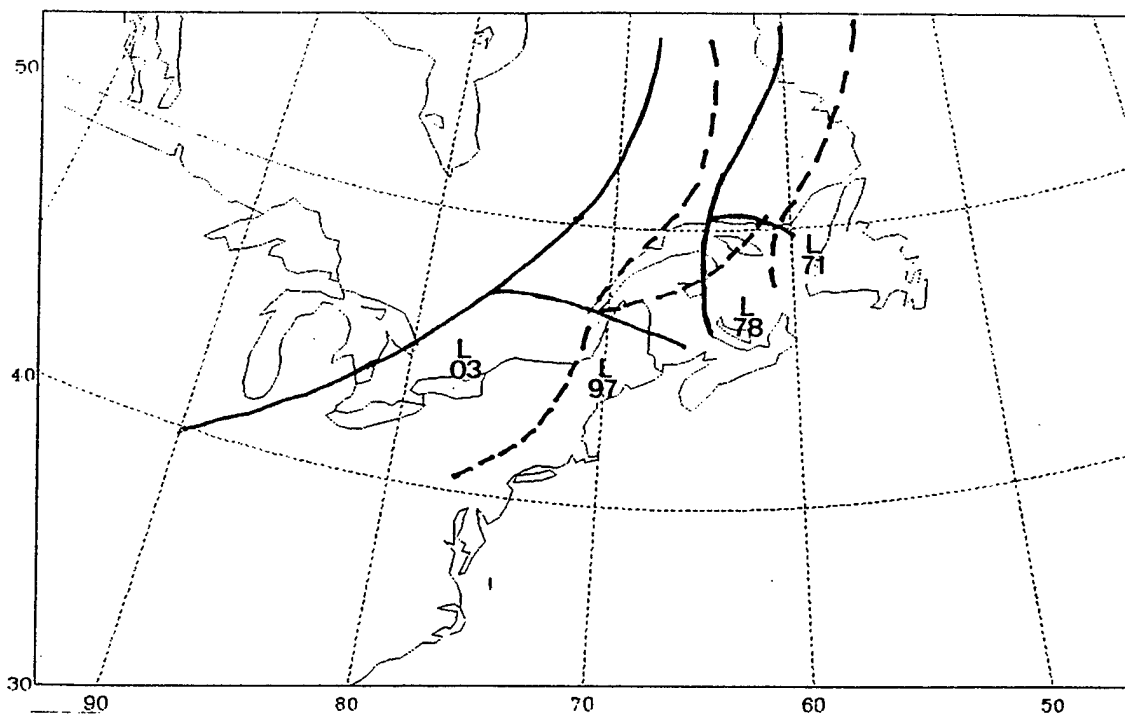


Figure 7. Composite Arctic front positions in twelve hour increments from 20/12Z to 22/00Z January 1989 (from Cameron 1993).

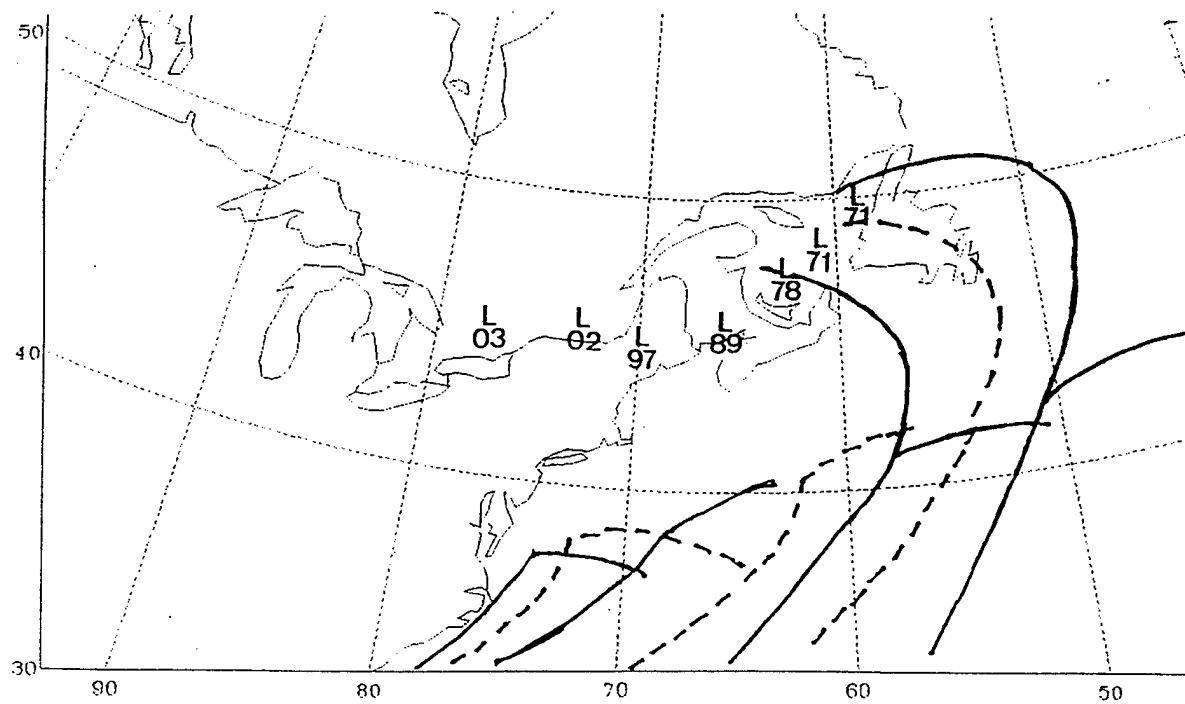


Figure 8. Composite coastal front positions in six hour increments from 20/12Z to 22/00Z January 1989 (from Cameron 1993).

forecast positions of the ERICA IOP 5A cyclone at 6-h intervals starting from 20/1200Z are depicted in Fig. 9. The initial analyzed position is just north of Lake Ontario. Note that the

Table 1. Position and intensity forecasts for IOP 5A. Position errors are read as the distance and direction that the NORAPS low is from the MQI analyzed low.

	20 km NORAPS (mb)	20 km MQI analysis (mb)	60 km NORAPS analysis (mb)	NMC hand analysis (mb)	Position error (nm)
20/1200Z	1004	1003	1003	1003	0
20/1800Z	1000	998	1000	999	15/south
21/0000Z	996	995	997	995	28/southeast
21/0600Z	987	985	986	986	43/northeast
21/1200Z	973	975	973	970	71/northwest
21/1800Z	966	964	970	964	105/northwest
22/0000Z	967	965	969	966	128/west

minimum central pressure of 964 mb occurs at 21/1800Z close to the southwestern edge of Newfoundland. The storm deepens 31 mb in the 18-h period from 21/0000Z to 21/1800Z with a model pressure difference of +2 mb (Fig. 10). After 18 h (21/0600Z), the forecast shows an increasing bias in the cyclone position, with NORAPS tending to place the storm center somewhat to the northwest of the observed position.

2. Time Series Comparisons

To further examine model performance, a time series of SLP, surface temperature, wind speed and direction from Sable Island (WSA) during a cold frontal passage will be examined. This station is located on a small island (43.9° N, 60.0°W), while the available every hour, and are plotted with the hourly model output in Fig. 11. A point verification is

a challenging test for a numerical weather prediction model.

In comparing the time series in Figs. 11 a-b, NORAPS generally has similar SLP but warmer near-surface temperatures when compared to the observations until frontal passage, which occurs 22 h (21/1000Z) into the simulation. The surface observations show a sharp jump in temperature near the frontal passage, which is captured skillfully by the model. Prior to frontal passage (21/0000Z - 21/0900Z), NORAPS shows a $24 \text{ mb } (9 \text{ h})^{-1}$ pressure fall as compared to the observational rate of $27 \text{ mb } (9 \text{ h})^{-1}$. After frontal passage, the model remains approximately 5 mb too high at this point for the remainder of the period. The earlier warm bias of the surface temperatures begins to diminish and NORAPS forecasts the surface temperatures after frontal passage exceedingly well.

NORAPS captures the observed wind speed and direction well (Figs. 11 c-d). The NORAPS wind speed is nearly equal with the observations until frontal passage. At frontal passage, the observations show a momentary drop in wind speed with a gradual veering of the winds to the west. NORAPS follows both of these trends except that the wind speed remains nearly steady during frontal passage and remains somewhat weak for the remaining period.

C. SUMMARY OF MODEL PERFORMANCE

From previous investigations of the IOP 5A cyclone, it was demonstrated that the coarse grid NORAPS model produced a realistic simulation of the rapid cyclogenesis event. The important large-scale features such as the location and intensity of the 500 mb and 300 mb troughs, vorticity centers, jet streaks and upper-level divergence areas were all represented well. The reader is referred to Spinelli (1992) and Cameron (1993) for a detailed

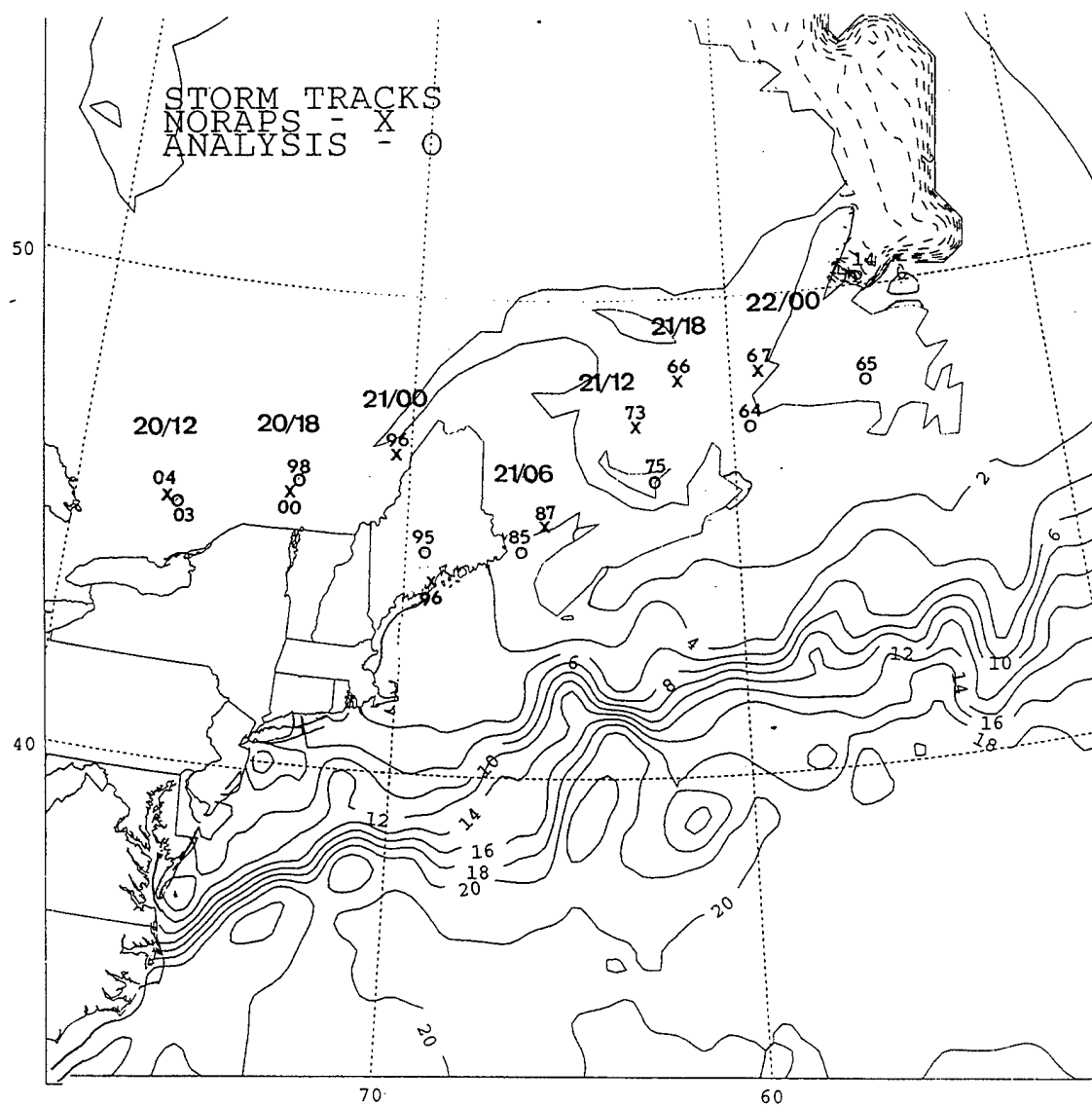


Figure 9. Sea surface temperatures (solid, 1°C) on 20 January 1989. NORAPS (crosses) and the MQI analysis (circles) 6-h surface cyclone positions and central sea level pressures between 12 UTC 20 January and 0000 UTC 22 January 1989.

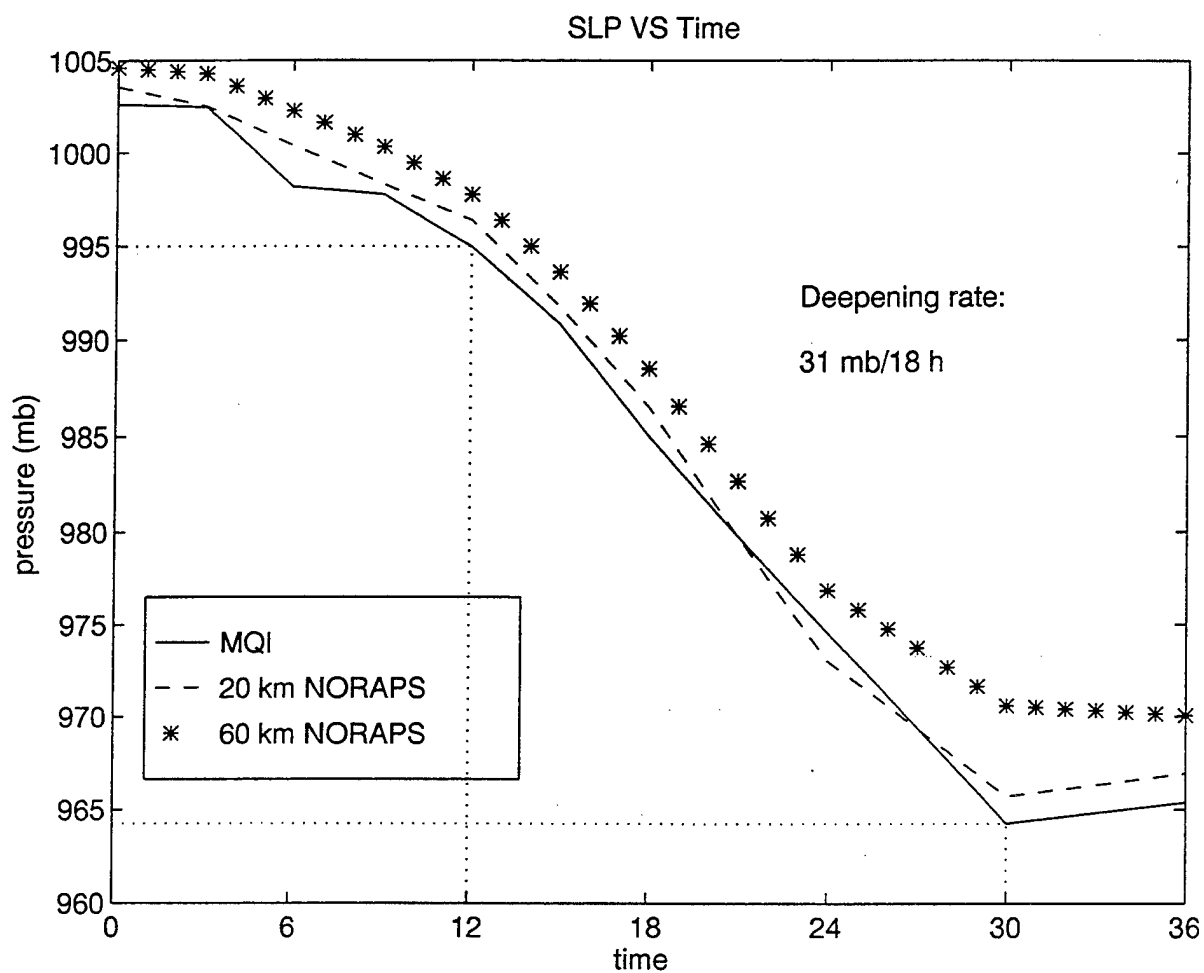


Figure 10. Analyzed (MQI) and simulated sea level pressure (mb) at the center of the cyclone for the 36-h simulation period.

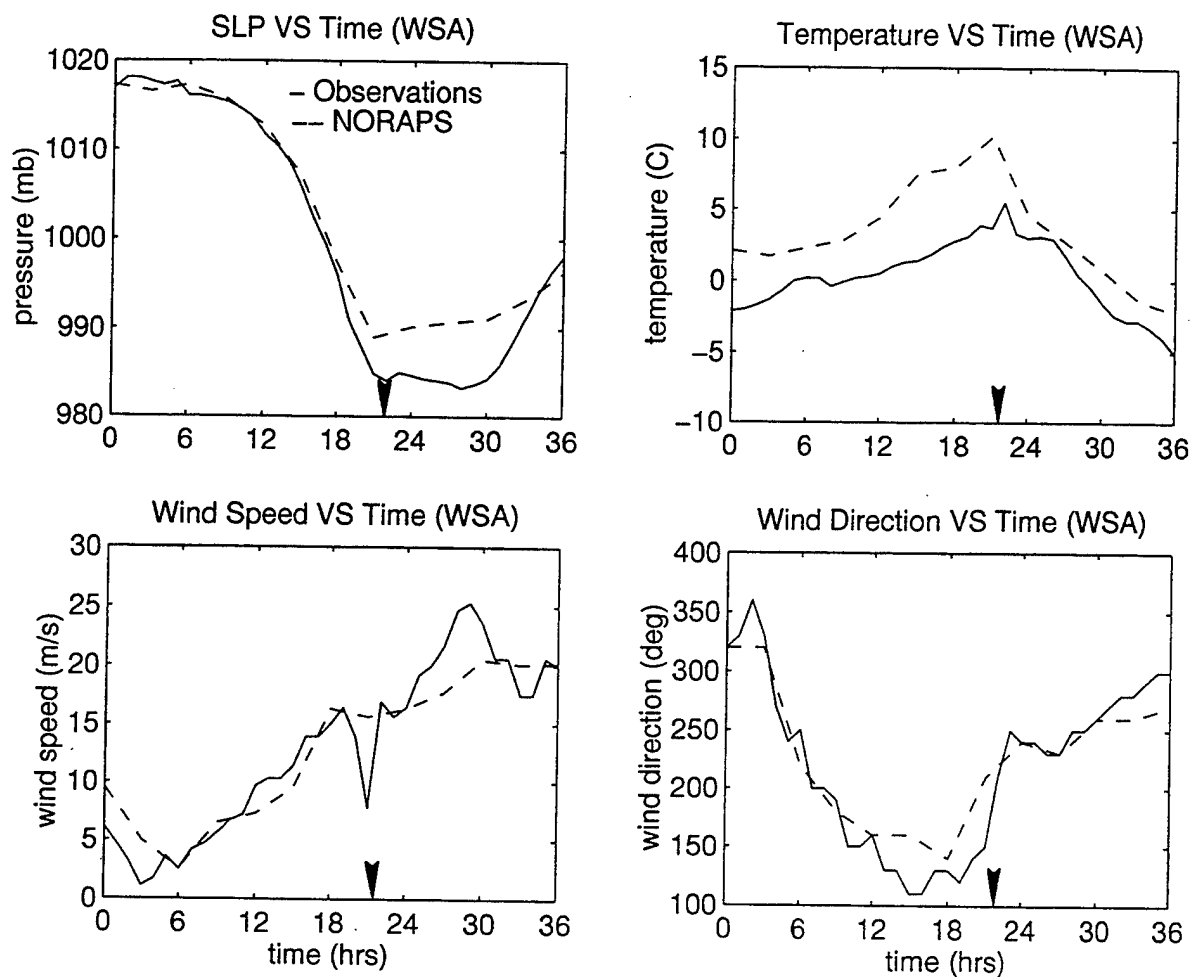


Figure 11. Time series comparisons from Sable Island (WSA) during cold frontal passage: (a) sea level pressure (mb); (b), temperature (1°C); (c), wind speed (m/s); (d), wind direction (degrees).

analysis of the coarse grid NORAPS model performance in simulating ERICA IOP 5A.

Although it is evident that the overall performance of the coarse grid NORAPS model in predicting the rapid cyclogenesis was successful, a higher resolution model was used to investigate the mesoscale features of IOP 5A. In comparing the forecast fields against observations, it is shown that the latest version of NORAPS demonstrated considerable skill in forecasting the mesoscale features of IOP 5A. Moreover, the model simulation provides a high resolution and dynamically consistent data set. Therefore, it will be used in the subsequent analyses of the structure, development and evolution of IOP 5A.

IV. MESOSCALE EVOLUTION

The following sections present the IOP 5A cyclone development and frontal evolution in three stages: the incipient development stage (20/1200Z - 21/0000Z); the explosive development stage (21/0000Z - 21/1800Z) and the mature cyclone stage (21/1800Z-22/0000Z). Six hour surface temperature and pressure analyses (MQI) are presented in Fig. 12 along with the NORAPS 6 h forecasts for the same periods. Frontal evolution will be described to address specific details of IOP 5A's frontal life cycle from its incipient phase through warm-core seclusion. The frontal analysis is based on a detailed examination of the surface observations obtained from the ERICA dataset.

The rate of change of the gradient of potential temperature following a parcel is used to examine the kinematics of the simulated frontogenesis. The horizontal frontogenesis function in pressure coordinates is defined as:

$$\begin{aligned} \frac{d}{dt} |\nabla_p \theta| = & \nabla_p \theta^{-1} \left(- \left[\left(\frac{\partial \theta}{\partial x} \right)^2 \frac{\partial u}{\partial x} + \left(\frac{\partial \theta}{\partial y} \right)^2 \frac{\partial v}{\partial y} \right] - \left[\frac{\partial \theta}{\partial x} \frac{\partial \theta}{\partial y} \left(\frac{\partial v}{\partial x} + \frac{\partial u}{\partial y} \right) \right] \right. \\ & \left. - \left[\left(\frac{\partial \theta}{\partial x} \right) \left(\frac{\partial \theta}{\partial p} \right) \frac{\partial \omega}{\partial x} + \left(\frac{\partial \theta}{\partial y} \right) \left(\frac{\partial \theta}{\partial p} \right) \frac{\partial \omega}{\partial y} \right] + \left[\frac{\partial \theta}{\partial x} \frac{\partial}{\partial x} \left(\frac{\partial \theta}{\partial t} \right) + \frac{\partial \theta}{\partial y} \frac{\partial}{\partial y} \left(\frac{\partial \theta}{\partial t} \right) \right] \right). \end{aligned} \quad (1)$$

For this study only, the confluence and shear terms, the first two terms on the right hand side of the equation, will be used to estimate $d/dt |\nabla_p \theta|$. The remaining terms were not found to be significant. The 1000 mb level of the NORAPS model was used to produce fields of surface frontogenesis. In addition, model vertical soundings will be evaluated and compared

to actual soundings observed during the experiment. Model cross sections will also aid in determining frontal position and structure.

There remains significant interest in frontal evolution as noted in Neiman and Shapiro (1993), Mass and Schultz (1993), and McGinnigle (1988). In addition, forecasting the structure and development of sub-synoptic scale features in coastal areas remains a difficult task, largely because timely synoptic observations end at the shoreline. Even with special collection efforts such as the ERICA study, large ocean areas or sparsely populated land areas may not be adequately sampled, leaving large gaps where significant mesoscale activity may develop. In an effort to combat the sparsity of data, gridded data sets are often used in place of unverified analyses. Therefore, this study utilizes a data base consisting of hourly NORAPS forecast fields augmented with the special data available from the ERICA studies. The ability of the high resolution model to resolve the mesoscale features and frontal evolution of a rapidly deepening cyclone will continue to be documented with detailed model station soundings and cross sections compared with the observed fields.

A. INCIPIENT DEVELOPMENT STAGE (20/1200Z-21/0000Z)

Horizontal surface analysis of pressure and temperature with associated frontal positions are presented in 6-h intervals to illustrate the cyclone's mesoscale frontal structure during this period (Figs. 12a,c,e,g,i,k,m) (left panels). NORAPS simulated fronts are also depicted (Figs. 12b,d,f,h,j,l,n) (right panels) for comparison. The 36-h analyzed and forecast storm track shown in Fig. 9 depicts sea surface temperatures valid at initialization. Of particular note is the strong temperature gradient marking the Gulf Stream off the coast of North Carolina. The ice edge is also present further north along the coast of eastern Quebec

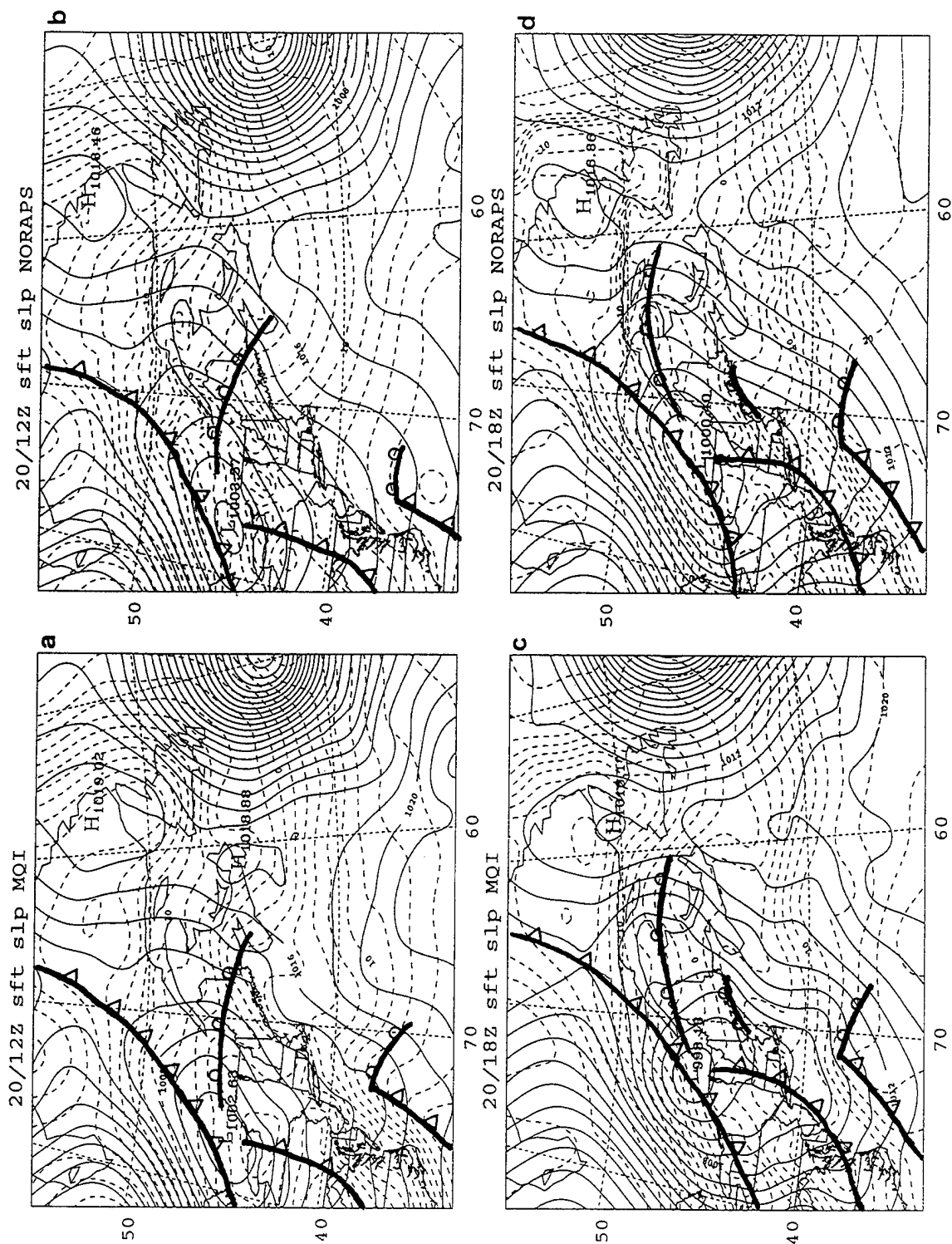


Figure 12. Six-hourly surface MQI analyses (left panels) and NORAPS forecasts (right panels) of pressure (mb, contour interval 2 mb) and temperature (dashed, contour interval 2° C) for 20 January 1989; (a-b) and (c-d), 1200Z and 1800Z respectively, 21 January; (e-f), (g-h), (i-j), and (k-l) 0000Z, 0600Z, 1200Z, and 1800Z respectively, (m-n) 22/0000Z January 1989. Fronts (conventional symbols) are also depicted.

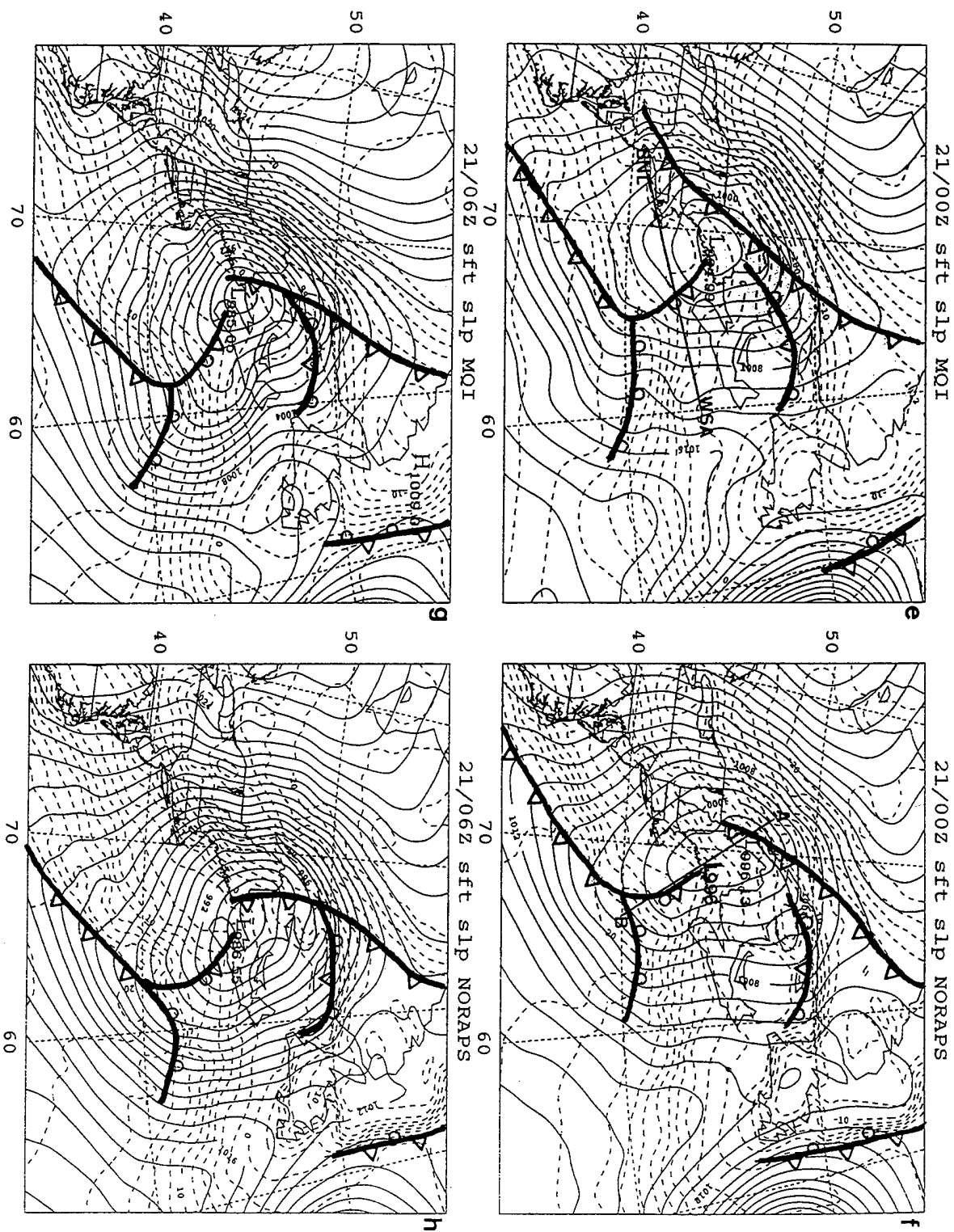


Figure 12.. (Continued)

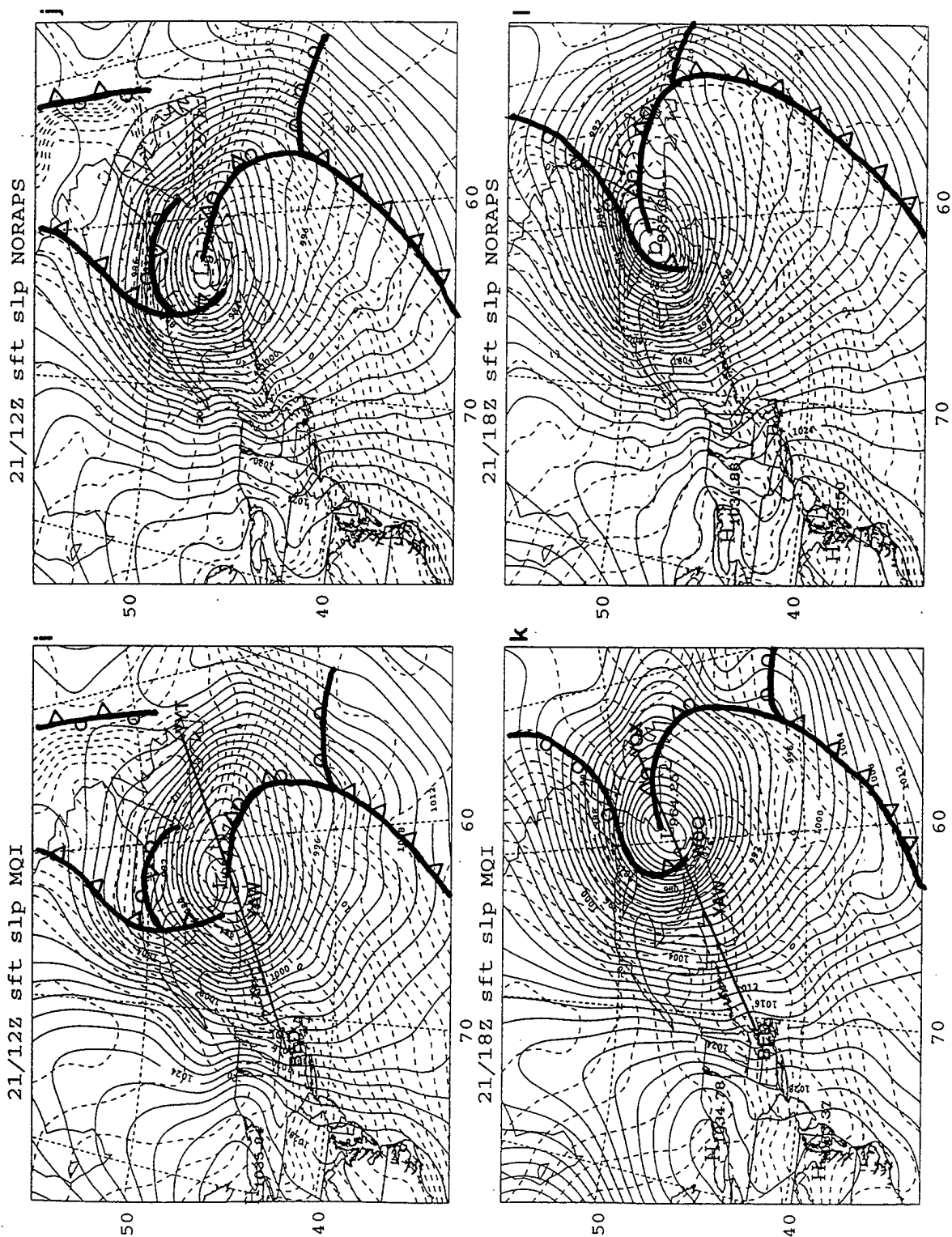


Figure 12.. (Continued)

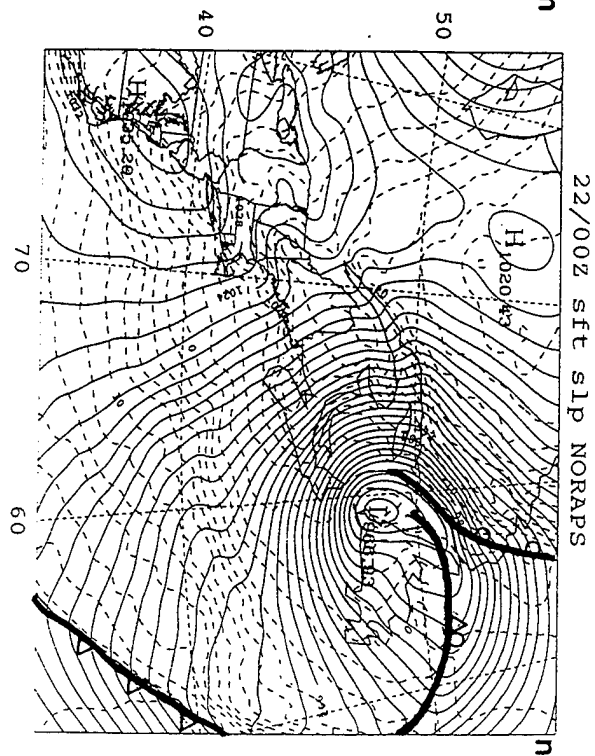
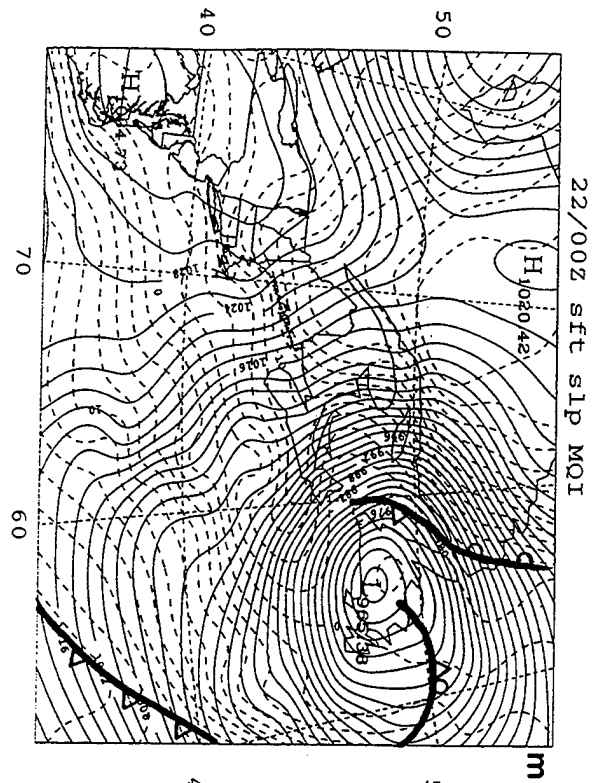


Figure 12.. (Continued)

and continuing south to the tip of Newfoundland. Not depicted is the broken ice coverage in the northern portion of the Gulf of St. Lawrence near the coast of southern Quebec.

At the beginning of the period (Fig. 12a), the surface low is located just north of Lake Ontario with a central pressure of 1003 mb. Further to the east, the IOP 5 storm is weakening southeast of Newfoundland. A complex pattern with four distinct baroclinic zones are evident. In addition to the primary warm and cold fronts associated with the incipient IOP 5A cyclone, a pre-existing Arctic front extends southwest from central Quebec, upstream of the low through Michigan, Illinois and ending in northeastern Missouri (full extent not shown). This front is very intense north of the Great Lakes as evidenced by the tight temperature gradient. A weak northern warm frontal band extends from the low center, east through Quebec and into New Brunswick. The polar front extends south of the low along the pressure trough through western New York, central Pennsylvania, Virginia and across western North Carolina. This cold front is not clearly seen in the surface temperature analysis at this time, but is evident in the pressure pattern and is carried on operational NMC charts (not shown). Additionally, a pre-existing mesoscale coastal front off the North Carolina coast associated with strong sea surface temperature gradients is evident. A very weak warm front intersects the coastal front along the temperature ridge line and extends to the southeast. There is also a weak coastal front beginning to form along the southern coast of Maine, which extends to Massachusetts. There is a warm tongue along the Southeast Coast. This feature, along with the Arctic and polar fronts are evident at 850 mb as well (Fig. 13).

By 20/1800Z, the low center moves east and deepens five mb to 998 mb (Fig. 12c). The northern portion of the Arctic front moves east at 20 kts and catches up with the surface

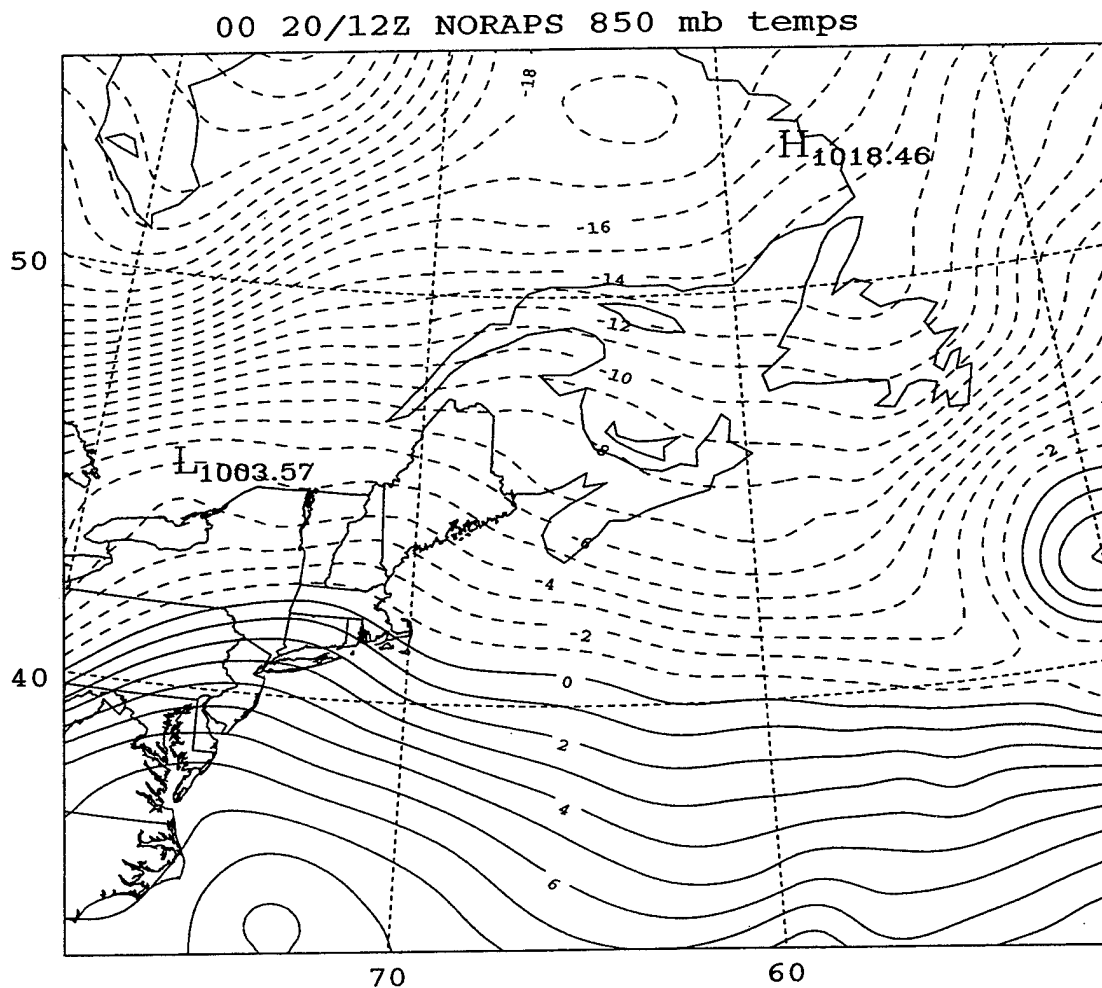


Figure 13. 850 mb temperature (solid, positive values, dashed, negative values, contour interval 1°C) valid at 20/1200Z January 1989.

low in southern Quebec. The portion of the front southwest of Lake Ontario began to dissipate. A weak warm front is still evident north and east of the surface low. This front intersects the Arctic front at the low position in southern Quebec and extends east, crossing New Brunswick into the partially ice covered Gulf of St. Lawrence. The polar front pushes east and extends southwest into South Carolina. The thermal packing of this front is more noticeable at this time. The coastal front and associated warm front are notably stronger as well. Figure 14 depicts surface frontogenesis at 6 h intervals starting at 20/1200Z and ending

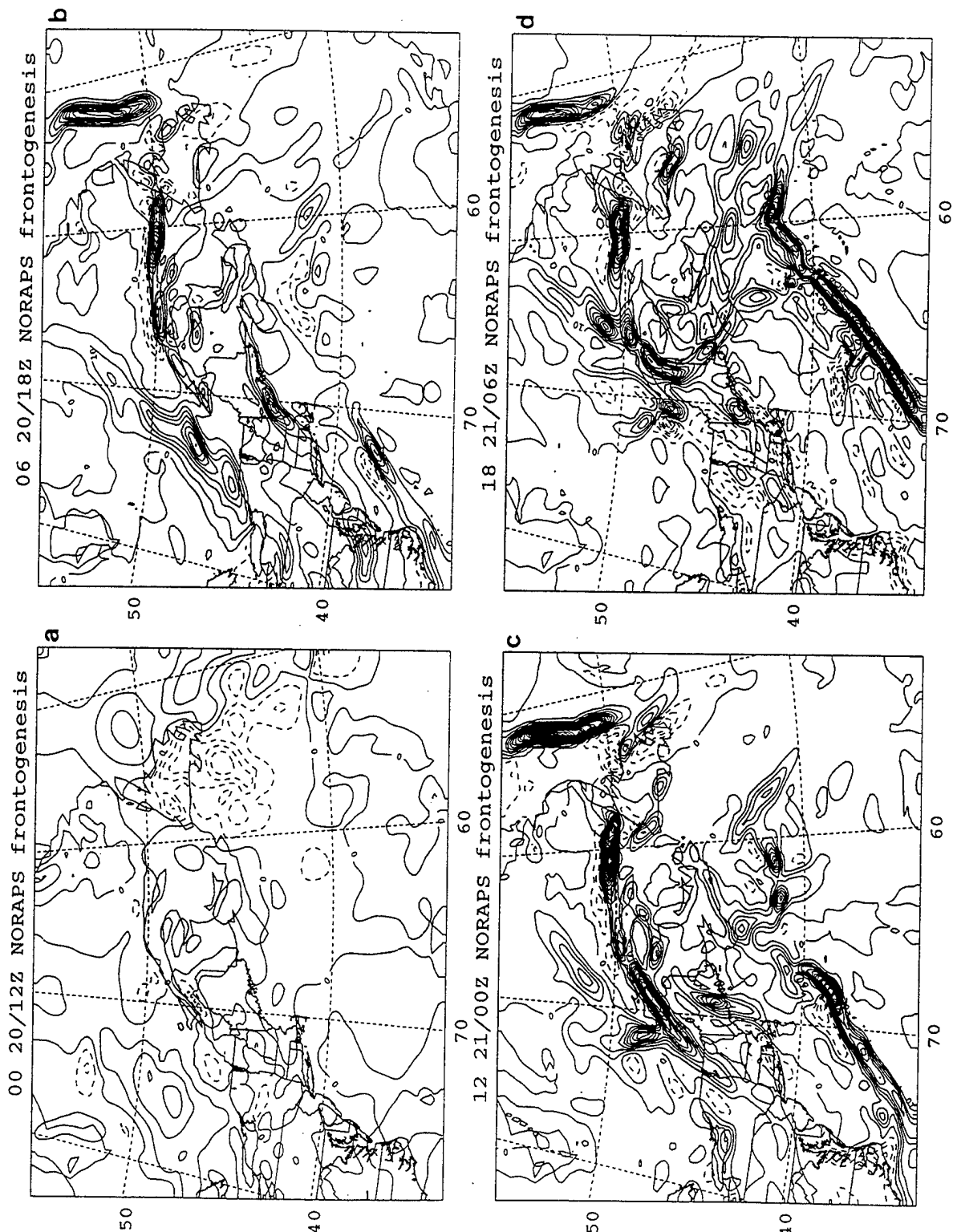


Figure 14. Surface frontogenesis (solid, positive values; dashed negative values; contour interval $5^{\circ}\text{C}/\text{day}/100\text{ km}$) at 6-h intervals of the modeled storm at (a) 0, (b) 6, (c) 12, (d) 18, (e) 24, (f) 30, and (g) 36 h into the simulation.

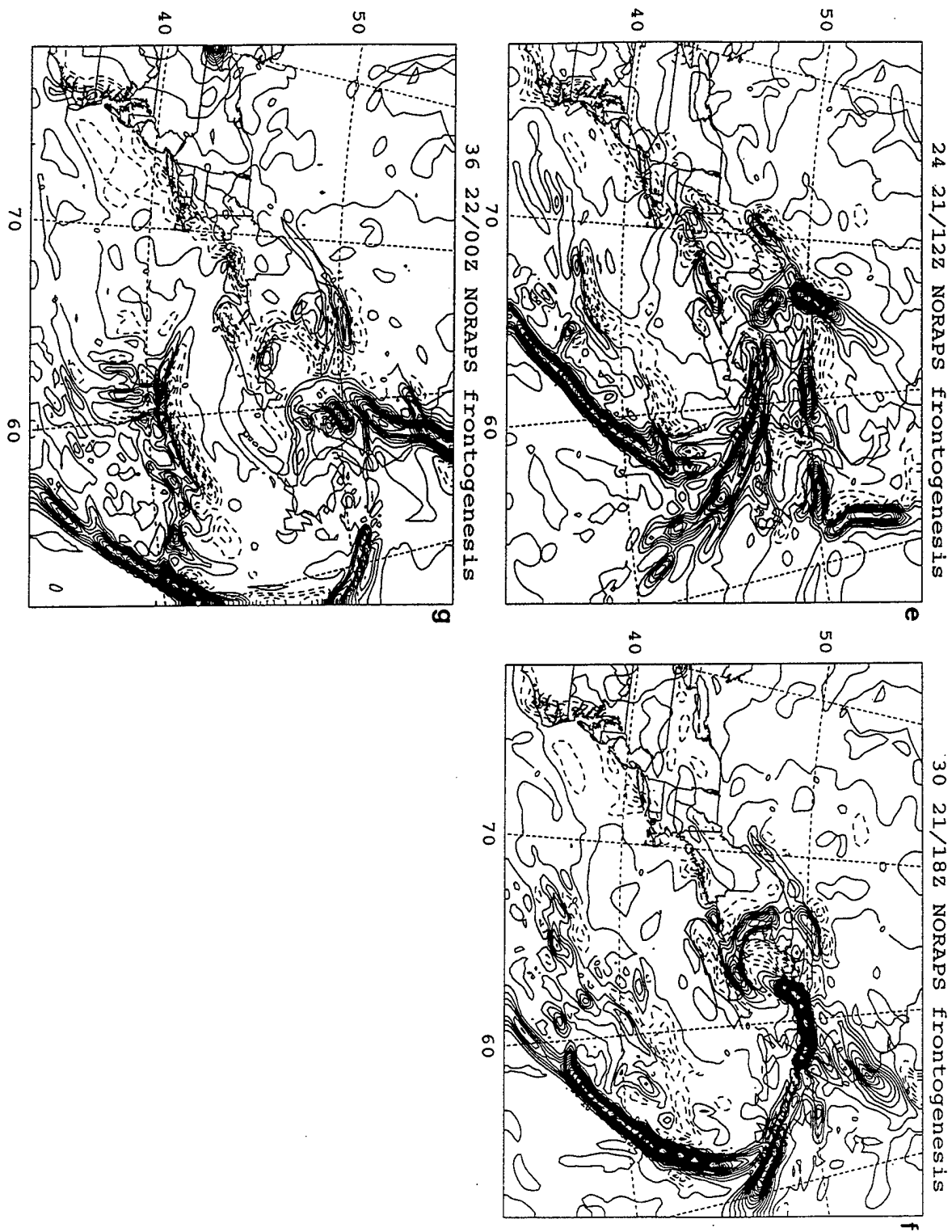


Figure 14. (Continued)

at 22/0000Z. Figure 14b shows five areas of positive values. These areas correlate directly with the locations of the Arctic front; polar front, the associated warm front; the two coastal fronts off the Virginia coast and southern Maine; and the strongly baroclinic ice edge off eastern Canada to the north. The NORAPS depicts the location of each of these fronts well. Of particular note is how well NORAPS represents the position and thermal packing behind the polar and coastal fronts. The analysis puts the polar front in the pressure trough just ahead of the thermal packing located in southeastern Virginia. Further east there is a weakening of the thermal gradient just off the coast and then the thermal gradient strengthens behind the coastal front. NORAPS shows these features well. Satellite imagery (Fig. 15) at 20/1801Z is in agreement with the position of both fronts and shows the distinct separation of the comma cloud mass associated with the incipient low and polar front to the north and the cloud mass to the southeast associated with the coastal front.

By 21/0000Z, the synoptic-scale low moves to the southeast and is positioned over central Maine with a pressure of 995 mb. The mesoscale details associated with this movement will be discussed shortly. Rapid deepening of the storm is now beginning to occur. The Arctic front has moved east as well (Fig. 12e) and is located just west of the low. Over the last 6 h, the polar front has weakened considerably and has combined with the coastal front, which has intensified over the western North Atlantic to form an occlusion. This occlusion is classified as a warm occlusion since the coldest air is ahead of the warm front. This newly combined frontal system will be referred to as the synoptic cold front hereafter. The synoptic warm frontal boundary associated with this cold front can clearly be seen in the isotherm field and on the surface frontogenesis chart as a separate area of

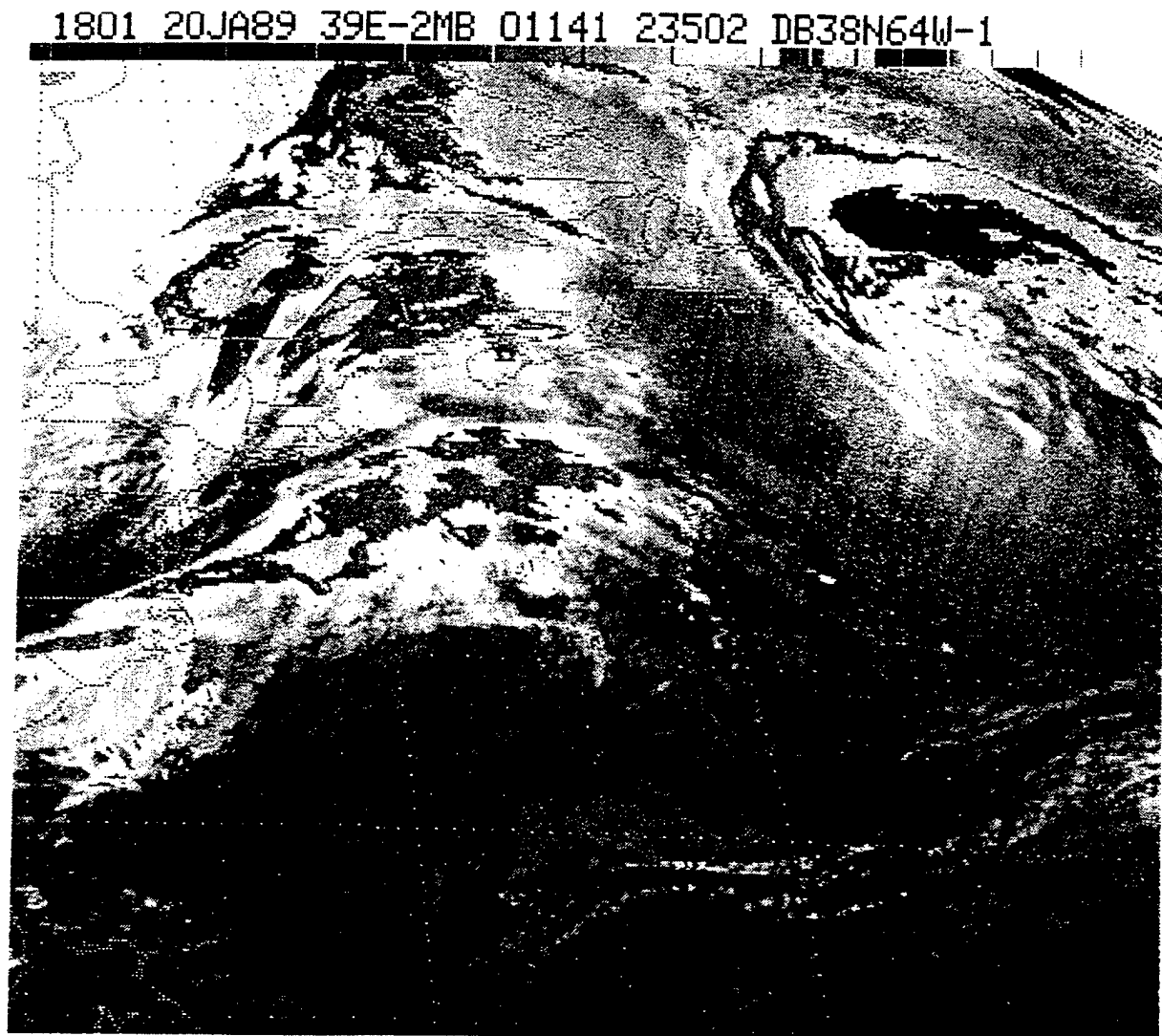


Figure 15. Goes enhanced IR satellite imagery at 20/1801Z January 1989.

positive values (Fig. 14c). The surface frontogenesis also indicates that the previous synoptic warm frontal band associated with the incipient low has now moved along the intensifying baroclinic zone along the northern Gulf of St. Lawrence and southern Quebec and become stationary. This increased intensification of the baroclinic zone in the northern portion of the Gulf of St. Lawrence is due to greater convergence along the coastal mountain ridge

associated with the eastward moving cyclone.

An examination of the 21/0000Z 850 mb temperatures (Fig. 16) reveals that a distinct rotation of the thermal ridge over New England from a southwest-northeast orientation to a more north-south alignment had occurred over the last 6 h. The presence of the warm tongue has become more pronounced as can be seen by the 6° C contour line which now extends north of 40° N.

GOES infrared satellite imagery valid at 21/0001Z (Fig. 17) shows a distinct comma head with the largest cloud mass ahead of the low, over New Brunswick and southeast of Nova Scotia. A developing dry slot south of the cyclone is also evident. This mature comma cloud structure formed when the comma cloud pattern in the polar air upstream of the main frontal band merged with the main cloud mass associated with the old coastal front. The cloud mass merging and evolution during the early part of the rapid deepening is similar to the "instant occlusion" scenario as described by Mullen (1983). The cloud band in Fig. 17 shows a distinct western border marking the limiting streamline of the warm conveyor belt structure as described by Carlson (1980), which separates the dry and moist air streams.

The NORAPS forecasts of the temperature and wind in the vertical will now be assessed. To do this, a vertical cross section (Fig. 18) at 21/000Z from Brookhaven, Long Island (BNL) 40.9° N, 72.9° W to Sable Island (WSA) 43.9° N, 60.0° W is compared to the model cross section in Fig. 19. This section contains five stations and provides adequate resolution in the horizontal. The location of the cross section is indicated in Fig. 12e.

The left edge of the cross section in Fig. 18 depicts the weak coastal baroclinic zone southwest of the coastal low. The cross section depicts the occluded front near station N234.

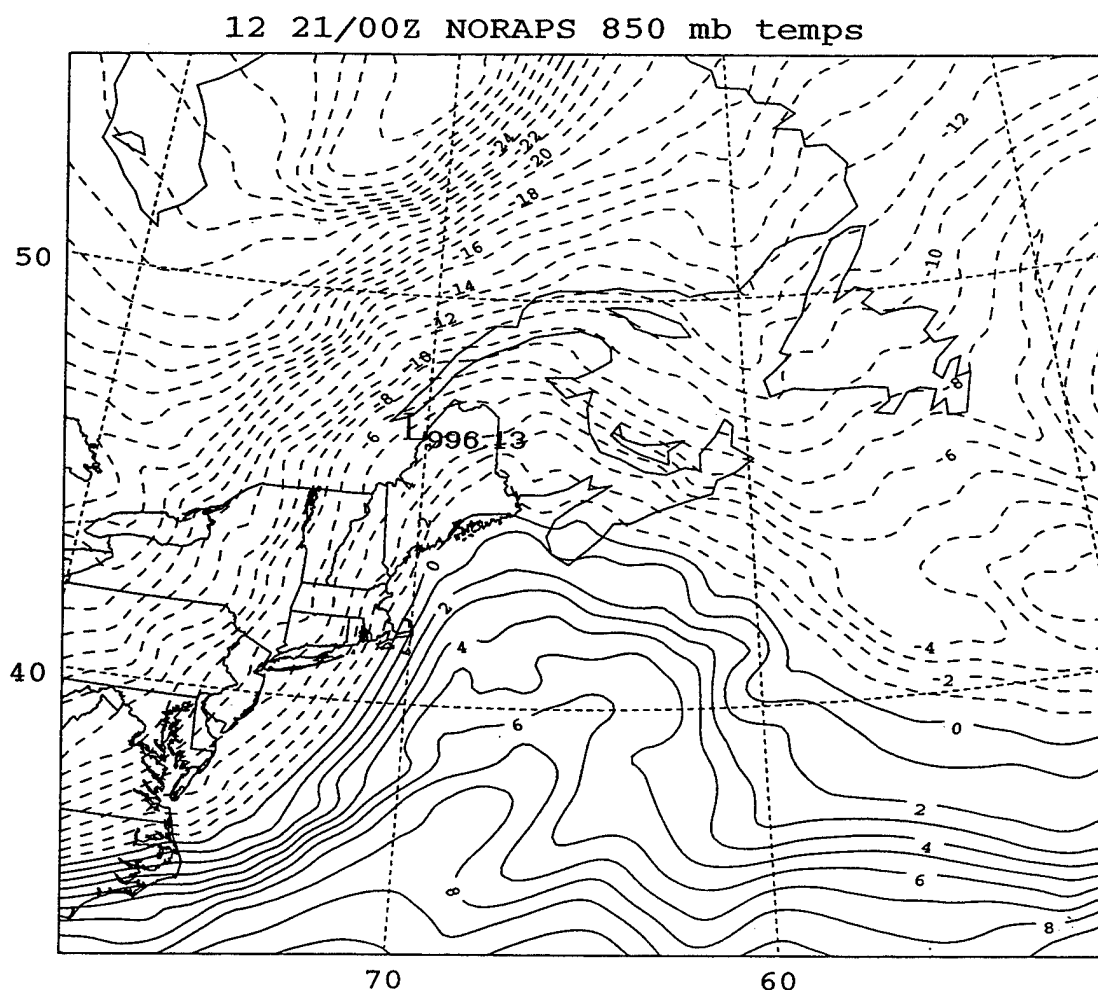


Figure 16. 850 mb temperature as in Fig. 13, except for 21/0000Z January 1989.

The nearly vertical theta lines in the western part of the cross section represent the leading edge of continental polar air that has now moved southward from eastern Canada. The location of the occlusion is clearly evident in the tongue of warm air near station N234 approximately 15 nm south of Maine. Further east, the cross section terminates in the lower theta air just north of the warm front. NORAPS moisture values indicate 80%-90% saturation in the vicinity of the warm tongue while the observed soundings only indicate 50%-80%. The model cross section (Fig. 19) describes all of these features generally well and of particular note is how well NORAPS handles the change in wind direction to the south at the

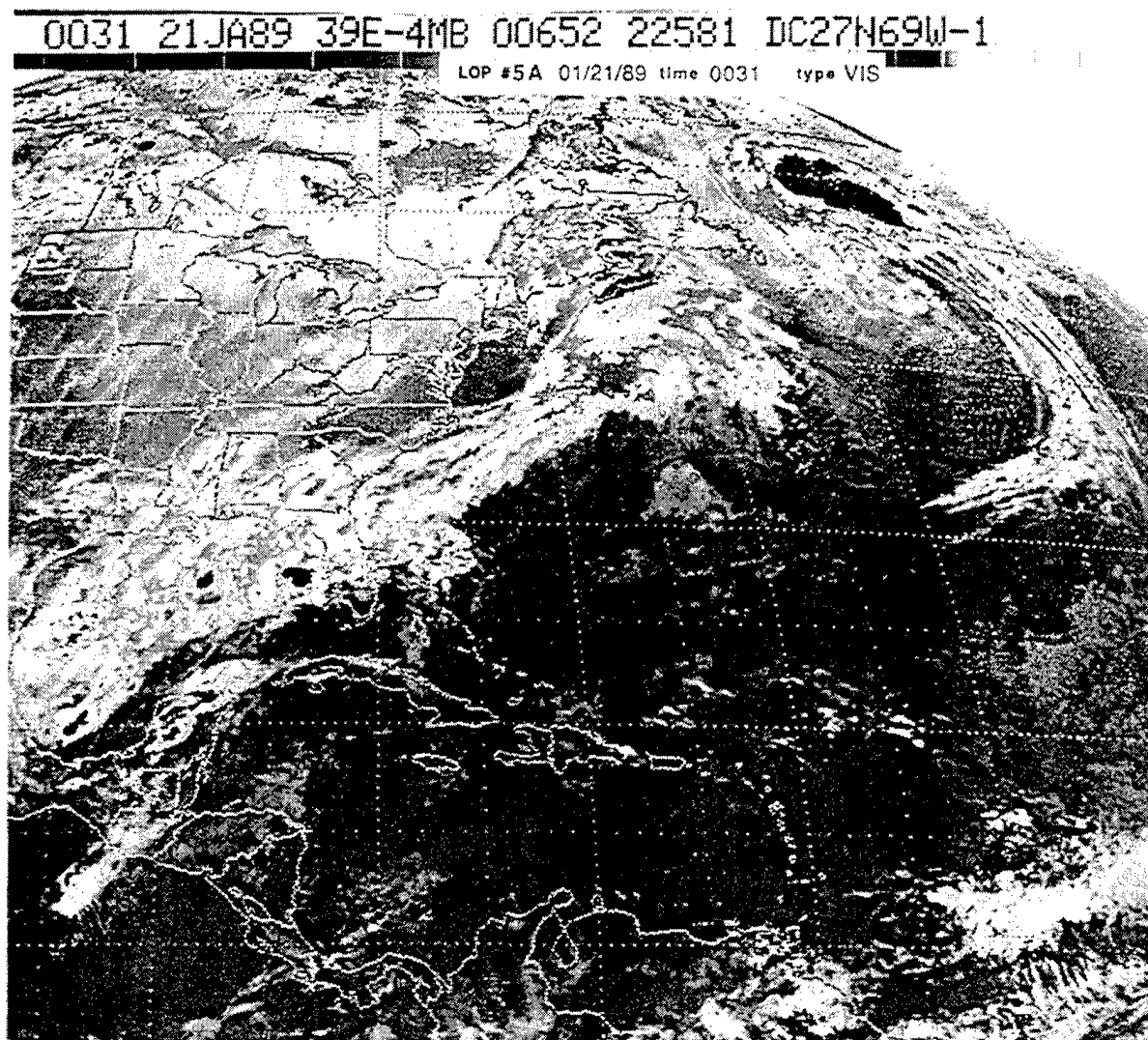


Figure 17. Goes enhanced IR satellite imagery at 21/0001Z January 1989.

base of the warm tongue.

The NORAPS forecast fields and satellite data illustrate the complexities and uniqueness of the IOP 5A cyclone. Specifically, this cyclone does not form along a single, broad baroclinic zone as discussed by Neiman and Shapiro (1993) or by Mass and Schultz (1993). In particular, the cloud and frontal analysis show several important pre-existing

baroclinic zones near the incipient cyclone, an intensifying coastal front with a distinct warm tongue to the south and a strong Arctic front present west of the low.

B. EARLY MESOSCALE DEVELOPMENT

Spinelli (1992) performed a subjective hourly hand analysis which revealed the presence of a secondary low pressure center well to the southeast of the primary center just prior to explosive deepening (20/1500Z) (Fig 4). Her analysis of this secondary low provided the motivation for further analysis of this area using an objective technique. For this study, an objective analysis at 3 h intervals was performed on the data using the Multiquadric Interpolation technique as described by Nuss and Titley (1994). A mesoscale comparison of how well NORAPS forecast fields compared to MQI analyses was performed. Comparisons of the MQI analysis and the NORAPS model output with verifying observations are depicted in Fig. 20 for the period of 20/1200Z to 21/0300Z. The following discussion will focus on the MQI analysis (left panels) with comments on the NORAPS model (right panels) where they differ significantly.

From 20/1200Z to 20/1800Z (Figs. 20a, c,e) the primary IOP 5A low quickly tracked to the northeast at a speed of 35 kts and deepened from 1003 mb to 998 mb. At the same time, a developing low pressure area in southeastern New York also moved northeast and was located near 42.7N 72.5W (southern Vermont) at 20/1800Z. While the wind pattern did not indicate a cyclonic circulation, minimum pressure in the area dropped from approximately 1007 mb to 1002 mb during the 3 h period. The NORAPS depiction agrees well with the analysis through 20/1800Z.

From 20/1800Z to 20/2100Z the cyclone moved southeast to 45.5°N, 71.4° and

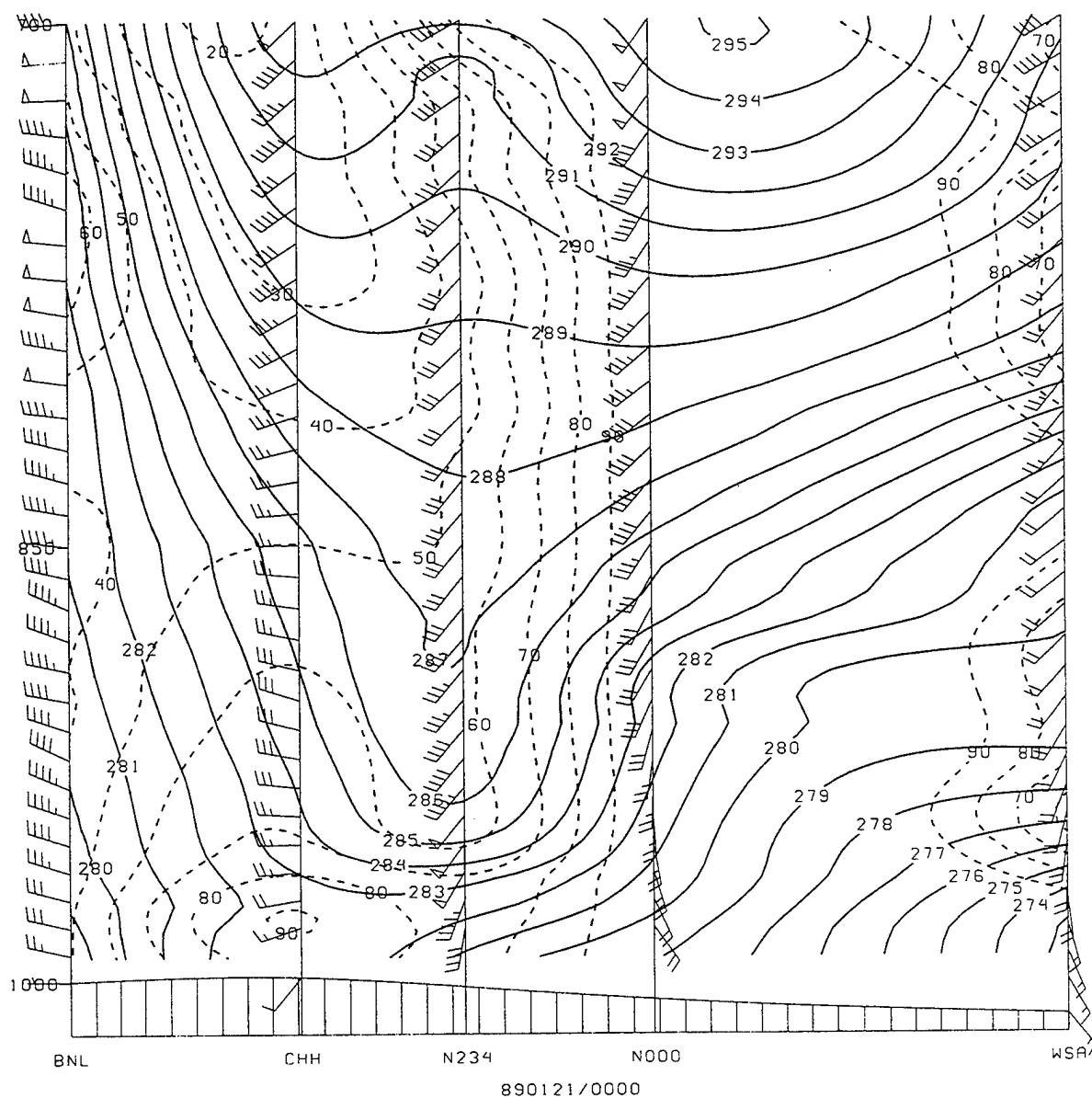


Figure 18. Analysis vertical cross section of potential temperature (solid, contour interval 1°K); relative humidity (dashed, contour interval 10%; wind barbs are at observation points) valid at 21/1200Z January 1989.

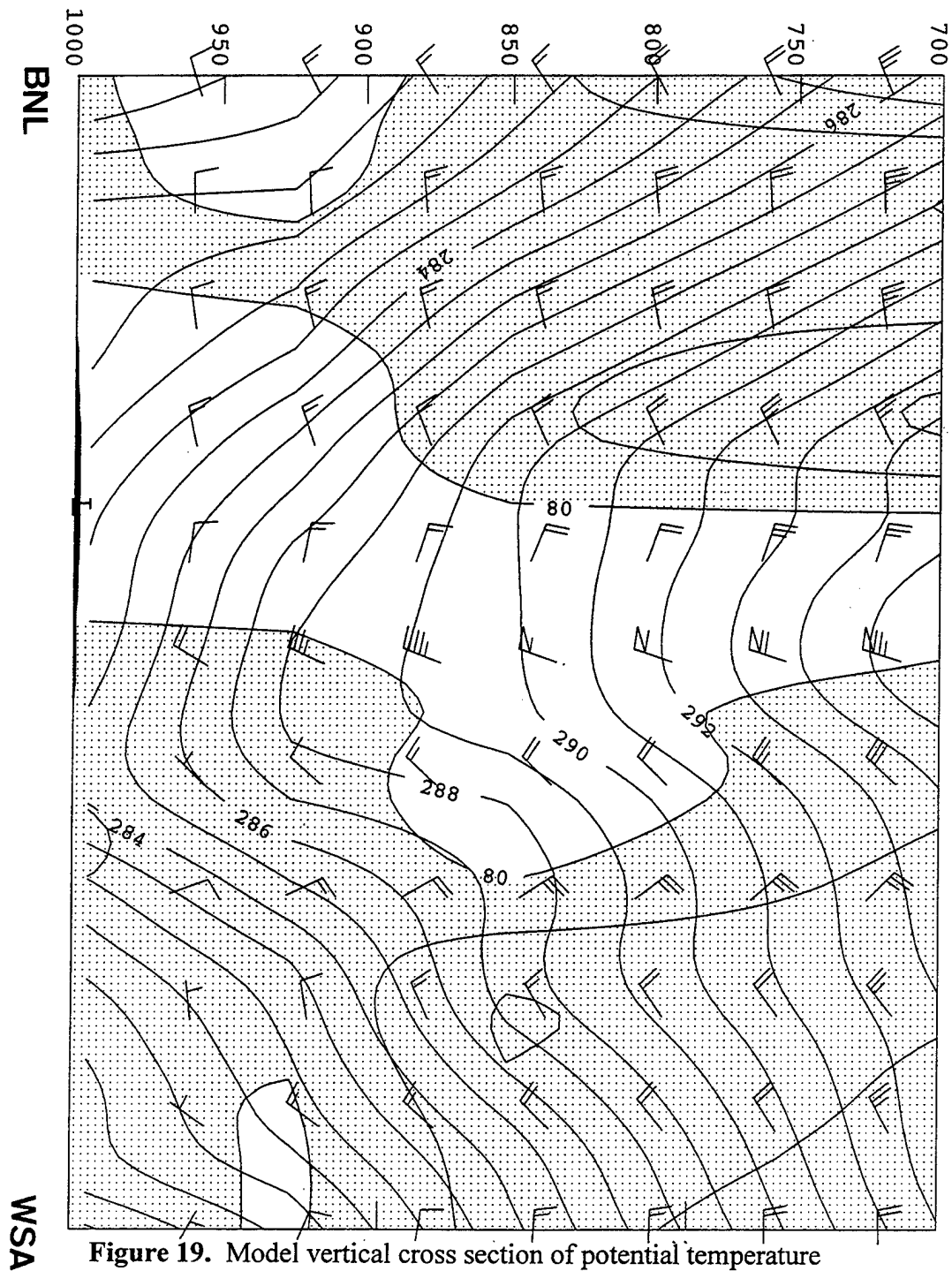


Figure 19. Model vertical cross section of potential temperature (solid, contour interval 1°K); relative humidity (stippled area > 80%) valid at 21/1200Z January 1989.

remained at 998 mb. The low pressure area to the south moved eastward to near the southwest corner of Maine and SLP dropped in the area down to 999 mb (Fig. 20g). This represents a deepening of $9 \text{ mb } 6 \text{ h}^{-1}$ for this coastal region. The observations now begin to indicate a cyclonic circulation, showing a distinct wind shift from northerly at Manchester Airpark, NH (MHT) to westerly at Beverly Municipal, MA (BVY) to southerly at the buoy IOSN with lowest pressures being reported by the coastal stations (station identification not shown).

The fine mesh NORAPS model did an exceptional job at forecasting the secondary cyclogenesis. The corresponding NORAPS depiction of the secondary development is best seen in Figs. 20 f,h. The area of broad troughing is very similar to the analyzed troughing 6 h into the simulation. By 20/2100Z, NORAPS develops a 1001 mb secondary cyclone near 43.3N 70.7W (southwest Maine), while the MQI analysis is showing a strong pressure trough with approximately 999 mb for the area. Although 2 mb weak in pressure, NORAPS does an excellent job in positioning the new low just 25 nm northeast of the cyclonic circulation evident in the observations previously described. Although this low is not specifically indicated in the analysis, the analyzed pressures for this area are more representative of the observations. Due to the univariate nature of the MQI analysis, it may not have been capable to place a low center there based only on the pressure field. NORAPS continues to move the northern primary cyclone to the northeast and deepens it to 998 mb. Based on the topography (Fig.21), and the sub-synoptic scale flow in the area, it is likely that this secondary low pressure area is a result of lee cyclogenesis on the lee side of the northern Appalachian Mountains.

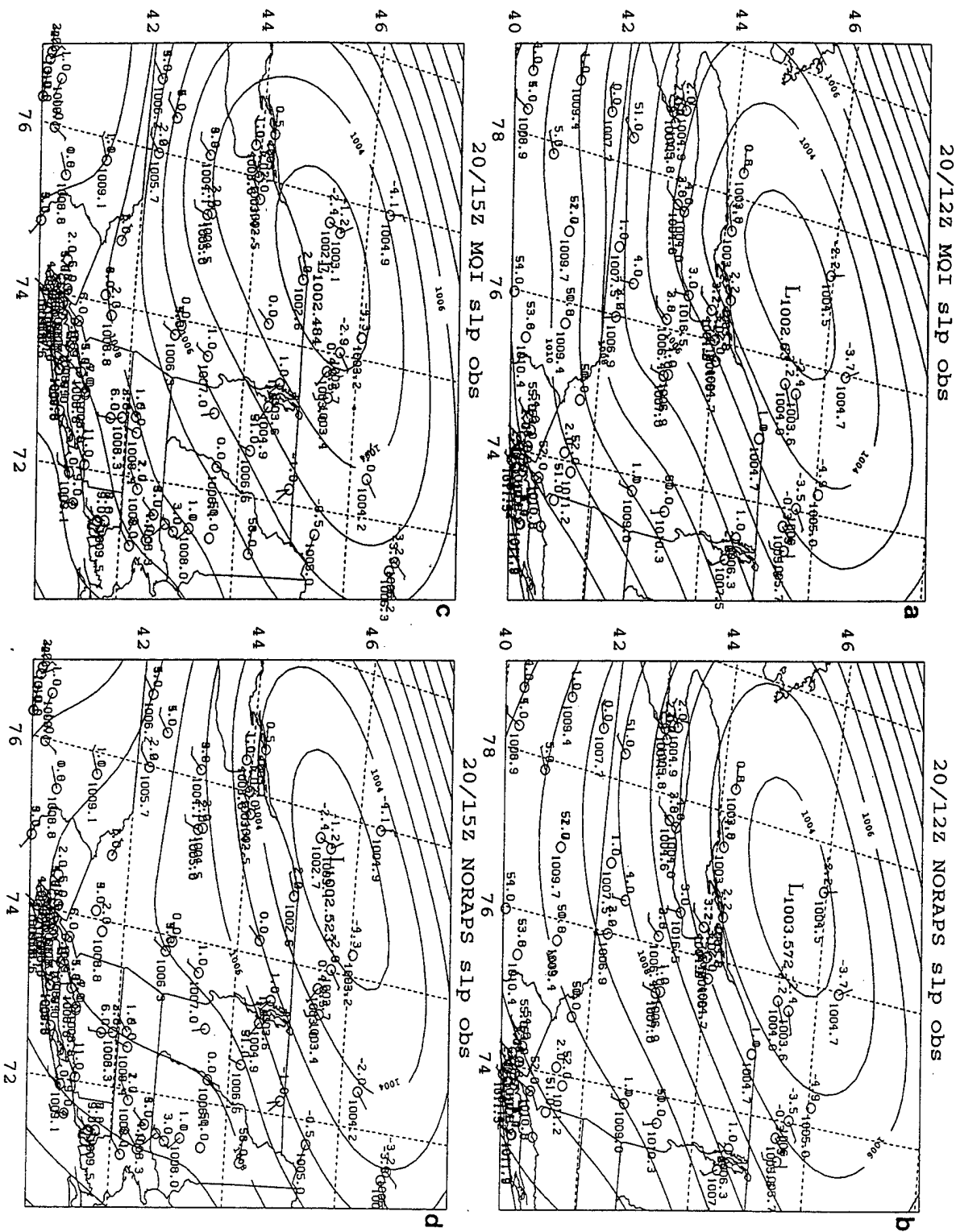


Figure 20. Three-hourly surface MQI analyses (left panels) and NORAPS forecasts (right panels) (isobars, solid, contour interval 1 mb) with verifying observations 20 January 1989; (a-b), (c-d), (e-f), and (g-h) 1200Z, 1500Z, 1800Z, and 2100Z respectively, 21 January; (i-j), (k-l), (m-n), 0000Z, 0300Z, and 0600Z, respectively. Six-hour intervals: 21 January; (o-p) and (q-r) 1200Z and 1800Z respectively, (s-t) 22/0000Z January 1989.

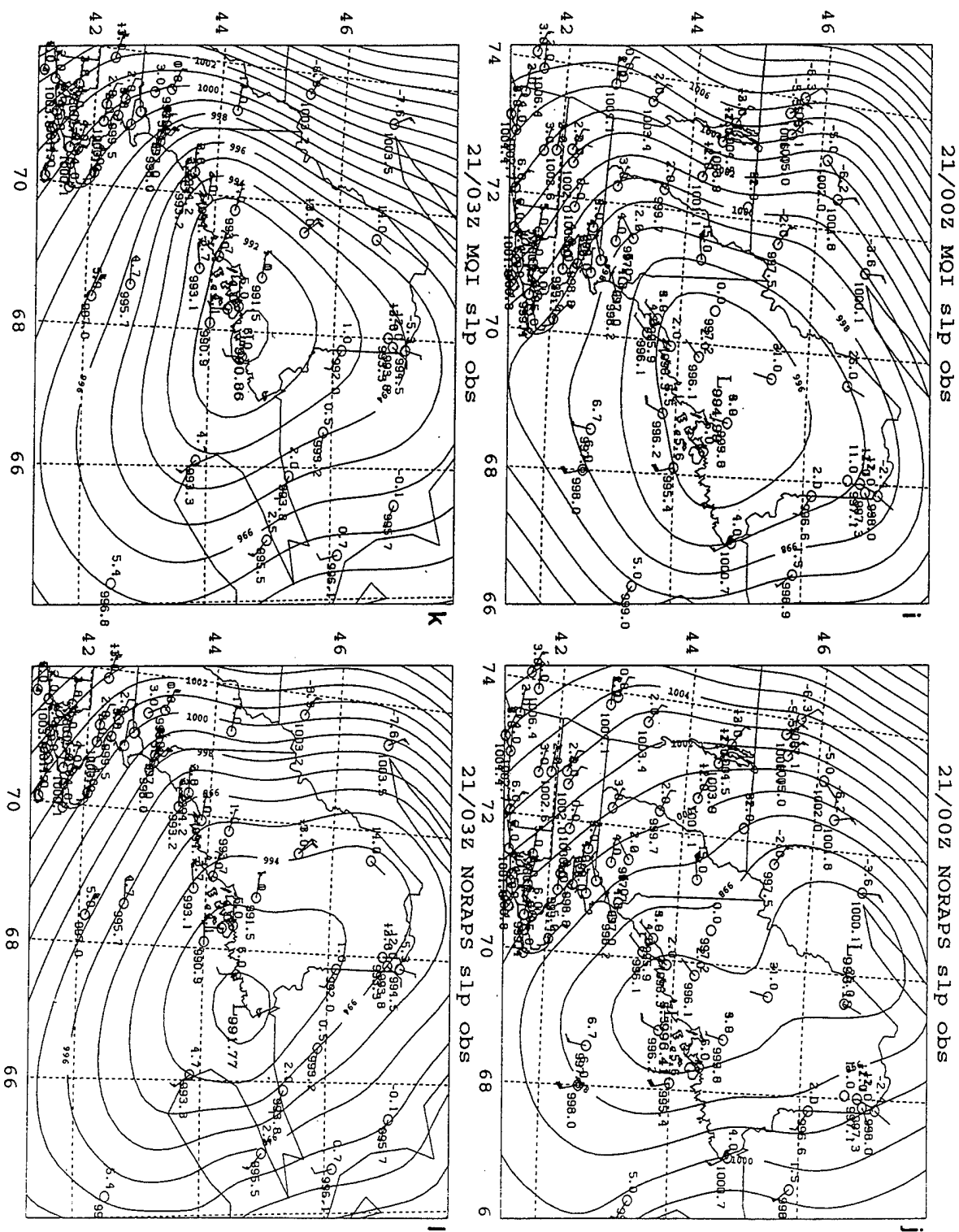


Figure 20. (Continued)

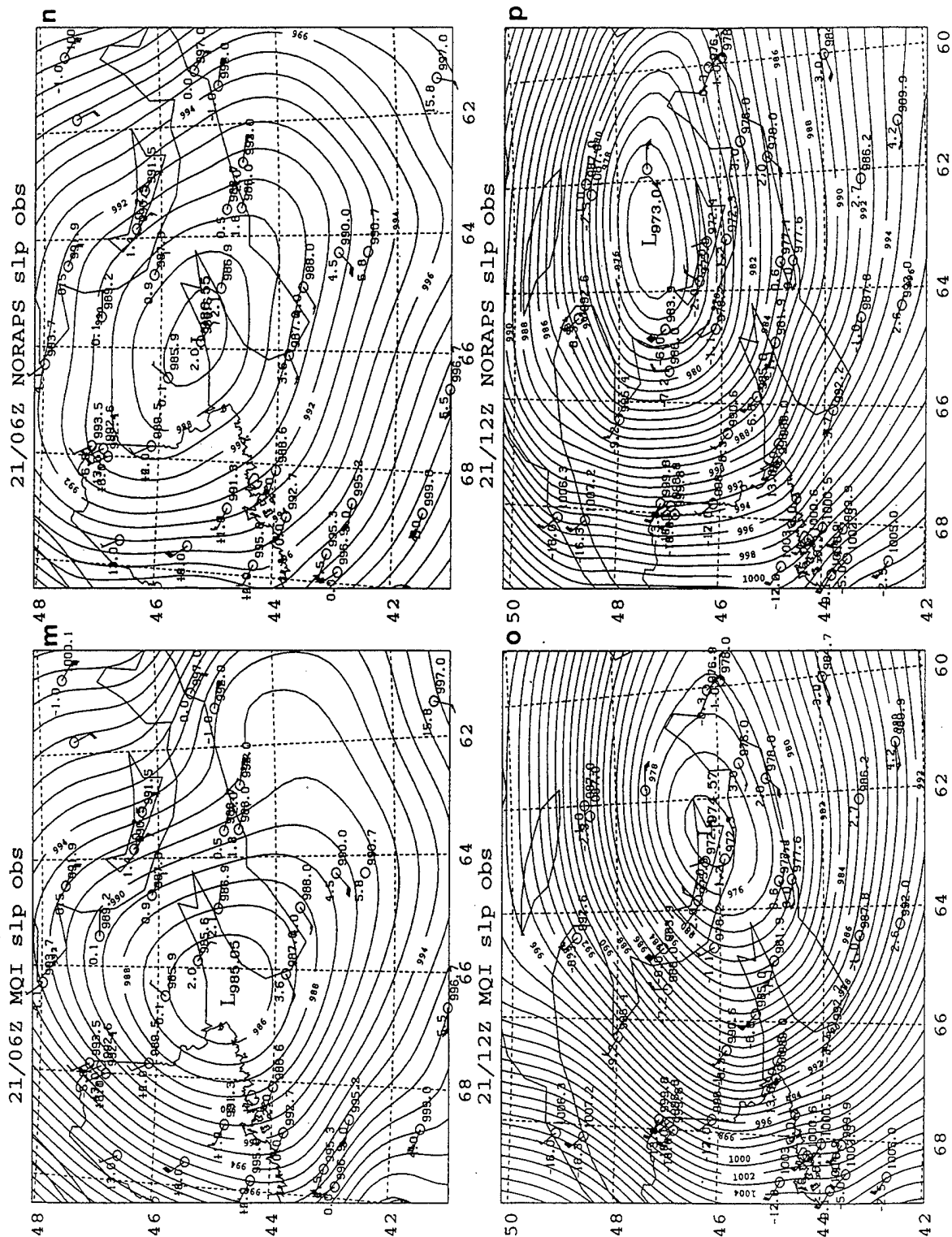


Figure 20. (Continued)

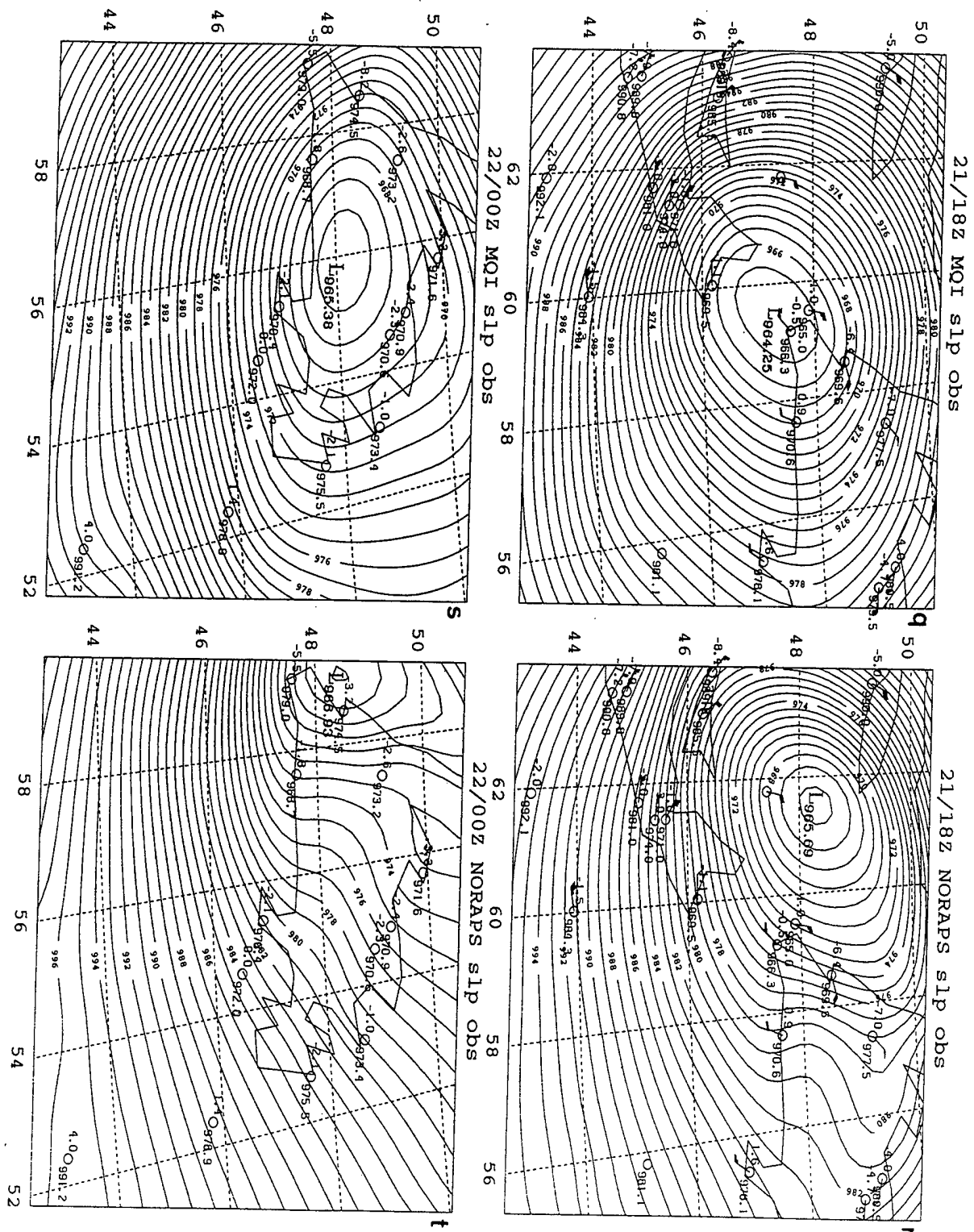


Figure 20. (Continued)

As shown in Fig.21, the ridge line of the mountain range runs southwest to northeast along the northwest Maine border. From 20/2100Z to 21/0000Z, the primary cyclone appeared to "jump" over the mountains to the southeastern side of the ridge near 44.8N 69.5W (central Maine) by 21/0000Z (Fig.20a). This indicates a speed of movement of approximately 25 kts. The central pressure dropped 2 mb to 995 mb by this time. However, it is not clear as to whether this low jumped across the mountains to combine with the lower pressure area near the coast, or dissipated while the secondary low pressure area developed into the primary IOP 5A cyclone. The sparse data in this mountainous area may make it impossible to conclusively determine which scenario best fits.

NORAPS static stability fields for the time period 20/1500Z to 21/0000Z (Fig. 22) depict a significantly lower static stability over the New England coastal region than what was over the primary IOP 5A cyclone's path north of New York, Vermont and New Hampshire. This reduced static stability along the coast favors continued development of the coastal low pressure area. By 21/0000Z, NORAPS moves the northern low to the east near 46.6N 70.5W and deepens it to 996 mb. The coastal low continued to track along the coast to near 44.0N 69.2W. This position places it approximately 35 nm south of the analyzed low. A northwest to southeast model cross section bisecting the secondary low along the coast at 21/0000Z is shown in Fig. 23. Evident in the cross section is the strong low-level winds crossing the northern Appalachian Mountains and the model low pressure area located on the leeward or coastal side of the mountains. A 66 m/s jet streak (into the paper) is seen at approximately 300 mb in the top right side of the figure. This position places the developing coastal low pressure system in a favorable position with the transverse circulation associated with the jet

steak as evidenced by the strong upward vertical motion over the low center (Uccellini et. al 1985; Wash et. al 1988).

From these detailed comparisons of the analyses and forecast model, it is concluded that IOP 5A evolved from two separate low centers that the NORAPS model portrayed in an accurate manner. Lee side cyclogenesis and strong upper-level forcing enhanced by a lower static stability likely played a role in the development of the secondary mesoscale low to the south of the primary cyclone. This low deepened rapidly and likely became the new IOP 5A cyclone. The ability of the high resolution NORAPS model to accurately forecast the secondary low confirms the speculation that previous failed attempts to model this low was due to a lack of adequate resolution.

C. EXPLOSIVE DEVELOPMENT STAGE (21/0000Z - 21/1800Z)

During this period, IOP 5A experienced its greatest intensification, deepening 31 mb in 18 h. From 21/000Z to 21/0300Z, the primary cyclone continued to move to the southeast to approximately 44.5°N 67.9°W and deepened 4 mb to 991 mb (Fig. 20g). NORAPS combined the two previous low centers to form the new IOP 5A cyclone at the entrance to the Bay of Fundy near 44.5°N, 67.0°W (Fig. 20h).

By 21/0600Z (Fig. 12g), the southern portion of the Arctic front has dissipated and is now located just west of the cyclone center. There is now a noticeable cyclonic rotation of the Arctic front towards the low center. The synoptic cold front continues to move east and the associated warm front pushes further to the northeast. The previous warm front intersects the Arctic front in New Brunswick and extends to the northeast into the Gulf of St.

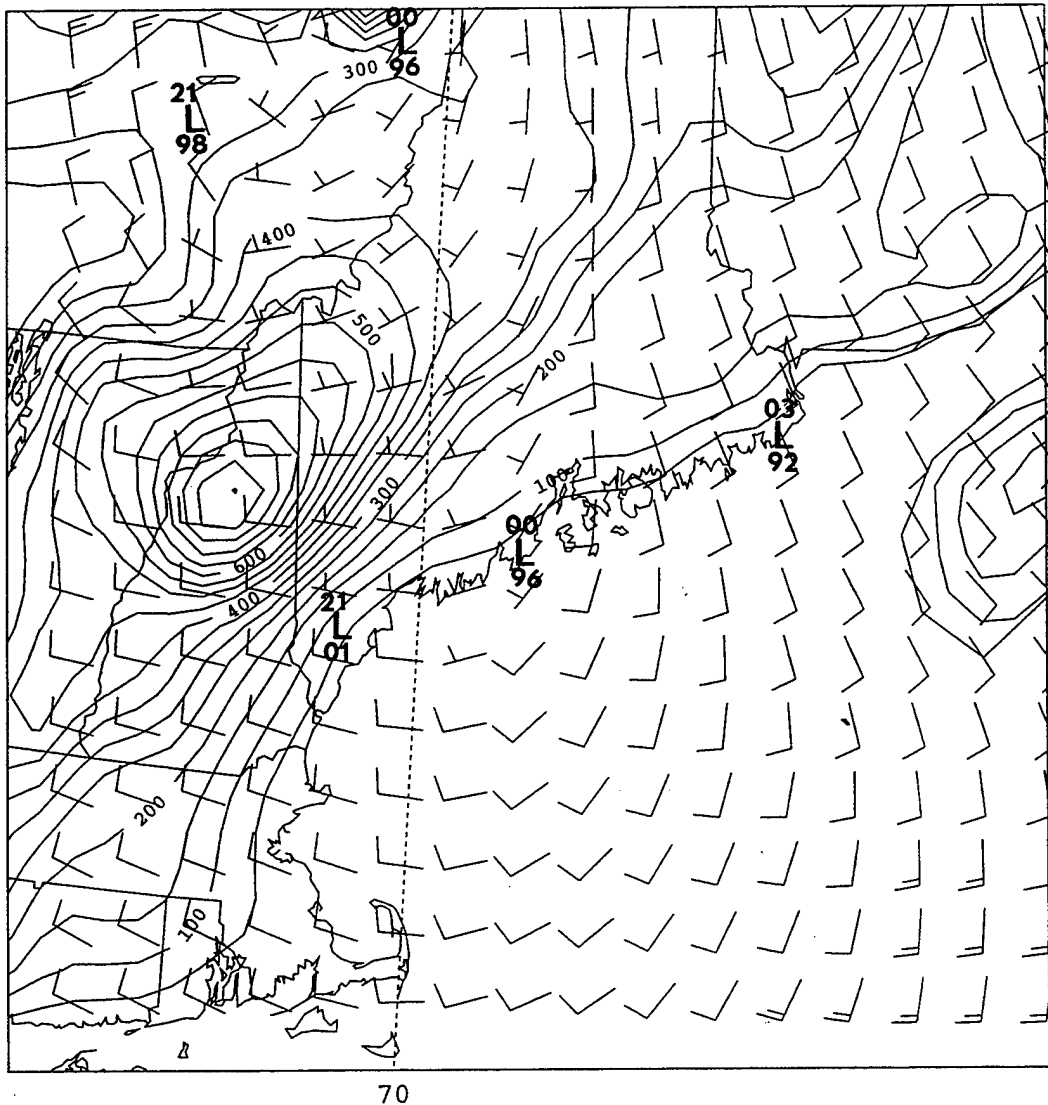


Figure 21. NORAPS surface terrain height (solid, contour interval 50 m) and wind flow for 21/0000Z January 1989. 3-h NORAPS surface cyclone positions (from 20/2100Z to 21/0300Z) with last two digits of sea level pressure (mb) are also displayed.

Lawrence. Cold-air advection northwest of the surface low continues to amplify the bent-back appearance of the isotherms at the 850 mb level (Fig. 24). The thermal ridge, north of 44°N shifted to a more southeast to northwest orientation due to the circulation about the cyclone center. Frontogenesis fields (Fig. 14d), shows an intensification of the synoptic cold

and warm fronts. The cyclonic curvature of the Arctic front is also evident in the frontogenesis field over northern Maine and New Brunswick.

Very strong cold-air advection accompanied by convective cloud lines in the 21/0601Z satellite imagery (Fig. 25) were present offshore from North Carolina to Massachusetts in the cold air behind the front. This area corresponds well with the large ($> 1600 \text{ watts/m}^2$) surface latent heat fluxes simulated by NORAPS in this area (Fig. 26). Not shown are the large dewpoint depressions observed in this area which suggests the potential for large latent heat fluxes. The limiting streamline along the western cloud boundary has continued to grow with colder cloud top temperatures evident over the warm conveyor belt during the last 6 h. A model cross section (location shown in Fig. 25), which bisects the northern portion of the warm conveyor belt is shown in Fig. 27. The stippled region are model saturated values ($> 80\%$). NORAPS does an excellent job in depicting the dry edge of the limiting streamline. The contrast in the moisture content of the two air streams is readily evident in the gradient of relative humidity across the limiting streamline, which separates the moister airstream ahead of the trough from the dryer air in the upper troposphere west of the trough.

By 21/1200Z, the IOP 5A cyclone had moved from the Bay of Fundy northeast to a position on the eastern side of Prince Edward Island in the Gulf of St. Lawrence. A deepening rate of 13 mb h^{-1} from 21/0600Z to 21/1200Z is observed, and the central pressure dropped to 975 mb (Fig. 12i). Two observations in the area of the MQI low report pressures as low as 972 mb (Fig. 20o). Thus, the NORAPS pressure of 973 mb appears to be more accurate (Fig. 12p). However, NORAPS positions the low approximately 60 nm north of

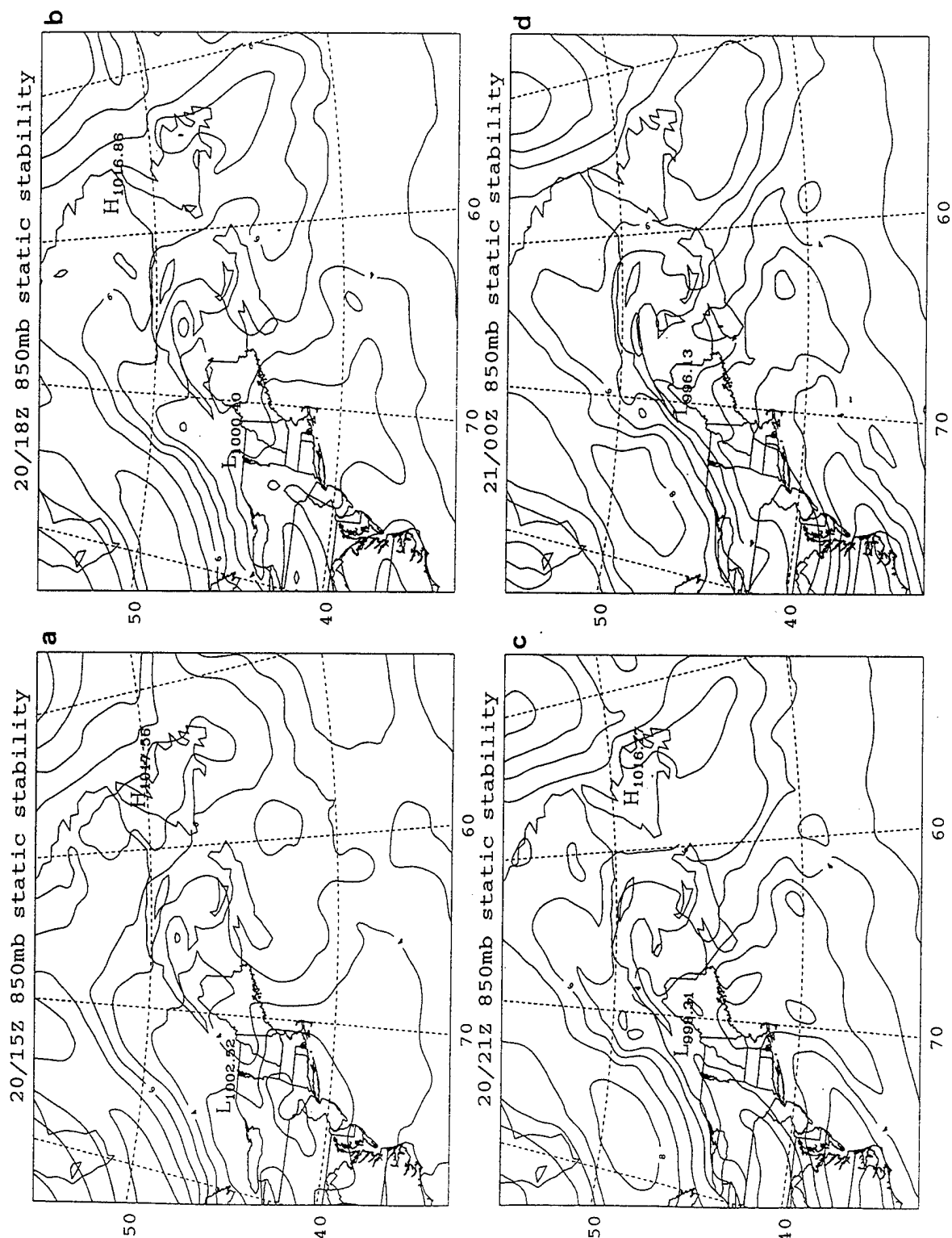


Figure 22. 850 mb model static stability ($1^{\circ}\text{K}/100\text{ mb}$) in 3-h increments from (a) 20/1500Z, (b) 20/1800Z, (c) 20/2100Z and (d) 21/0000Z January 1989.

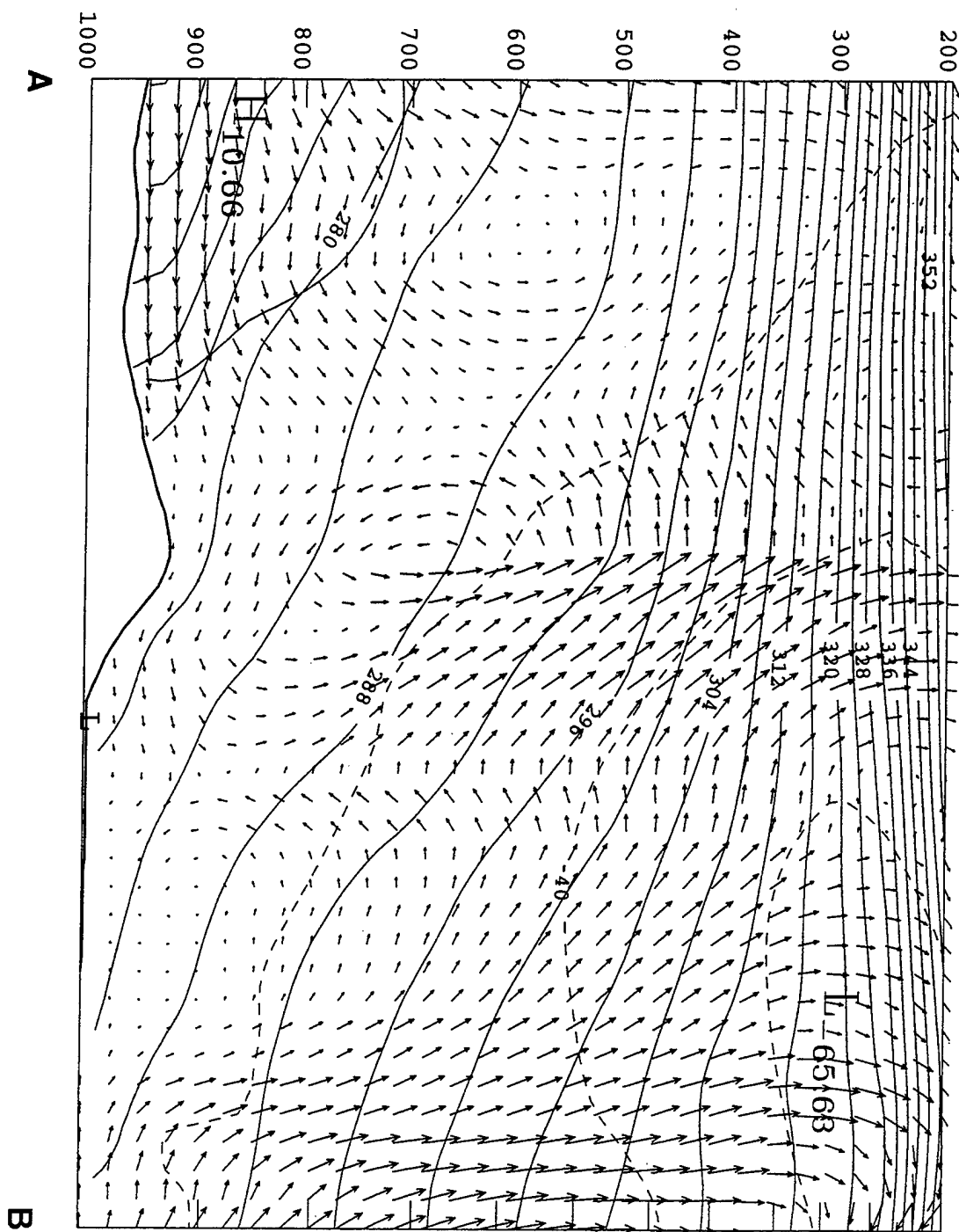


Figure 23. Model cross section of potential temperature (solid contour, K), section normal wind speed (contour interval 20 m s^{-1}) and cross section circulation vectors (m s^{-1}) along line AB of Fig. 12f at 21/0000Z January 1989.

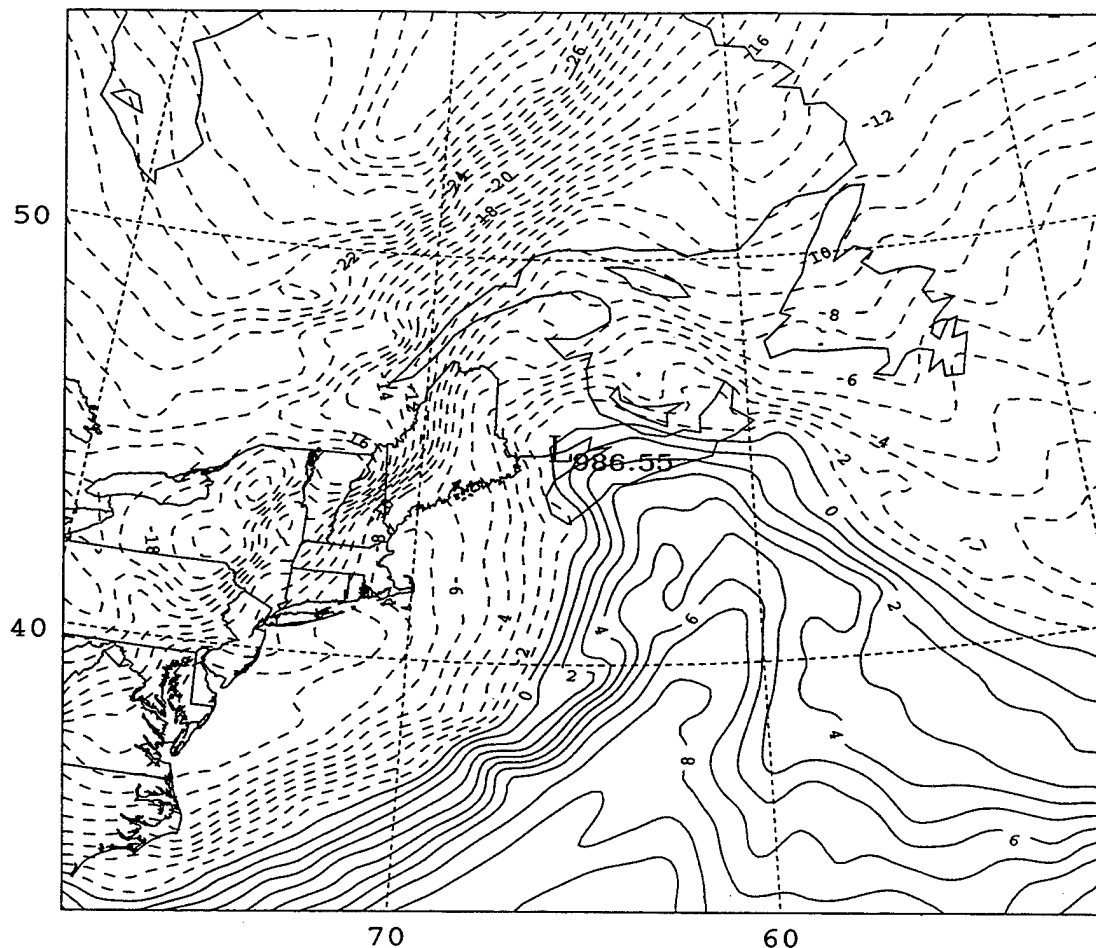


Figure 24. 850 mb temperature as in Fig. 13, except for 21/0600Z January 1989.

Prince Edward Island. The Arctic front continues to intensify and move east with a now pronounced cyclonic turning toward the low position. The synoptic cold front continues to move eastward with the occlusion nearly intersecting the Arctic front at the low position. The observations (Figs. 20 m, o) have been showing colder temperatures for the last 6 h ahead of the occlusion and warm front, verifying the warm occlusion classification. The surface temperature field south and east of the low center is showing a cyclonic rotation of the thermal ridge.

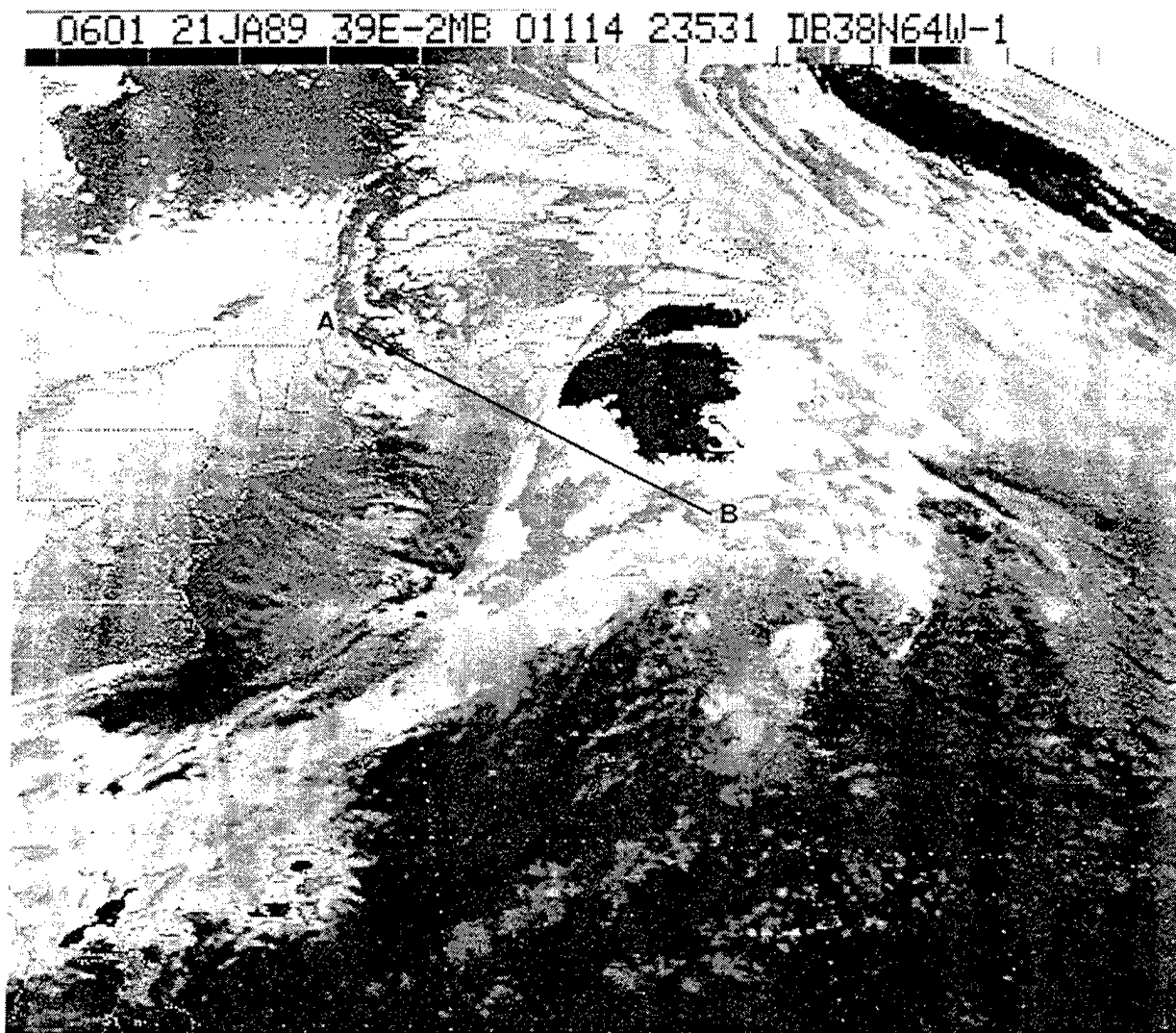


Figure 25. Goes enhanced IR satellite imagery at 21/0601Z January 1989

The rotation of the thermal ridge is more apparent at the 850 mb level as depicted by NORAPS (Fig. 28).

A fracture, or weakening of the surface temperature gradient along the northern portion of the cold front, similar to the Shapiro and Keyser (1990) T-bone model is becoming evident in the surface isotherm pattern. Similar weakening is also in the surface frontogenesis

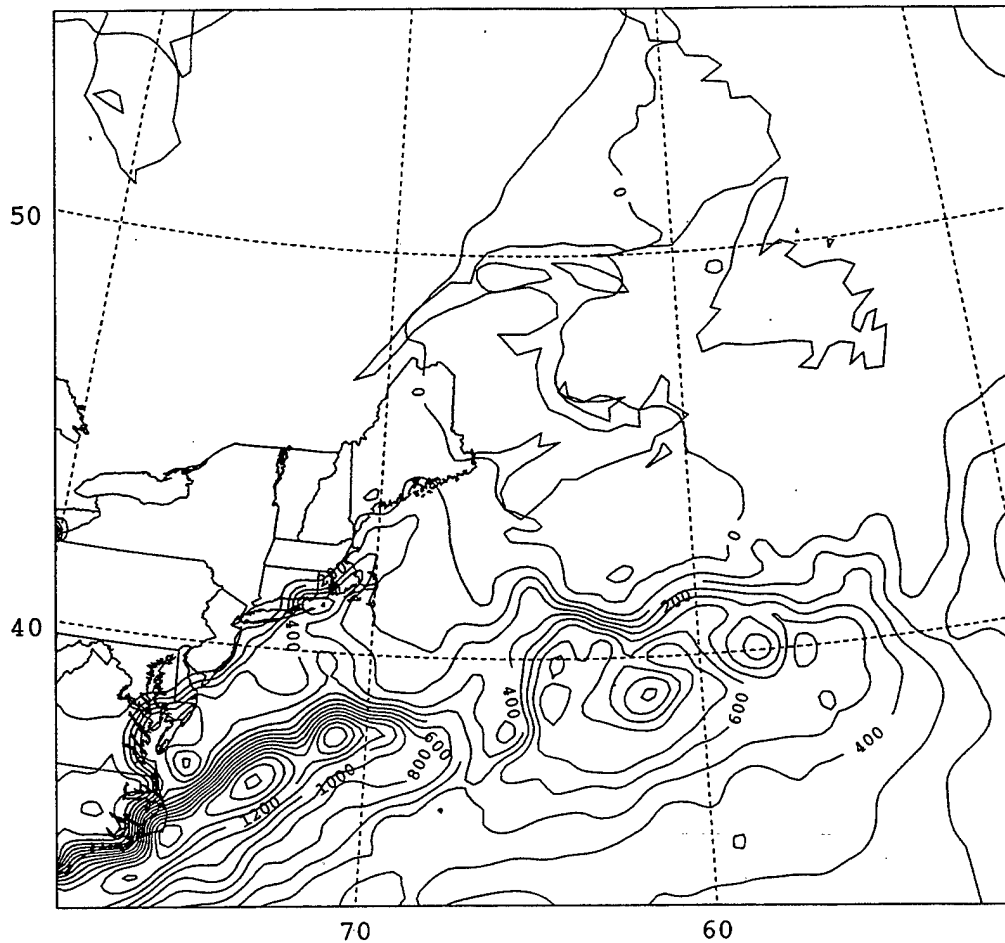


Figure 26. Surface latent heat flux (contour interval 100 watts/m²), valid at 21/0600Z January 1989.

fields (Fig. 14e). However, the position of the surface low west of this fracturing indicates that the cold front might be catching up with the warm front as seen by Mass and Schultz (1993), who found similar weakening of the Lagrangian frontogenesis field in the northern portion of the cold front, but found no similar fracturing of the surface thermal field for a continental cyclone case. However, above the boundary layer (800 mb) Mass and Schultz

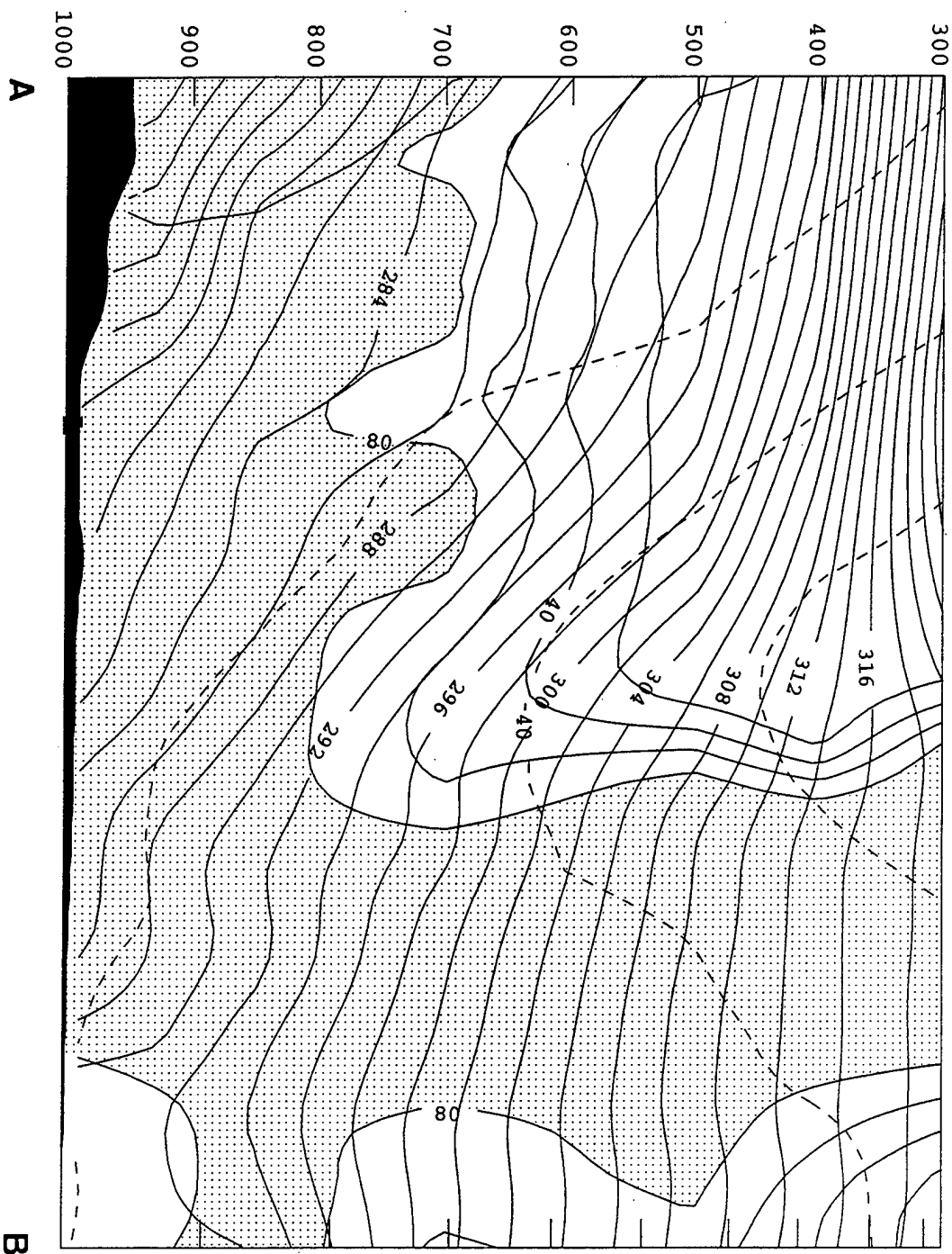


Figure 27. Model vertical cross section of potential temperature (dark solid, contour interval 2°K); relative humidity (light solid, contour interval 20%; stippled area $>80\%$); and section normal isotachs (dashed, contour interval 20 ms^{-1}) valid at 21/0600Z January 1989.

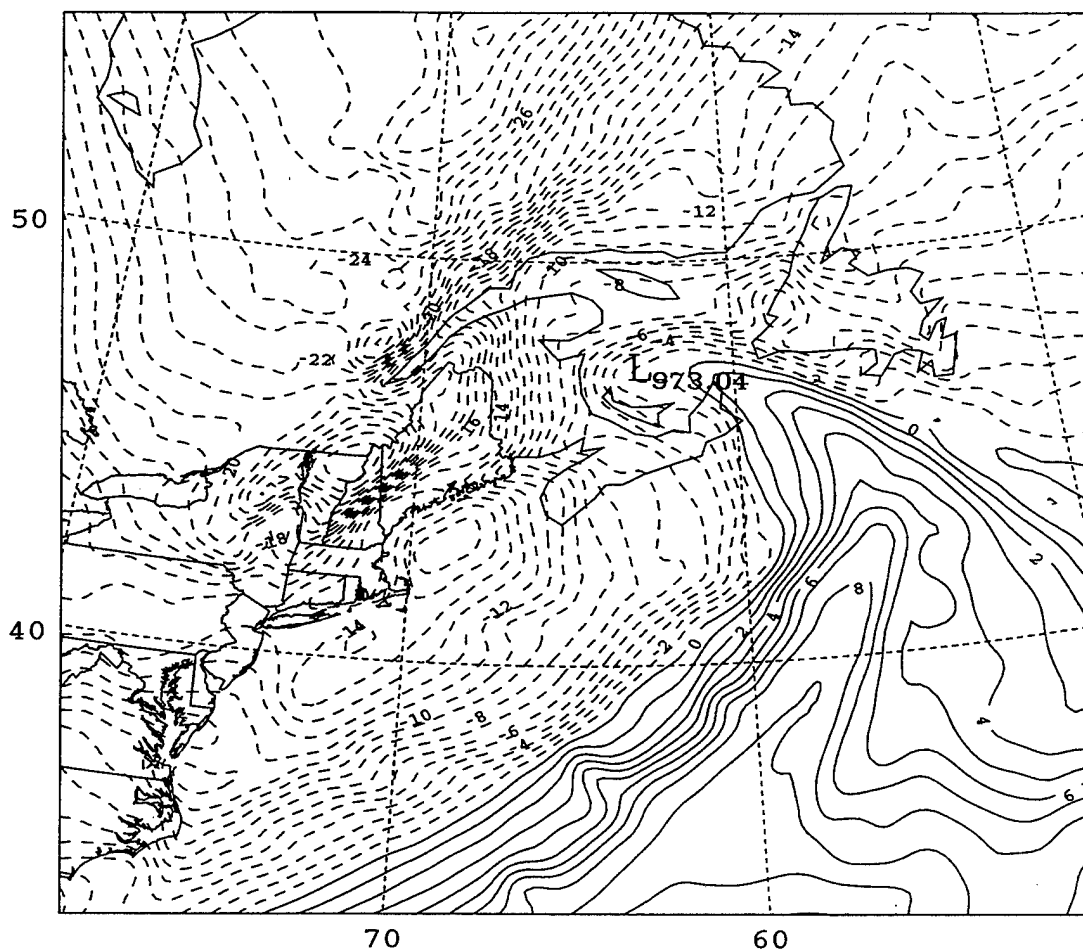


Figure 28. 850 mb temperature as in Fig. 13, except for 21/1200Z January 1989.

found similar thermal and frontogenetical structures to those of the T- Bone model of Shapiro and Keyser (1990). Mass and Schultz (1993) believe one possible answer for the differing surface structures is in the profound difference in the trajectories of air parcels within the cold and warm frontal zones. Another possible answer may be due to the enhanced friction over land, which contributes some frontogenetical forcing that helps maintain continental cold fronts near the surface. However, over the ocean, especially over the western basins during winter where there is a rapid modification of the cold air masses from the large surface heat fluxes, a frontolytic environment is produced. Thus, temperature gradients

within the area of weak frontogenesis along the northern cold front can attenuate rapidly, producing a fractured cold-frontal surface (Mass and Schultz 1993). Satellite imagery (Fig. 29) valid at 21/1201Z, shows a distinct mature comma head cloud with the largest cloud mass still well ahead of the low.

A vertical cross section at 21/1200Z from Bedford, Massachusetts (BED) 42.4° N, 71.3° W (Fig. 30) passes south of the surface low, crosses the warm tongue near station N111 then terminates at St. Johns, Newfoundland (YYT) 47.7° N, 52.8° W. The location of the cross section is shown in Fig. 12j. Starting from the east, this cross section verifies the location of the Arctic front to be between 850 mb and 800 mb near Halifax, Nova Scotia (YAW). This cross section continues to the northeast, intersecting the occluded front near station N111, approximately 10 nm southeast of Nova Scotia. NORAPS shows the Arctic front to be somewhat shallower between 850 mb and 925 mb (Fig. 31). Otherwise, both the observed and modeled cross sections are in excellent agreement with each other in the thermal structure. NORAPS moisture values show a deep moist tongue to 925 mb east of the occlusion. This structure is also seen in the observed cross section. The model wind fields also correspond well with the observed fields again noting the shift in the winds over the occlusion.

The IOP 5A cyclone continues to rapidly deepen from 21/1200Z to 21/1800Z, at a rate of $11 \text{ mb } 6 \text{ h}^{-1}$. This deepening rate is significantly greater than the $3 \text{ mb } 6 \text{ h}^{-1}$ rate shown in the NORAPS coarse grid OI analyses for this period. During this time, the 975 mb low moved rapidly northeast across the Gulf of St. Lawrence at 30 kts and deepened to 964 mb

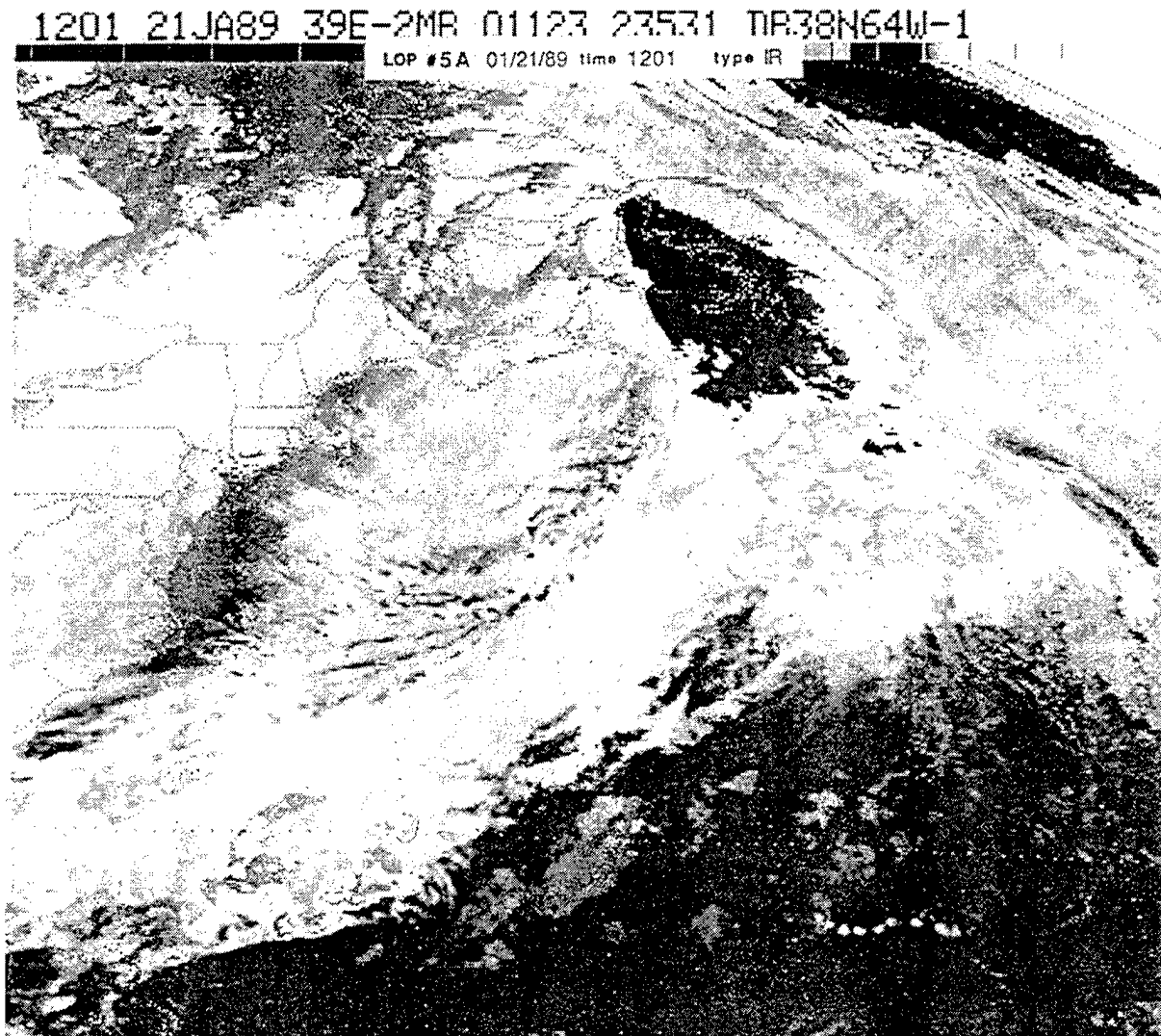


Figure 29. Goes enhanced IR satellite imagery at 21/1201Z January 1989.

(Figs. 20 o,q). NORAPS also presents a westward bias in the track with a 105 nm error to the northwest. There is now a significant change in the frontal evolution. The Arctic front has weakened and combined with the previous baroclinic zone along the ice edge to the east. The baroclinic zone to the east was advected onshore by the strong southeasterly flow caused

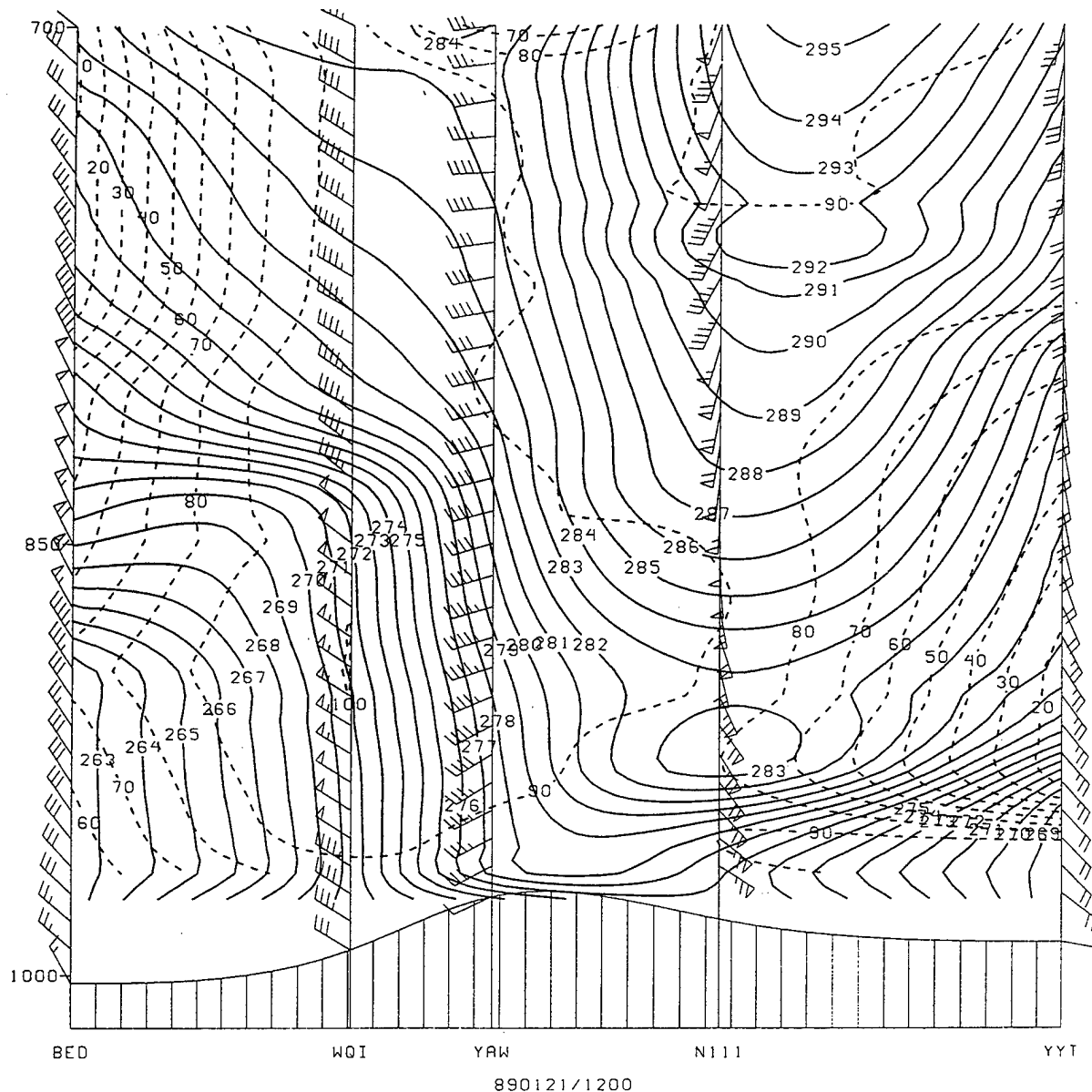


Figure 30. Analysis vertical cross section of potential temperature (dark solid, contour interval 1°K); relative humidity (dashed, contour interval 10%) valid at 21/1200Z January 1989.

by the stronger pressure gradient from the eastward moving cyclone. There is now strong cyclonic turning of the Arctic front into the low center, giving the appearance of a bent-back warm front in the mature stage. This bent-back thermal structure is evident at the surface

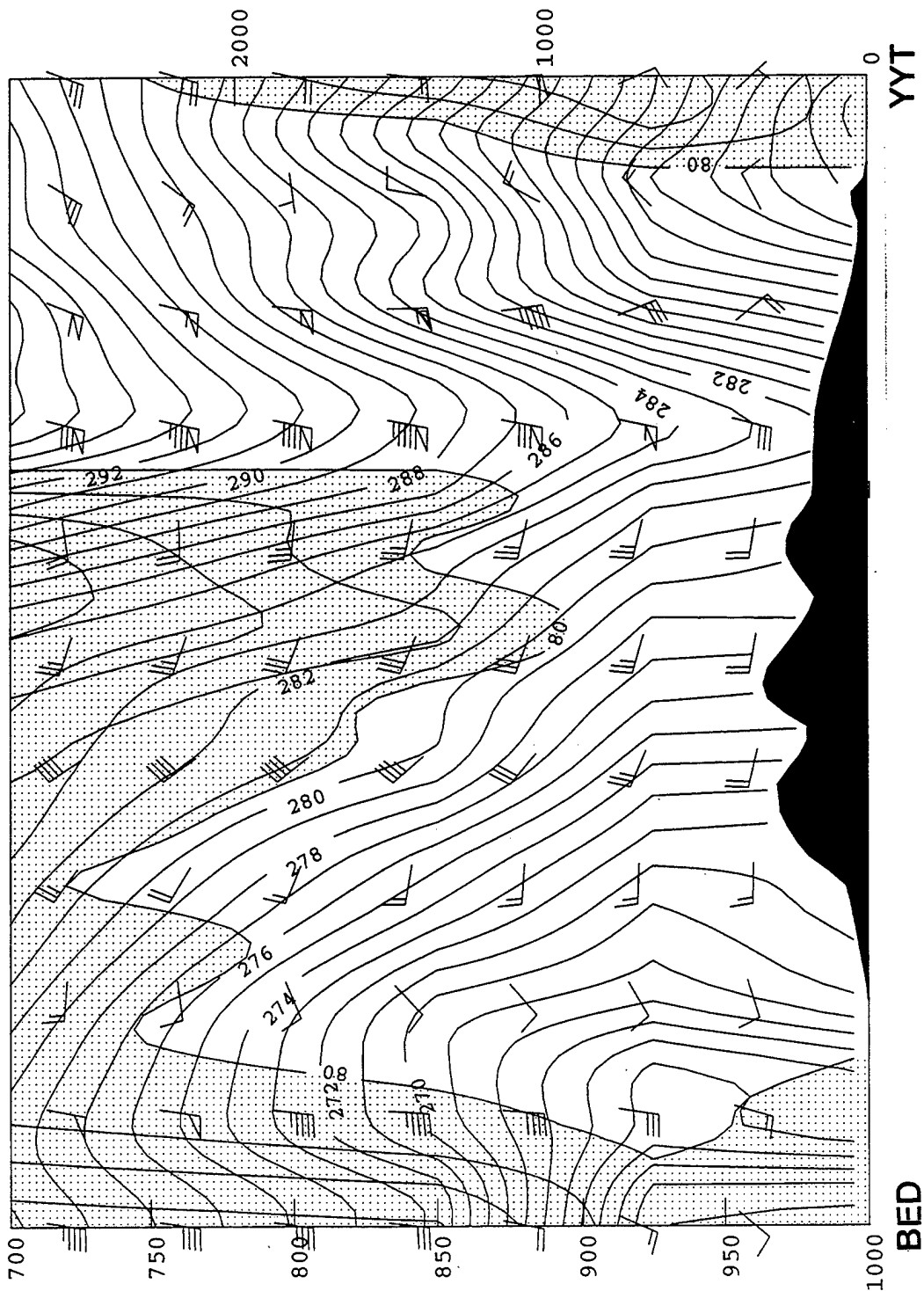


Figure 31. Model vertical cross section of potential temperature (dark solid, contour interval 1°K); relative humidity (light solid, contour interval 20%; stippled area $>80\%$) valid at 21/1200Z January 1989.

but more so at the 925 mb (not shown) and 850 mb level (Fig.32) Cold air encircling around the cyclone center has now totally enclosed a region of warmer air forming a warm-core seclusion, similar to the seclusion process as described by Shapiro and Keyser (1990). This seclusion process is different than Bjerknes and Solberg's (1922) seclusion process, which resulted from the topographic retardation of the front. Frontogenesis fields for this time depicts strong frontogenesis values to the north and southwest of the low center correlating well with the maximum baroclinicity and wind speeds found in the observations west of the low (Fig 20q). The previous stationary front along the northern portion of the Gulf of St. Lawrence has dissipated. Satellite imagery at 21/1701Z (Fig. 33) shows a mature cyclone vortex cloud pattern with the coldest cloud top temperatures ahead of the low.

A vertical cross section from Bedford, Massachusetts (BED) 42.6°N, 71.1°W, crossing the southern extent of the Arctic front, through the warm surface low and front, and terminating in Gander, Newfoundland (YQX) 49.0°N, 54.8°W, is presented in Fig. 34. The location of the cross section is shown in Fig. 12k. The model cross section is shown in Fig. 35. A pool of Arctic air dominates the west side of the cross section between 900 mb and 700 mb. There is warming of the theta air below 950 mb as it passes over the relatively warmer waters of the Gulf of Maine. The southern extent of the Arctic front is evident between Halifax, Nova Scotia (YAW) and Queensport, Nova Scotia (WOQ) where the tightest packed theta lines intersect the surface. The surface warm tongue in Fig. 12 k is seen in the temperature ridge between stations WOQ, and YQX. There is a drying out in the eastern part of the cross section as evidenced by the sharp relative humidity gradient. This structure resembles the warm conveyor belt structure described earlier in Fig.27. The model cross

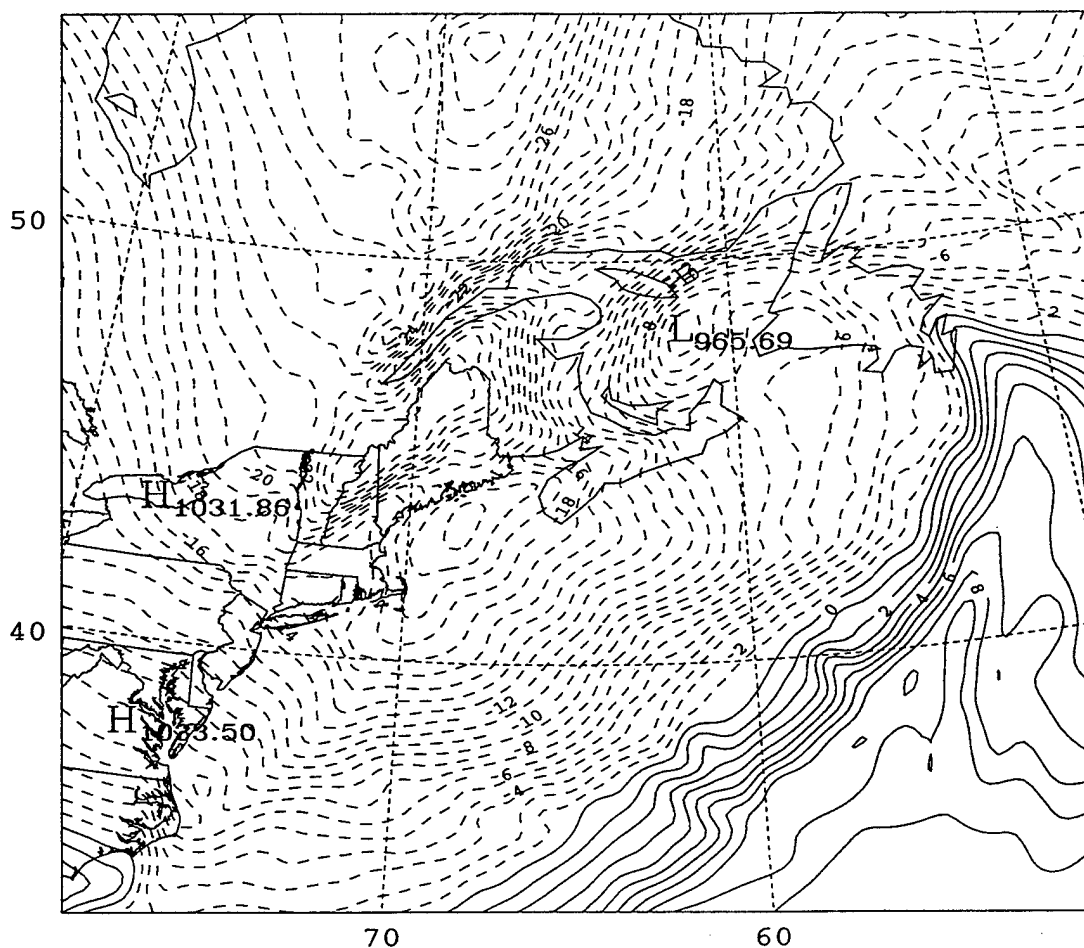


Figure 32. 850 mb temperature as in Fig. 13, except for 21/1800Z January 1989.

section (Fig. 35) shows similar structure in the vertical. A dry tongue ($< 20\%$ RH) extends down to 750 mb which separates the very moist areas of the warm and cold conveyor belts. Below the dry slot high relative humidity values ($>90\%$) dominate near the surface.

The Arctic front location is also evident in the observed sounding taken at Halifax, Nova Scotia (YAW) as illustrated by the frontal inversions and deep moisture layers (Fig. 36). The model sounding at this location also depicts a low-level inversion with high moisture values (Fig. 37) closely resembling the actual sounding.

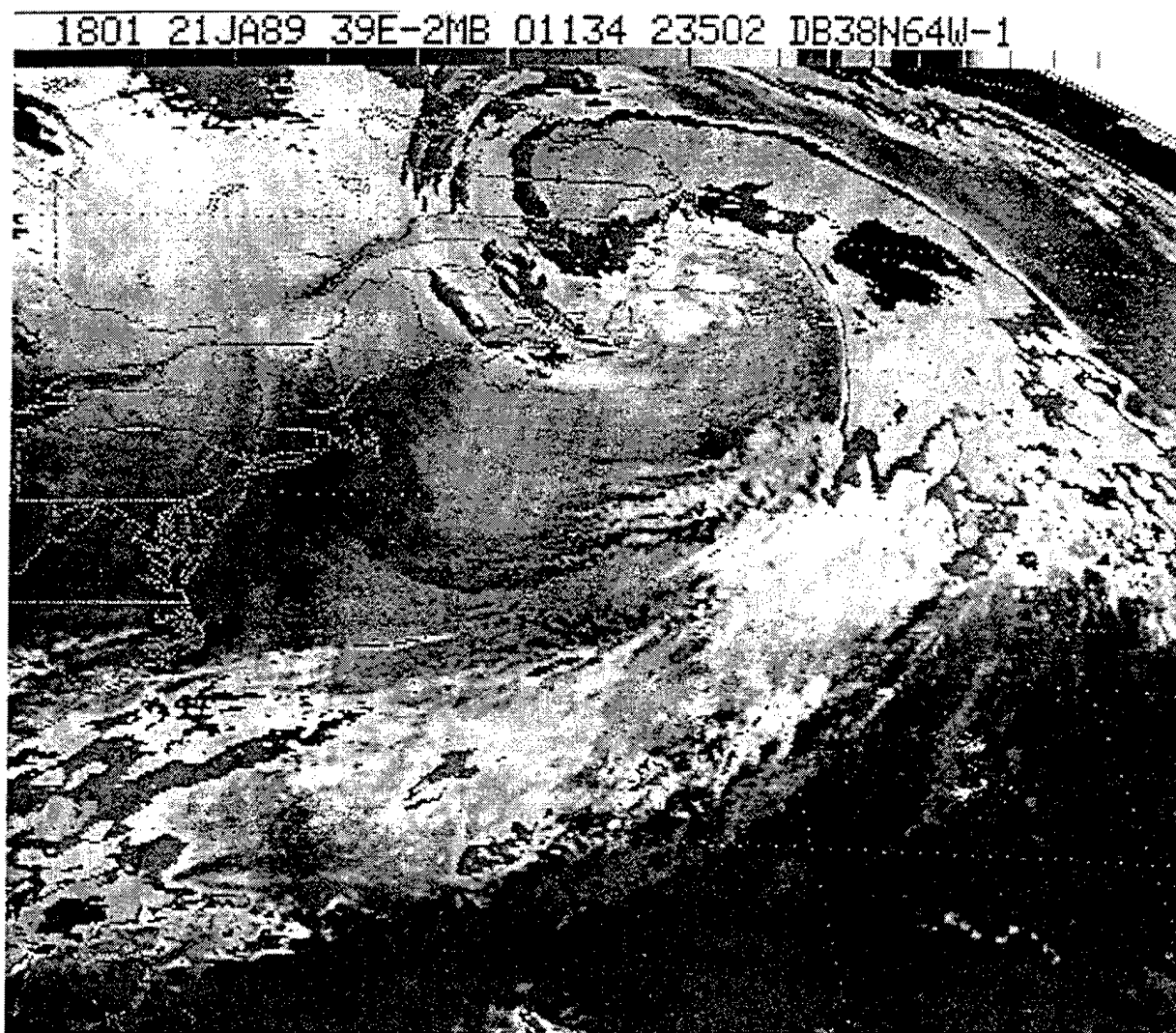


Figure 33. Goes enhanced IR satellite imagery at 21/1801Z January 1989.

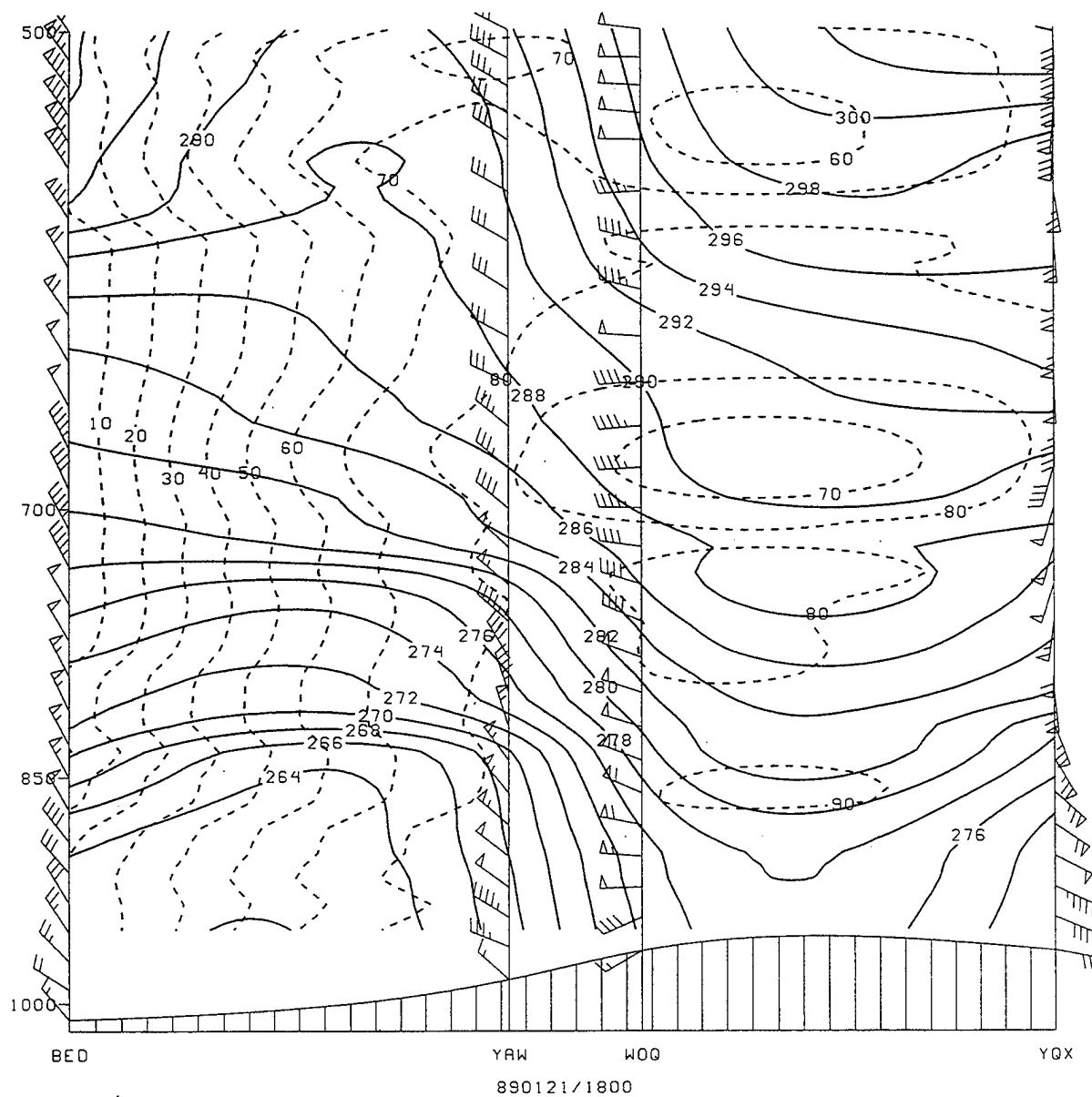


Figure 34. Analysis vertical cross section of potential temperature (dark solid, contour interval 1°K); relative humidity (dashed, contour interval 10%) valid at 21/1800Z January 1989.

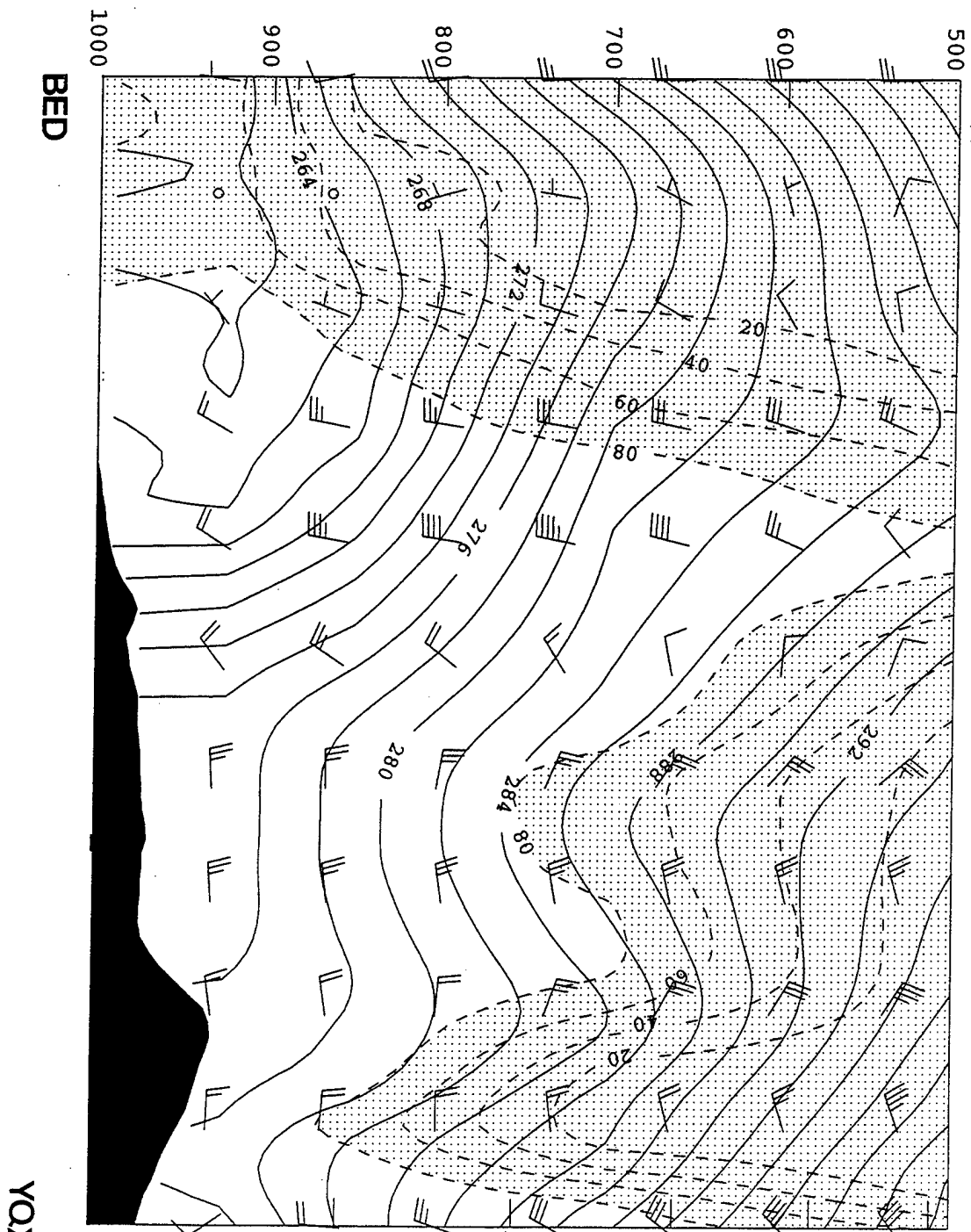


Figure 35. Model vertical cross section of potential temperature (dark solid, contour interval 1°K); relative humidity (light solid, contour interval 20%; stippled area >80%) valid at 21/1800Z January 1989.

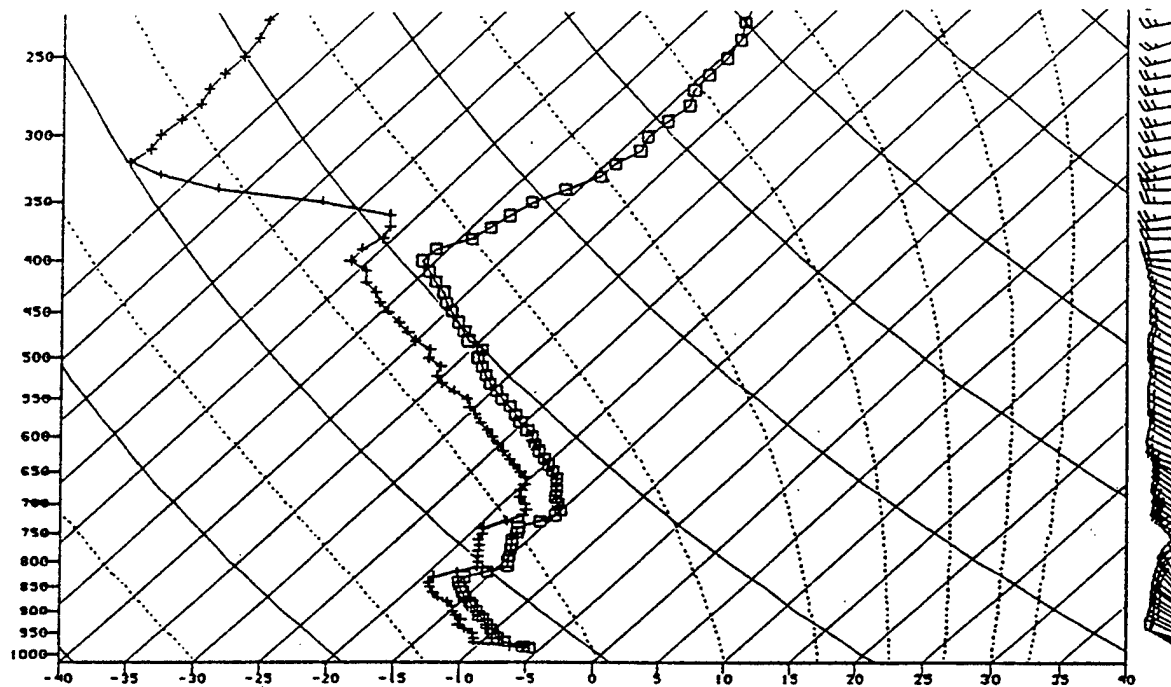


Figure 36. Observed sounding from Halifax, Nova Scotia (YAW) at 21/1800Z January 1989 (boxes denote temperature, crosses denote dew point) (from Cameron 1993).

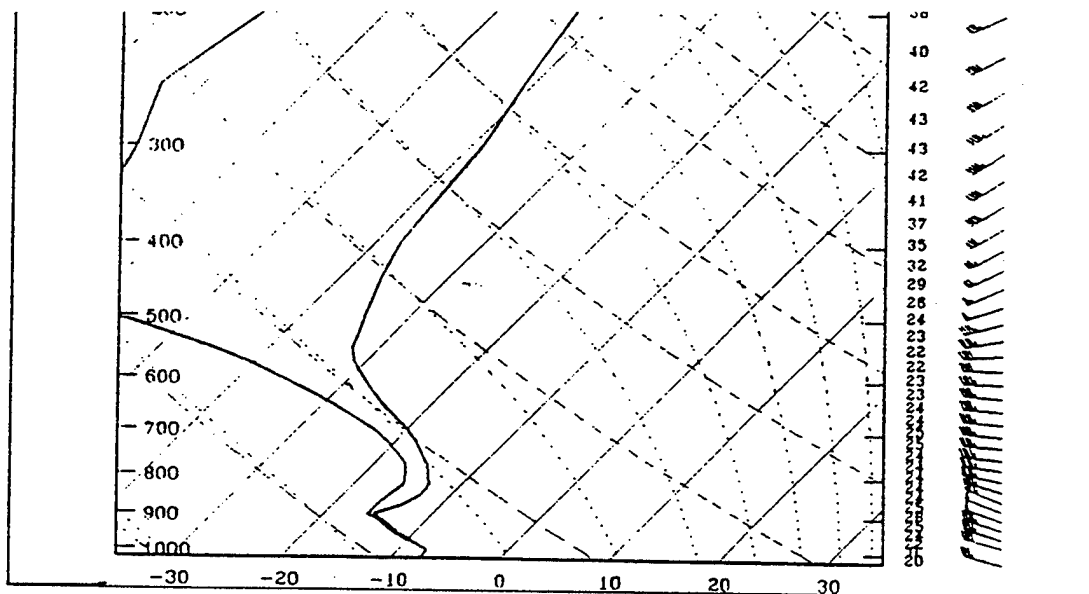


Figure 37. Model sounding for Halifax, Nova Scotia (YAW) at 21/1800Z January 1989 (right line denotes temperature, left line denotes dewpoint) (from Cameron 1993).

D. MATURE CYCLONE STAGE (21/1800Z - 22/0000Z)

In the final stages of development, the IOP 5A cyclone moves east over Newfoundland to 48.0°N, 55.9°W, and fills one millibar to 965 mb by 22/0000Z. The Arctic front and occluded front are now clearly separated as the cyclone moves further to the east. The surface warm tongue has continued a cyclonic rotation and the system looks noticeably more like a mature occluded cyclone. However, inspection of the surface isotherms (Fig. 20 m) reveals the continued presence of the warm-core seclusion noted at 21/1800Z. NORAPS shows this feature is present at the surface and 850 mb level (Fig. 38) as well. NORAPS has also positioned the low near St. Georges Bay, 130 nm west of the analyzed low. Model pressure is 2 mb weak at 967 mb. The separation of the Arctic and occluded fronts is also evident in the surface frontogenesis pattern (Fig. 14g). Frontogenesis has noticeably weakened north of the low where 6 h earlier it was at its strongest values.

Satellite imagery at 21/2100Z (Fig. 39) shows a dissipating comma head with a front still visible. The main cloud band to the east of the low has moved away from the cyclone center to the east. The system, now fully mature and vertical begins to fill as it moves out over the North Atlantic Ocean.

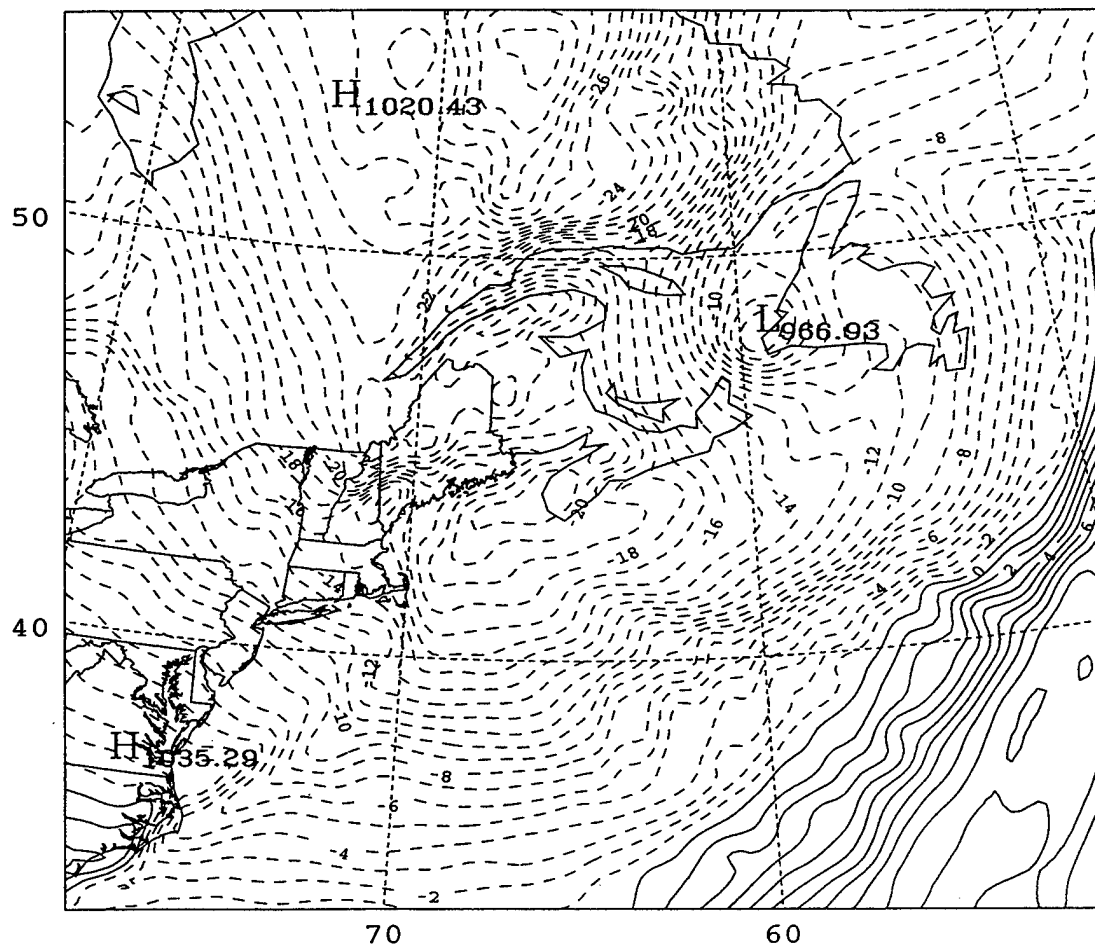


Figure 38. 850 mb temperature as in Fig. 13, except for 22/0000Z January 1989.

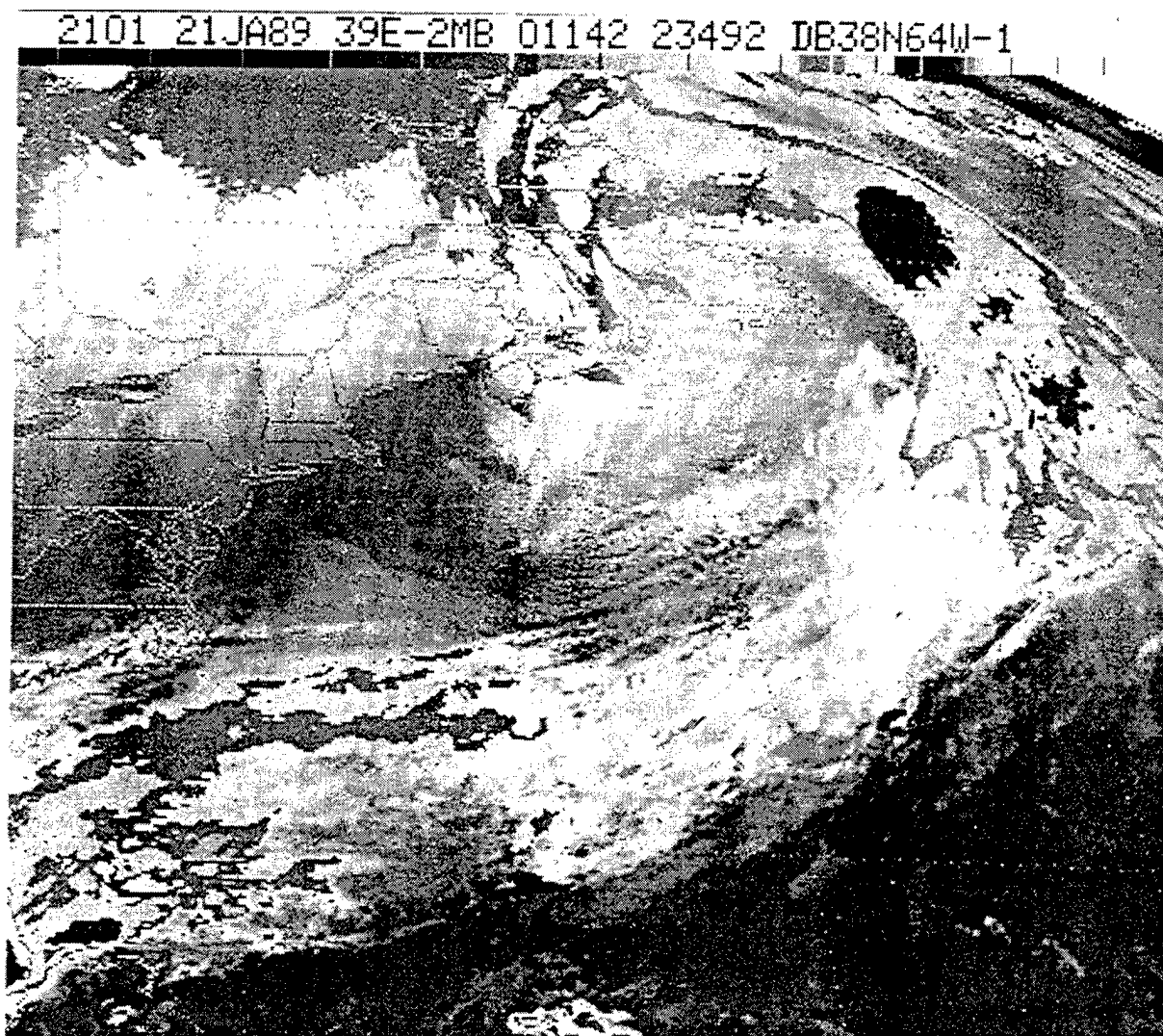


Figure 39. GOES enhanced IR satellite imagery at 21/2101Z January 1989.

V. SUMMARY AND RECOMMENDATIONS

A. SUMMARY

Using both observational data and output from the NORAPS mesoscale model, this paper describes the frontal evolution and mesoscale structure of an intense cyclone that evolved from a coastal low pressure system that eventually became the IOP 5A cyclone. The storm simulation was quite successful, skillfully capturing the intensity and movement of the cyclone, as well as most of its structural characteristics. Problems with the simulation include modest position and intensity errors during the latter portions of the simulation as well as minor differences with the observed moisture structure.

The model simulation of the January 1989 IOP 5A cyclone as well as the observed storm itself, suggest both similarities and differences with the T-bone conceptual model of Shapiro and Keyser (1990). Like the Keyser-Shapiro model, thermal seclusion and some fracturing of the cold front were present at the surface and even more so at 850 mb. However, the storm also shows a classic occlusion extending to the southeast of the storm (Fig. 12 i). In addition, the evolution of these frontal features is quite different than other studies. In particular, pre-existing frontal zones intensify during the rapid cyclogenesis and evolve into the cyclone frontal structures rather than forming as a result of the cyclogenesis.

A composite of the Arctic front evolution is presented in Fig. 40 at 12 h intervals from 20/1200Z to 22/0000Z. The Arctic front was a well defined baroclinic zone at the incipient stages of development. This front intensified as the cyclone developed and was consistently located in the immediate vicinity of the low throughout the IOP. The southern

portion of the Arctic front appeared to bend southeastward or wrap cyclonically around the low center in the later stages of development. The portion of the polar front south of the incipient low weakened as it moved over the warmer waters and joined with the pre-existing coastal front.

Figure 41 shows a composite of the coastal front positions every 6 h from 20/1200Z to 22/0000Z. The coastal front began as a weak baroclinic zone along the Mid-Atlantic states, located well to the southeast of the incipient low. The front continued to rotate cyclonically and intensify, in the presence of a strong warm tongue, conveyor belt and developing low. The northern portion of the front occluded and extended into the low by 21/0000Z. The warm front associated with the incipient system moved northeast, weakened and became stationary along the strongly baroclinic coastal zone along the southern border of Quebec.

Additionally, ERICA data was used to determine the mesoscale structure of the over-land coastal development period. The observed pressure and wind fields verified that coastal cyclogenesis occurred prior to explosive cyclogenesis. The mesoscale vortex, which appears to have formed as the result of topographic effects, developed south of the primary cyclone, deepened and tracked along the Maine coast and likely became the IOP 5A cyclone. Lower static stability, and strong upper-level forcing from a jet streak combined to aid in the development and subsequent intensification of the coastal system.

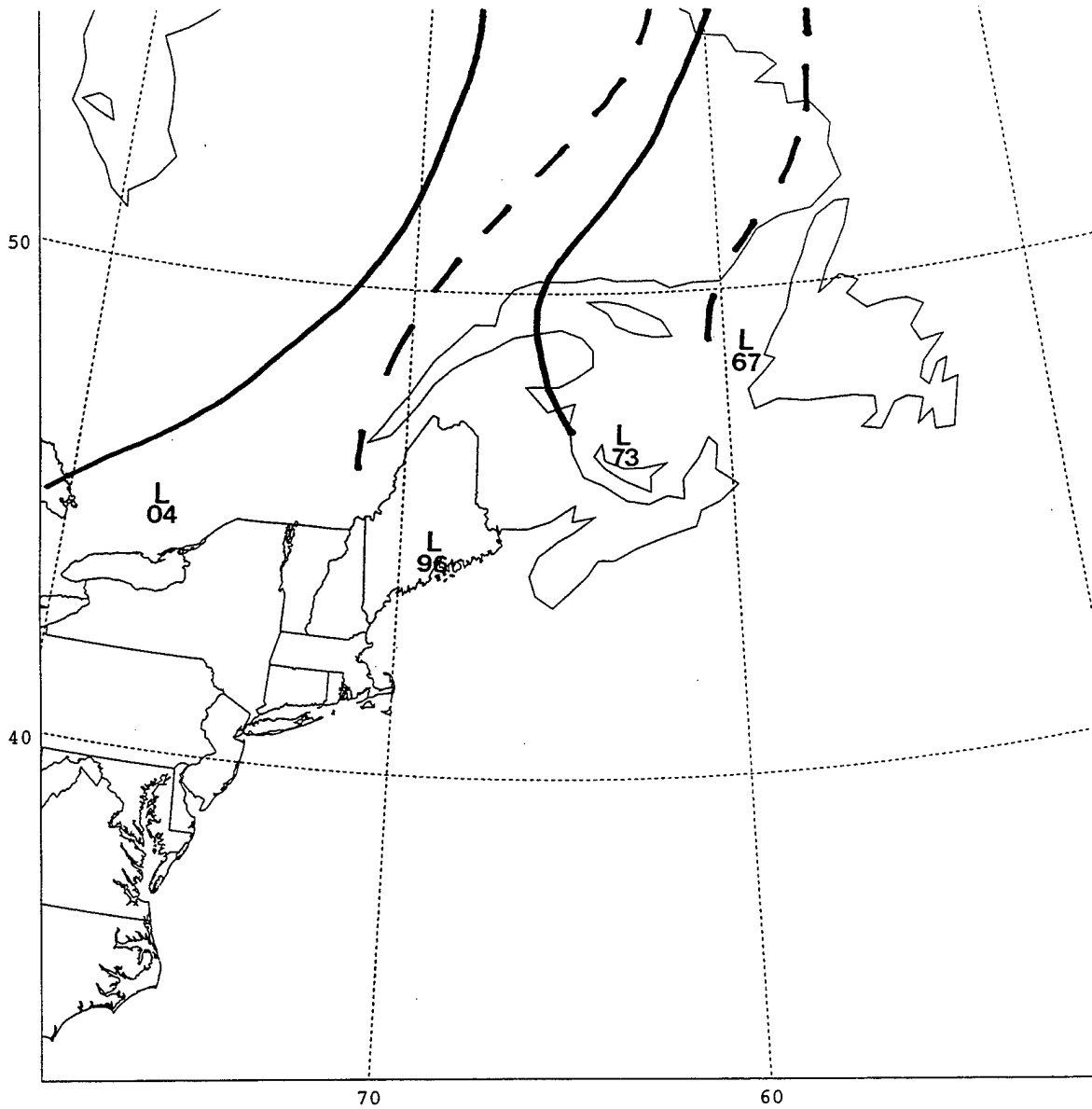


Figure 40. Model composite Arctic front positions in twelve hour increments from 20/12Z to 22/00Z January 1989.

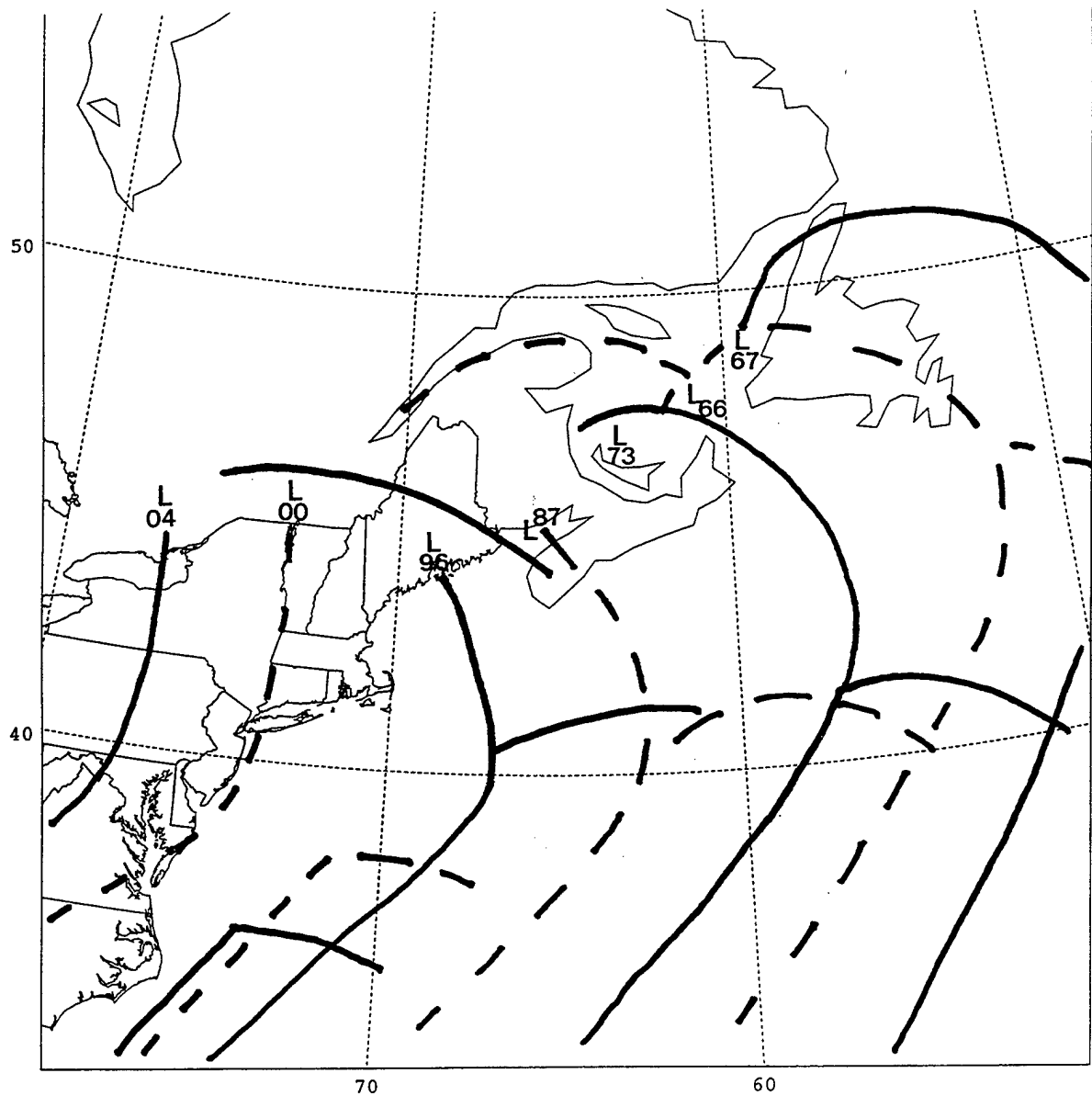


Figure 41. Model composite synoptic front positions in six hour increments from 20/12Z to 22/00Z January 1989.

B. RECOMMENDATIONS

The success of the nested NORAPS simulation encourages further numerical experimentation with other ERICA type storms to determine the different types of frontal evolutions observed. Specifically, further diagnosis of the development of the warm-core seclusion and cyclone center would aid in determining the intensity and depth of the mesoscale circulations associated with the warm core structure. Additionally, trajectories similar to those of Mass and Schultz (1990) derived from a model simulation, could explain many of the structural elements of the storm (i.e., conveyor belts and fronts) by using air-parcel trajectories associated with these features. Further diagnostics of the frontogenesis function can determine which components were most important during the break along the northern section of the cold front and bent-back warm front structure in the latter stages of development. Also an adiabatic mountainless simulation could quantitatively determine the roles of the topography or weaker stability along the baroclinic coastal area in the mesoscale cyclogenesis. The success of mesoscale analyses and numerical forecasts provides the tools to understand and predict future cases of explosive coastal development.

LIST OF REFERENCES

- Barker, E. H., 1992: Design of the Navy's multivariate optimum interpolation analysis system. *Wea. And Forecasting.*, 7, 220-231.
- Bosart, L. F., 1981: The Presidents' Day snowstorm of 18-19 February 1979: A subsynoptic-scale event. *Mon. Wea. Rev.*, 109, 1542-1566.
- Bjerknes, J., and Solberg, H., 1922: Life cycle of cyclones and the polar front theory of atmospheric circulation. *Geofys. Publ.*, 3, No. 1, 1-18.
- Cameron, S. R., 1993: Mesoscale frontal evolution of the ERICA IOP 5A cyclone. M.S. thesis, Naval Postgraduate School, Monterey, California, September 1993.
- Carlson, T. N., 1980: Airflow through midlatitude cyclones and the comma cloud pattern. *Mon. Wea. Rev.*, 108, 1498-1509.
- Hadlock, R., and C. W. Kreitzberg, 1988: The Experiment on Rapidly Intensifying Cyclones over the Atlantic (ERICA) field study: Objectives and plans. *Bull. Amer. Meteor. Soc.*, 69, 1309-1320.
- _____, E. Harnett, and G. Forbes, 1989: The Experiment on Rapidly Intensifying Cyclones over the Atlantic (ERICA) Field phase summary. [Available from ERICA Data Center, Department of Physics and Atmospheric Science, Drexel University, Philadelphia, PA 19104.], 388 pp.
- Hodur, R. M., 1987: Evaluation of a regional model with an update cycle. *Mon. Wea. Rev.*, 115, 2707-2718.
- Kuo, H. -L., 1974: Further studies of the influence of cumulus convection on large-scale flow. *J. Atmos. Sci.*, 31, 1232-1240.
- Langland, R. H., and C. -S. Liou, 1994: Operational implementation of a turbulence kinetic energy closure boundary-layer flow. Preprints, *10th Conf. on Numerical Weather Prediction.*, Portland, OR, Amer. Meteor. Soc., 450-453.
- Liou, C. -S., R. M. Hodur, and R. H. Langland, 1994: Navy Operational Regional Atmospheric Prediction System (NORAPS): A triple nest mesoscale model. Preprints, *10th Conf. on Numerical Weather Prediction.*, Portland, OR, Amer. Meteor. Soc., 423-425.

- Louis, J. -F., 1979: A parametric model of vertical eddy fluxes in the atmosphere. *Bound. Layer Meteor.*, **17**, 187-202.
- Manobianco, J., 1989: Explosive East Coast cyclogenesis over the West-Central North Atlantic Ocean: A composite study derived from ECMWF operational analyses. *Mon. Wea. Rev.*, **117**, 2365-2383.
- Mass, C. F., and D. M. Schultz, 1993: The structure and evolution of a simulated midlatitude cyclone over land. *Mon. Wea. Rev.*, **121**, 889-917.
- McGinnigle, J. B., M. V. Young, and M. J. Bader, 1988: The development of instant occlusions in the North Atlantic. *Meteor. Mag.*, **117**, 325-340.
- Mullen, S. L., 1983: Explosive cyclogenesis associated with cyclones in polar air streams. *Mon. Wea. Rev.*, **111**, 1537-1553.
- Neiman, P. J., and Shapiro, M. A., 1993: The life cycle of an extratropical marine Cyclone. Part I: Frontal-cyclone evolution and thermodynamic air-sea interactions. *Mon. Wea. Rev.*, **121**, 2153-2176.
- Nuss, W. A., and D. W. Titley, 1994: Use of multiquadric interpolation for meteorological objective analysis. *Mon. Wea. Rev.*, **122**, 1611-1631.
- _____, and R. A. Anthes, 1987: A numerical investigation of low-level processes in rapid cyclogenesis. *Mon. Wea. Rev.*, **115**, 2728-2743.
- Sanders, F., and J. R. Gyakum, 1980: Synoptic-dynamic climatology of the "bomb." *Mon. Wea. Rev.*, **108**, 1589-1606.
- _____, 1986: Explosive cyclogenesis in the west-central North Atlantic Ocean, 1981-84. Part I: Composite structure and mean behavior. *Mon. Wea. Rev.*, **114**, 1781-1794.
- Shapiro, M. A., and D. Keyser, 1990: Fronts, jet streams and the tropopause. *Extratropical Cyclones: The Erik Palmen Memorial Volume*. C. W. Newton and E. O. Holopainen, Eds., Amer. Meteor. Soc., 167-191.
- Spinelli, J. M., 1992: An investigation of the ERICA IOP 5A cyclone. M.S. thesis, Naval Postgraduate School, Monterey, California, December 1992.
- Tiedtke, M., W. A. Heckley, and J. Slingo, 1988: Tropical forecasting at ECMWF: The influence of physical parameterization on the mean structure of forecasts and analysis. *Quart. J. Roy. Meteor. Soc.*, **114**, 639-664.

Uccellini, L. W., D. Keyser, K. F. Brill and C. H. Wash, 1985: Presidents' Day cyclone of 18-19 February 1979: Influence of upstream trough amplification and associated tropopause folding on rapid cyclogenesis. *Mon. Wea. Rev.*, **113**, 962-988.

Wash, C. H., J. E. Peak, W. F. Calland, and W. A. Cook, 1988: Diagnostic study of explosive cyclogenesis during FGGE. *Mon. Wea. Rev.*, **116**, 431-451.

INITIAL DISTRIBUTION LIST

	No. Copies
1. Defense Technical Information Center 8725 John J. Kingman Rd., STE 0944 Ft. Belvoir, VA 22060-6218	2
2. Dudley Knox Library Naval Postgraduate School 411 Dyer Rd. Monterey, CA 93943-5101	2
3. Professor Carlyle H. Wash (Code MR/Wx) Department of Meteorology Naval Postgraduate School Monterey, CA 93943-5000	3
4. Paul A. Hirschberg National Weather Service 1325 East-West Highway, Station 13236 Silver Spring, MD 20910	1
5. Commander, Carrier Group Three Unit 25059 FPO AP 96601-4303 Attn: LCDR Timothy Lane	2
6. Director Naval Meteorology and Oceanography Division Naval Observatory 34 th and Massachusetts Avenue NW Washington, DC 20390	1
7. Commander Naval Meteorology and Oceanography Command Stennis Space Center MS 39529-5001	1
8. Commanding Officer Fleet Numerical Meteorology and Oceanography Center Monterey, CA 93943-5001	1

- | | |
|---|---|
| 9. Commanding Officer
Naval Research Laboratory
Stennis Space Center
MS 39529-5004 | 1 |
| 10. Chief of Naval Research
800 N. Quincy Street
Arlington VA 22217 | 1 |